12-14-2018

Distributed Predictive Control for MVDC Shipboard Power System Management

Nasibeh Zohrabi

Distributed predictive control for MVDC shipboard power system management

By

Nasibeh Zohrabi

A Dissertation
Submitted to the Faculty of
Mississippi State University
in Partial Fulfillment of the Requirements
for the Degree of Doctor of Philosophy
in Electrical Engineering
in the Department of Electrical and Computer Engineering

Mississippi State, Mississippi

December 2018

Distributed predictive control for MVDC shipboard power system management

By

Nasibeh Zohrabi

Approved:

Joni Klüss
(Major Professor)

Sherif Abdelwahed
(Co-Major Professor/Dissertation Director)

Yong Fu
(Committee Member)

Masoud Karimi Ghartemani
(Committee Member)

James E. Fowler
(Graduate Coordinator)

Jason M. Keith
Dean
Bagley College of Engineering

Name: Nasibeh Zohrabi

Date of Degree: December 14, 2018

Institution: Mississippi State University

Major Field: Electrical Engineering

Major Professor: Dr. Joni Klüss

Title of Study: Distributed predictive control for MVDC shipboard power system management

Pages of Study: 141

Candidate for Degree of Doctor of Philosophy

Shipboard Power System (SPS) is known as an independent controlled small electric network powered by the distributed onboard generation system. Since many electric components are tightly coupled in a small space and the system is not supported with a relatively stronger grid, SPS is more susceptible to unexpected disturbances and physical damages compared to conventional terrestrial power systems. Among different distribution configurations, power-electronic based DC distribution is considered the trending technology for the next-generation U.S. Navy fleet design to replace the conventional AC-based distribution. This research presents appropriate control management frameworks to improve the Medium-Voltage DC (MVDC) shipboard power system performance.

Model Predictive Control (MPC) is an advanced model-based approach which uses the system model to predict the future output states and generates an optimal control sequence over the prediction horizon. In this research, at first, a centralized MPC is developed for a nonlinear MVDC SPS when a high-power pulsed load exists in the system. The closed-loop

stability analysis is considered in the MPC optimization problem. A comparison is presented for different cases of load prediction for MPC, namely, no prediction, perfect prediction, and Autoregressive Integrated Moving Average (ARIMA) prediction. Another centralized MPC controller is also designed to address the reconfiguration problem of the MVDC system in abnormal conditions. The reconfiguration goal is to maximize the power delivered to the loads with respect to power balance, generation limits and load priorities.

Moreover, a distributed control structure is proposed for a nonlinear MVDC SPS to develop a scalable power management architecture. In this framework, each subsystem is controlled by a local MPC using its state variables, parameters and interaction variables from other subsystems communicated through a coordinator. The Goal Coordination principle is used to manage interactions between subsystems. The developed distributed control structure brings out several significant advantages including less computational overhead, higher flexibility and a good error tolerance behavior as well as a good overall system performance. To demonstrate the efficiency of the proposed approach, a performance analysis is accomplished by comparing centralized and distributed control of global and partitioned MVDC models for two cases of continuous and discretized control inputs.

Key words: Model Predictive Control, Distributed Control, Medium-Voltage DC (MVDC), Shipboard Power Systems, Islanded DC Microgrid

DEDICATION

To my beloved parents, Hossein and Mahboobeh, and my sisters, Somayeh, Yasaman and Farzaneh, who always picked me up on time and encouraged me to go on every adventure, especially this one. And also to my best Hasan who has been a constant source of support and encouragement during the challenges of graduate school and life.

ACKNOWLEDGEMENTS

I would like to thank the following individuals who helped me prepare for this dissertation work. First and foremost, I would like to express my sincere gratitude to Dr. Sherif Abdelwahed for the continuous support of my Ph.D. studies and research, for his patience, motivation, guidance, caring, and immense knowledge. I would also like to appreciate my current advisor, Dr. Joni Kluss, for all his support and helpful advice, especially in the last year of my Ph.D. studies.

I would like to thank the other Ph.D. committee members, Dr. Masoud Karimi and Dr. Yong Fu, for supporting me, giving me helpful suggestions and reviewing this dissertation. I would also like to thank Dr. Jian Shi for all his helpful advice, especially in the modeling part of the electric ship power systems. I am grateful to Mr. Hasan Zakeri for all his helpful suggestions and inspiring discussions, especially in the control part of my work, whose comments and questions always open new horizon of concepts.

I thank the Office of Naval Research (ONR) for the financial support during my studies.

I am extremely grateful to my parents and my sisters for their love, dedication and support through all these years that I have been far away from home. Finally, my special thanks goes to Hasan for always being there for me and providing unending inspiration.

TABLE OF CONTENTS

APPENDIX

LIST OF TABLES

LIST OF FIGURES

CHAPTER I

INTRODUCTION

1.1 Motivations

Shipboard power systems (SPSs) are going through fundamental transitions to provide reliable and abundant power supply to the future all-electric fleets. With DC distribution bus and power conversion in the center of this transition to achieve improved power density and efficiency, Medium-Voltage DC (MVDC) system is envisioned as the obvious choice for the on-board power generation and distribution. An SPS based on DC distribution reveals some important advantages, including: eliminating the need for the phase angle synchronization of sources, reducing fuel consumption, reducing the size and ratings of switchgears and cables and elimination of frequency constraints [4, 37]. In this research, we mainly develop the MVDC SPS by proposing appropriate control management frameworks.

The design of shipboard power system needs careful consideration of the variety of system specifications, operating constraints and design requirements under different operating scenarios and mission profiles to maintain a stable, reliable and economically efficient operation. Especially, for the state-of-the-art DC-based SPSs, with the extensive use of power electronic apparatus and the wide adoption of intelligent ship modernization techniques, the complexity and heterogeneity of on-board electrical systems significantly increases. Therefore, appropriate specifications, requirements and control frameworks that are tailored

specifically for DC-based SPSs need to be developed to address the requirements of electric ship design, simulation, control, optimization, management and automation. In this research, we perform a comprehensive study of both steady-state and transient design specifications and performance criteria for a DC-based shipboard power system, utilizing mathematical formulations to address necessary criteria of designing various aspects of a shipboard power system, including aspects related to control, protection and optimization.

During the last few decades, Model Predictive Control (MPC) has received a great deal of attention from both the research community and industry mostly because it is easy to apply to multivariable cases, it can handle constraints on control inputs and system states in the optimization program directly and it is straightforward to include nonlinearities in the control law [23, 76, 106]. In addition, the MPC approach can systematically handle physical limitations imposed on the control inputs and system states. It can also deal with different system models and types (linear and nonlinear models) and it is easily reconfigurable and can handle run-time modifications of control objectives. Utilization of appropriately defined/modified objective functions and constraints makes distinct architectures of MPC (centralized, decentralized and distributed structures) [53]. The general control problem formulation is based on: 1) prediction model, 2) objective function, 3) state and control constraints, and 4) controller architecture: centralized, decentralized and distributed. Among all the applications of MPC, one can mention aerospace, power systems, thermal management and automotive industries [23, 71, 84, 105, 15]. Recently, model predictive methods have gained attention of researchers for shipboard power system applications [17, 82, 115]. In

this research, a model predictive control approach is used as the main method in both centralized and distributed control of a nonlinear MVDC shipboard power system.

Through the evolution of computer and network communication technologies, the distributed control approach offers important advantages over the centralized architecture, which enable it to effectively handle the various real world problems [73, 10, 101]. In a distributed control structure, the centralized problem is decomposed into several local control units which compute their optimization problems in separate processors and communicate iteratively to reach a closed-loop system objective [32].

One of the main advantages of distributed control is its good error-tolerance behavior and robustness. This means if an unexpected failure happens in a subsystem, the other local controllers can still work and the entire system is not affected by a possible failure. High flexibility is another important benefit of a distributed framework. This structure simplifies any possible expansions and maintenance of the control system. If a new subsystem is added to the current system, one only needs to modify the subsystems which have interaction with the new subsystem; making it easily extendable. Moreover, it is easier to implement a distributed scheme due to its lower computational requirements. This is because a complex problem is replaced by several smaller-scale problems even though this structure may have suboptimal outcome compared with a centralized control. The performance highly depends on the degree of interaction between subsystems and the coordination algorithm [73, 10, 101].

The above-mentioned advantages of MPC and distributed control scheme motivate their usage in many practical applications including the MVDC shipboard power system. The

aim of this research is to develop appropriate centralized and distributed predictive control architectures for the MVDC shipboard power management to achieve the desired system performance. In the centralized case, a nonlinear MPC is used to control the MVDC system when dealing with a pulsed load such as free electron lasers under battle condition. Another MPC controller is designed to address the reconfiguration problem of the MVDC system in abnormal conditions. In the proposed distributed structure for the nonlinear MVDC system, the distributed MPC controller not only has the advantages of MPC (directly handling constraints and good optimization performance), but also has the characteristics of a distributed control framework of less computational overhead, high flexibility and a good error tolerance.

1.2 Literature Review and Related Works

The following subsections review the preliminary and present overview of the recent results and related works.

1.2.1 Medium-Voltage DC Naval Ship System and its Specifications

Unlike conventional terrestrial power systems, Shipboard Power Systems (SPS) are independent small-scale electrical networks that are responsible for providing sufficient energy to service loads, propulsion systems and other essential loads, such as weapon support systems, if present. As they are particularly valuable for use in naval fleets and a large number of electric components tightly coupled in a small space, these models are far more susceptible to physical damage and unexpected disturbances than conventional terrestrial

systems. So, the normal operation of the ship power system needs an appropriate control management framework by defining high-level objectives to achieve system performances.

Among different distribution configurations, Medium-Voltage DC distribution power system is considered the trending technology for future naval warships to replace the conventional AC-based distribution [44, 14, 47]. The general topology of a notional MVDC Next Generation Integrated Power System is given in [6]. It includes two main power generation modules (main PGM1 and main PGM2), two auxiliary power generation modules (auxiliary PGM1 and auxiliary PGM2), two ship propulsion motors, a high power pulsed load, an energy storage and four zonal loads. A ring-bus topology is chosen for the DC distribution system where buses along the port and starboard sides of the ship are connected at the bow and stern. Fig. 1.1 shows the general topology of the MVDC distribution power system in which all electrical power sources and electrical loads are connected to the MVDC bus via power electronics. The propulsion motors are connected to the DC bus via Variable Speed Drives (VSDs) which work as the power converters. Fig.1.2 demonstrates the zonal load center for the MVDC system [6]. The port bus and starboard bus are DC busses. So, the DC loads are fed trough isolated dc/dc converter (IDCDC) and low frequency AC loads are fed through a non-isolated inverter module (NIM).

Conventionally, the AC-based distribution system has been widely employed in the SPS design with well-established and documented standards and regulations such as MIL-STD-1399-300 [1] and MIL-STD-1399-680 [2]. However, currently, there are very limited efforts made to address the lack of standardized design criteria and performance metrics for the DC-based distribution SPS research, particularly for the latest MVDC SPS [4, 44]. In [4],

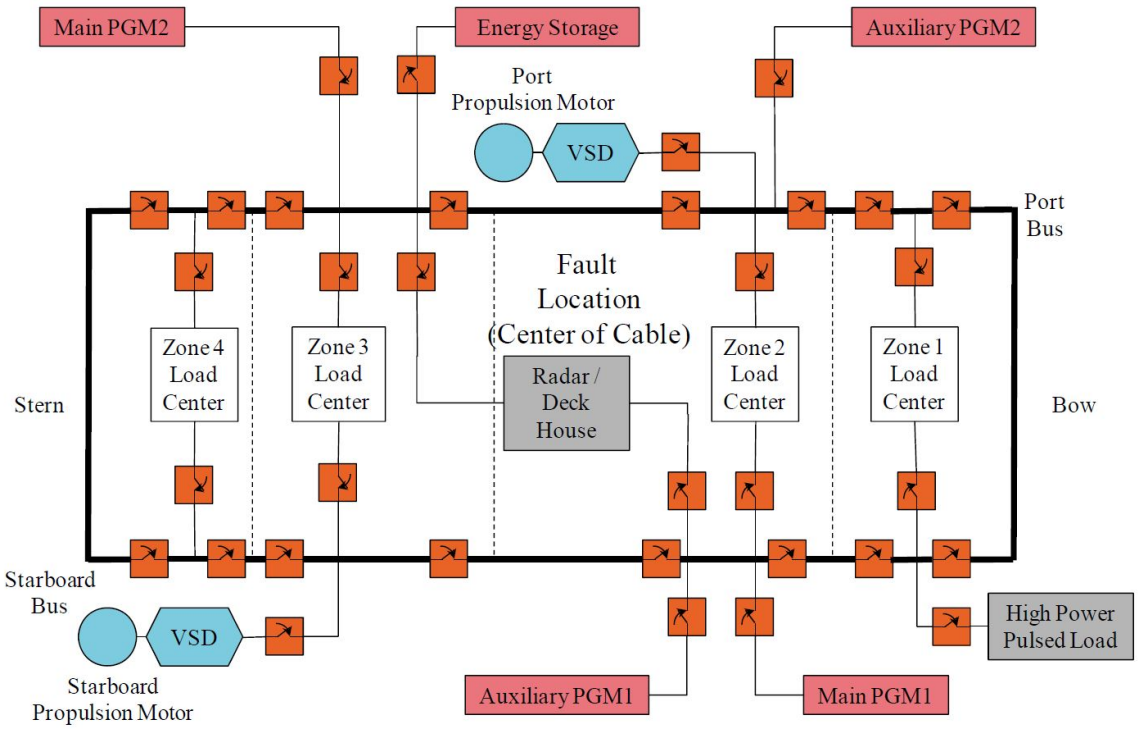

Figure 1.1: General Topology for Baseline MVDC System [5]

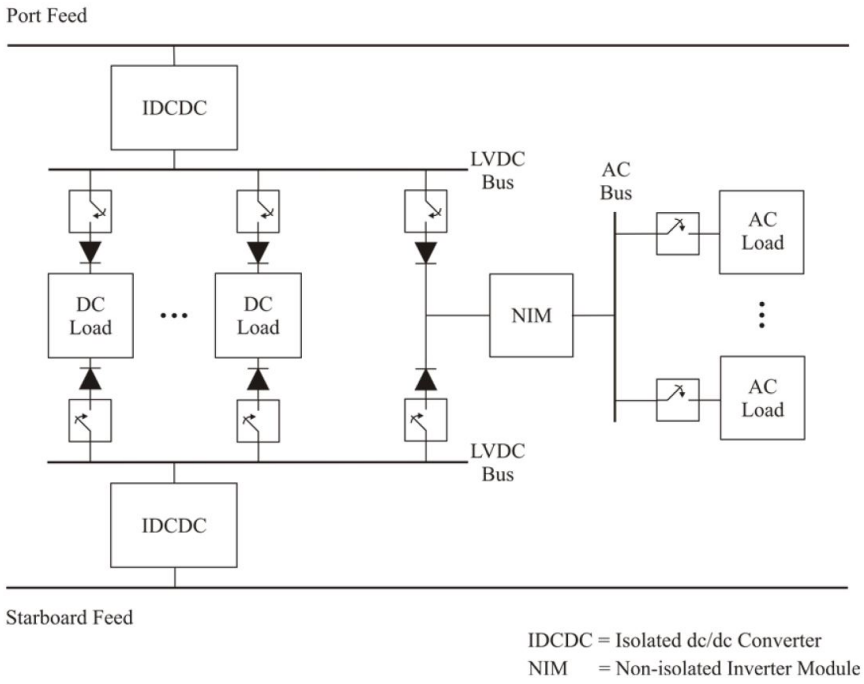

Figure 1.2: Notional MVDC Zone [6]

general direction and design concepts are studied which include limited implementation details and practical design considerations. This research work aims to address this issue by developing a list of significant design specifications and requirements along with their specific formulations for the steady-state and transient analysis of the MVDC SPS. The presented specifications and criteria can be utilized as guidelines and references for the SPS research community. Steady-state and transient specifications are essential to various aspects of the system design process including control, optimization, validation, simulation, model-based analysis, protection and testing. Chapter 2 provides more information on the system's model and also explains the most significant design specifications and requirements for the considered MVDC SPS.

1.2.2 Centralized Control Structure for an MVDC Ship Power System

In Chapter 3, two centralized model predictive control algorithms are designed for a nonlinear MVDC shipboard power system. First, an MPC controller is designed to control the MVDC system high power pulsed load under battle condition. Second, an MPC-based reconfiguration algorithm is presented to maximize the delivered power to the loads under abnormal conditions. The results presented in Chapter 3 based on centralized MPC are useful to design the distributed control structure with local MPC controllers for performance evaluation.

Effects of high power electrical loads such as pulsed loads and the necessity of controlling such loads in the power system have been studied thoroughly in the literature [36, 85, 96, 54]. In the shipboard power system, weaponry loads including electromagnetic

launch systems, electromagnetic guns, and free electron lasers are known as high power pulsed loads. These loads draw very high short-time current from system which can drop the voltage in the whole microgrid and drift the frequency, for a short period of time. In shipboard power systems, a large and prolonged voltage (or frequency) drop may shut down the propulsion system or take other sensitive loads offline [79]. Due to the size and weight constraints, it is infeasible to add more conventional generators to support the system for high power loads. Moreover, since shipboard power system is an independent network, there is no external generation support available if needed. There are several control studies that deal with this issue. Some methods may consider pulsed load as an unknown or a known disturbance to the power system and then apply an appropriate controller to reject the disturbance [36, 77]. This research work presents an efficient centralized MPC-based power management approach for mitigating the effects of stressful pulsed loads such as weaponry loads in the electric ships in Chapter 3. Chapter 4 (Scenario I) investigates distributed MPC control of a partitioned MVDC system when there is a pulsed load in the system and the results are compared with those obtained from centralized MPC controller.

In a shipboard power system, a fast reconfiguration is a critical activity to maintain a power balance requirement in the system and serve the vital loads. Therefore, in order to enhance survivability of the SPSs and reduce manning requirements, automatic reconfiguration is a necessary task for service restoration under abnormal conditions. A number of research works have been done on the reconfiguration problem of the shipboard power systems during the past decades [22, 95, 88, 18, 25].

For example, in [22], an automated self-healing reconfiguration methodology for service restoration in the naval SPSs is presented. An automatic rule-based expert-system method for reconfiguration of power systems on naval ships is proposed in [95]. An intelligent reconfiguration algorithm for microgrid is presented in [88] based on the genetic algorithms and graph theory. Another reconfiguration approach is presented in [18] which considers a balanced hybrid (AC and DC) SPS. All the above-mentioned research results are for the reconfiguration problem of the AC SPS. However, there are limited results available in the literature which consider the reconfiguration problem of the SPS with DC distribution system [25]. The reconfiguration algorithm presented in [25] for the DC SPS is based on the graph theory. In this research work, a reconfiguration algorithm is also developed for a nonlinear MVDC shipboard power system. A model predictive control approach is used for the SPS reconfiguration problem to optimize the objective function by maximizing power delivered to the loads without violating important system constraints such as power balance and power generation limits. The priorities of loads are also defined based on the mission of the ship.

1.2.3 Distributed Control Structure for an MVDC Ship Power System

Many centralized control design approaches are available for the control of shipboard power systems. Although these control methods can be applicable for the conventional terrestrial power systems, they may not be suitable for the naval ships. Since the SPS is an independent electric network without any external support, the centralized control structure may provide some limitations under battle mode or when dealing with sudden

disturbances and errors due to its complicated framework, i.e. one system, one controller. The model-based controllers can be prohibitive especially if a complex system model is used. The distributed control scheme facilitates any possible expansions and maintenance of the control subsystems without modifying the whole system's structure, so it is easily extendable.

Designers choose distributed architectures for control of large-scale systems over centralized architecture due to some key reasons. First, for a large-scale system, centralized schemes are based on designing a single controller for the entire plant, so they will be too complicated and expensive to implement as the size of the problem grows large, and they require substantial maintenance effort and cost [59, 62]. The second reason is robustness against implementation and hardware failure. Even though such failure can happen in both centralized case and distributed case, one should note that because the centralized controller is more complicated, the chance of failure is higher. And when the controller fails in the centralized scenario, the whole system will fail. On the other hand, in the distributed case, the failure can happen at either the coordinator or the subsystems. If a subsystems controller fails, then that subsystem can be taken out for maintenance without compromising the integrity of the whole system (the rest of the subsystems will continue to perform). Due to the fact that the coordinator is implementing a simple function, it will be easier and cheaper to provide redundancy for this important component. Such redundancy can reduce the probability of failure significantly. Reliability can be also enhanced with the distributed control structure because a single point of failure needs lower time-to-repair and it will not cause the entire process to fail. In addition, it is easier to troubleshoot a small system than

a large one. The local controllers can continue to operate in the event of failure of other controllers.

Recently, distributed control approaches have received more attention from academia and industry, and different results are available for AC shipboard power system [16, 55, 8]. In [16], the voltage and frequency control of an AC SPS is investigated according to a distributed control of multi-agent systems. A reconfiguration problem of an AC electric ship power system based on distributed control agents by using maximum flow algorithm is studied in [55]. In [8], a power management is proposed for an AC electric SPS to control load sharing by tuning no-load frequency in a distributed framework based on the Interaction Balance Principle. In this research work, a appropriate distributed predictive control structure is developed for a nonlinear MVDC system which is presented in Chapter 4 in detail. Model predictive control approach is used for the local controllers in the proposed distributed structure. A performance analysis is also carried out by comparing a centralized control and a distributed control on the global and partitioned models and considering different specifications in the MVDC system.

1.3 Summary of Contributions

This research aims to develop a distributed predictive control architecture for an MVDC shipboard power system management. It includes the model-based centralized and distributed management control frameworks to achieve different performance goals. The main contributions of this dissertation are listed as follows:

1) MVDC Shipboard Power System Model Formulations and its Design Specifications

(a) The MVDC SPS model structure and its mathematical formulations are presented.

(b) A comprehensive list of significant transient and steady-state specifications and performance criteria along with their mathematical formulations are provided.

(c) The necessary system constraints and operating conditions are presented for the MVDC naval ship system.

(d) These specifications are required to be met in various aspects of the electric ship design.

2) Centralized Model Predictive Control of the MVDC Shipboard Power System

(a) A nonlinear MPC approach is proposed for the MVDC SPS under a battle condition.

i. An MPC controller is designed to efficiently manage stressful high power pulsed loads in the SPS.

- In a shipboard power system, war fighting loads, such as electromagnetic guns, are known as pulsed loads that draw very high short time current.

ii. A comparison is performed for different cases for MPC: no prediction, perfect prediction and ARIMA prediction with different delays for the MPC controller.

iii. An improvement factor is defined based on this comparison.

(b) Stability Analysis

i. Closed-loop stability analysis is considered in the MPC optimization problem by adding a terminal cost in the objective function and considering an additional terminal state inequality constraint.

(c) An MPC-based reconfiguration algorithm is presented for the MVDC system when load demand changes (a load power increment or decrement).

i. The loads are categorized as vital loads, semi-vital loads and non-vital loads based on the missions of the ship.

ii. The main goal is to maximize the power delivered to the loads with respect to power balance and generation limits.

3) A distributed control structure is developed for a nonlinear MVDC shipboard power system.

(a) Each subsystem is controlled by a local model predictive controller.

(b) In the coordinator level, an optimization problem is iteratively solved to update a Lagrange multiplier vector to have a global optimal solution.

(c) The control inputs can be either continuous or discrete by using two different optimization methods in the MPC controller.

4) Performance analysis is performed by comparing a centralized control and a distributed control on the global and partitioned models and considering different specifications in the MVDC system.

(a) Comparison between centralized and distributed control architectures.

(b) Comparison based on continuous control inputs and discretized control inputs with different optimization methods.

(c) Considering changes in the load demand or a pulse load event in the system when comparing centralized and distributed control architectures.

1.4 Dissertation Organization

Chapter 2 provides a full description of the considered MVDC shipboard power system model and the control problem formulation used in this research. It also presents a list of significant transient and steady-state specifications and requirements of the MVDC SPS with detailed explanations and formulations. In Chapter 3, first, the basics of a model predictive control approach and its formulations are given. Then, the chapter proposes a centralized nonlinear MPC to control an MVDC shipboard power system when dealing with a pulsed load event in the system. The closed-loop stability of the nonlinear MPC for an MVDC SPS system is also guaranteed. Lastly, Chapter 3 proposes a reconfiguration method based on an MPC approach for a nonlinear MVDC system. Chapter 4 proposes an appropriate distributed control structure for a nonlinear MVDC SPS to develop power management architecture. This chapter also provides the comparison results between centralized and distributed control methods on the global and partitioned MVDC models for both continuous and discrete control inputs to show the validity of the proposed distributed approach. Moreover, this chapter presents two case scenarios to demonstrate the performance of distributed control structure for the MVDC system with a pulsed load or load changes. Finally, Chapter 5 includes the conclusion remarks and possible future works of this research.

CHAPTER II

MVDC SHIPBOARD POWER SYSTEM MODEL FORMULATIONS AND ITS DESIGN SPECIFICATIONS

The Shipboard Power System (SPS) is known as an independent controlled small-scale electric network which provides energy to the propulsion system and service loads on a ship [47]. Due to the specific roles of warships and the nature of their duties, the SPS is more susceptible to unexpected disturbances and physical damages in comparison to conventional terrestrial power systems. In addition, since a large number of electric and mechanical components are tightly coupled in a small space, and there is no external support from a relatively stronger grid, SPS includes a range of unique properties including limited generation capacities, a close physical and electrical proximity, being prone to disturbances, and a high stiffness for containing a wide range of dynamics of different origins [43, 42]. All these characteristics show that, unlike terrestrial power grid, there are strong interactions between components of the SPS. Therefore, the normal operation of the system requires considering various design features and system specifications simultaneously and rigorously maintaining them under all operating scenarios to enhance the system stability, survivability, security, and economics.

Among different distribution configurations that are currently available for SPS, power-electronic based DC distribution is considered the trending technology for the next-generation U.S. Navy fleet design to replace the conventional AC-based distribution [44, 47]. The introduction of Medium-Voltage DC (MVDC) electrical distribution in ships brings out a broad range of advantages and improvements including [37, 24, 100]:

- No phase angle synchronization requirements between sources and loads,
- Facilitating the connection of different types of generators, storage systems and loads,
- Reducing fuel consumption due to the use of variable speed prime movers,
- Reducing the size and ratings of switchgears and cables, and no need for the large low-frequency transformers,
- Eliminating frequency constraints from the design of generators and, as a result, reducing their size and weight, and
- Better management of power flow and limiting fault currents in emergency conditions.

Although DC distribution offers the above advantages as well as valuable insights into the ship modernization, energy technology and service innovation, it also poses significant challenges regarding SPS design, analysis and application development. Especially with the ever-growing density of power electronic apparatus that operate on a wide range of frequencies and the intelligent technologies integrated into the existing ship's infrastructure to support the normal operation of these power electronic devices, the complexity and heterogeneity of the SPS is expected to increase. Reliable, efficient and secure operations of an

SPS would require a more sophisticated and systematically-developed set of specifications, regulations and requirements to facilitate planning, implementation, testing and validation of future SPS design and analysis activities.

This research mainly investigates the control problem of an MVDC shipboard power system. This chapter aims to provide necessary information on the model under consideration and its formulations for the rest of this dissertation. In this chapter, a comprehensive study of both steady-state and transient design specifications and performance criteria is performed for a DC-based shipboard power system, utilizing mathematical formulations to address necessary criteria of designing various aspects of a shipboard power system, including aspects related to control, protection, validation, testing, model-based management and optimization. Several important transient performance criteria are presented here such as system stability, voltage performance, power ramp rate and droop gain ramp rate specifications. Additionally, significant steady-state design specifications, such as quality of service, fuel efficiency, availability, and survivability, are reviewed. Moreover, this chapter presents the necessary operating constraints which need to be maintained within their own pre-defined range to ensure the safe operation of an SPS. Therefore, a careful consideration of design specifications and performance criteria for DC-based shipboard power system distribution is required to be met under different operational constraints to maintain a reliable, stable, economically efficient, and operational fleet. The applications of these specifications and their formulations in the distributed control architecture are also discussed. This chapter has been published in [117, 116, 118].

2.1 Medium-Voltage DC Shipboard Power System Model and Formulations

The general topology of a baseline system for a notional MVDC Next Generation Integrated Power System model is given in [6] and shown in Fig. 2.1. It consists of two Main Turbine Generators (MTGs), two Auxiliary Turbine Generators (ATGs), two electrically driven propellers with Variable Speed Drives (VSDs), four zonal service loads, one pulsed load device such as electromagnetic launch systems or free electron lasers, and an energy storage device. A ring-bus topology is chosen for the distribution system where buses running along the port and starboard sides of the ship are connected at the bow and stern. Details about the baseline model can be found in [6] or [112, 90].

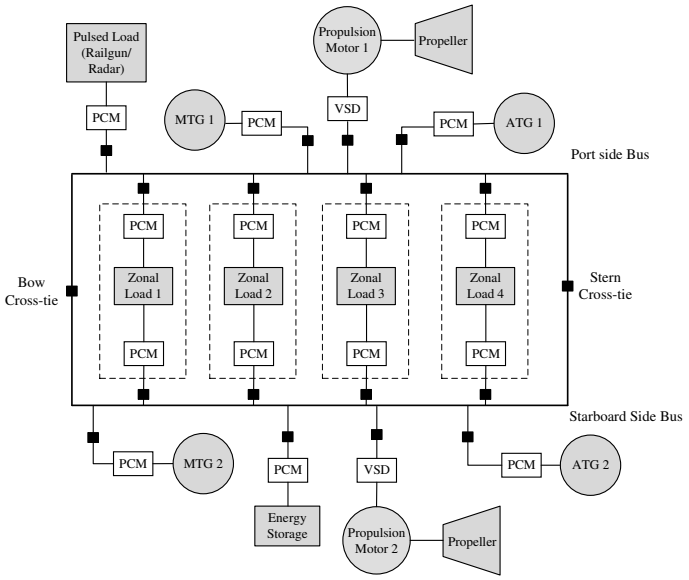

Figure 2.1: General Topology of the Baseline System for the MVDC SPS

The model used in this research is a nonlinear MVDC shipboard power system with 37 state variables which consists of one Main Turbine Generator (MTG), one Auxiliary Turbine

Generator (ATG), one electrical driven propeller with variable speed drives, four zonal service loads, one isolated pulsed load, and an energy storage device [112]. The distribution system has a ring-bus topology. All the modules are connected to the DC distribution bus by power electronics based Power Conversion Modules (PCMs) and DC disconnect switches. Fig. 2.2 demonstrates the general architecture of the considered MVDC system in this work.

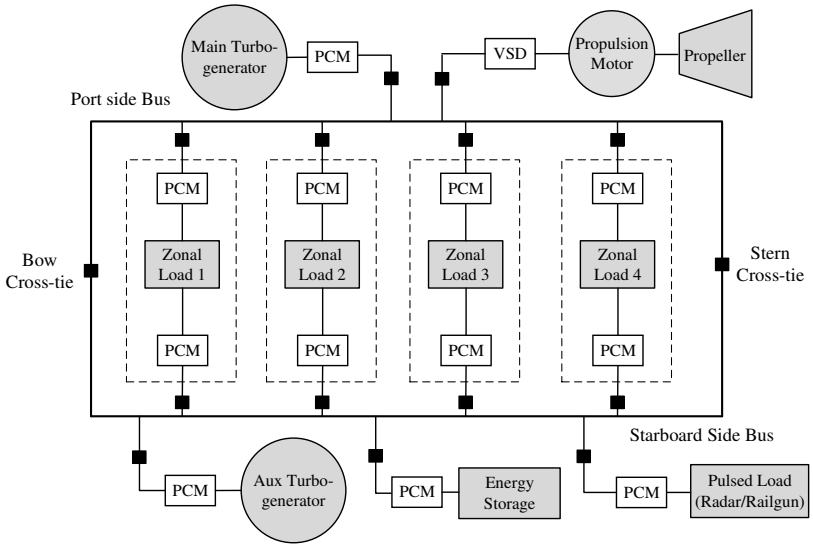

Figure 2.2: MVDC SPS Architecture used in this work

The general dynamics of a global nonlinear MVDC SPS model can be mathematically described by the following nonlinear differential-algebraic equation (DAE):

$$\begin{aligned} \dot{x}(t) &= f(x(t), u(t), t), \qquad x(0) = x_0 \\ 0 &= g(x(t), y(t)) \end{aligned} \tag{2.1}$$

where $x(t) \in \mathbb{R}^n$ is a vector of state variables included in dynamic components of the system such as gas turbines, synchronous machines and exciters. $u(t) \in U \subset \mathbb{R}^m$ denotes

the control inputs and $y(t)$ represents a vector of the algebraic state variables such as distribution network variables and other nonlinear algebraic state variables associated with on-board components where no derivatives are present. x_0 is a vector of initial values for the state variables.

The system described by equation (2.1) can be sampled and written in discrete time by sample time k, for the purpose of prediction and control, as:

$$\begin{aligned} x(k+1) &= f(x(k), u(k), k), \qquad x(0) = x_0 \\ 0 &= g(x(k), y(k)) \end{aligned} \tag{2.2}$$

Here, we use $x(t)$ and $x(k)$ to refer to the state variables of the continuous-time model and the discrete-time model, respectively. Under this definition, Table 2.1 shows a list of representative state variables of the MVDC SPS model used in this research. Table 2.2 provides a list of significant design parameters that will be used throughout this work to describe the design requirements. This model includes all of the required functional components in order to consider system specifications and performances criteria for the rest of this chapter. The full description and formulation of the considered model is included in the Appendix A. For further information and explanations about the MVDC model see [112].

2.2 Design Specifications and Requirements for the MVDC Shipboard Power System

Conventionally, the AC-based distribution system has been widely employed in SPS design during the past decade with relatively well-developed and documented standards and regulations such as MIL-STD-1399-300 [1] and MIL-STD-1399-680 [2] (for both

Table 2.1: A Short List of Important State Variables of the MVDC Model

Symbol	Description	Symbol	Description
v_{dc}	DC Bus voltage	v_s	Ship Speed
i_{gen1}	MTG current	ω_m	Rotor speed of propeller
i_{gen2}	ATG current	$\lambda_{rd}, \lambda_{rq}$	d-q axis flux linkage of IM rotor
i_{LC}	Induction motor (IM) current	λ_s	Stator flux linkage
ω_{r1}	Rotor speed of MTG	v_{fd}	Field winding excitation voltage
ω_{r2}	Rotor speed of ATG	v_{sc}	Super-capacitor voltage

low voltages below 1000 Volts and high voltages on or above 1000 Volts). Currently, there are very limited efforts made to address the lack of standardized design criteria and performance metrics for the DC-based distribution SPS research, especially for the latest Medium-Voltage DC SPS [4, 44]. In [4], general direction and design concepts are studied which include limited implementation details and practical design considerations. This section is intended to address this issue by preparing a survey of current related literature and providing a list of significant design specifications and requirements along with their specific formulations for the steady-state and transient analysis of the MVDC SPS. The presented specifications and criteria could generally be utilized as guidelines and references for the SPS research community.

Design specifications can be generally classified into two types: steady-state criteria and transient criteria. For the rest of this discussion, the term “steady-state” or “long-term performance” criteria mainly refer to specifications that impact ship planning, operational

Table 2.2: Applicable Design Parameters

Symbol	Description
v_{dc}^{ref}	Reference value of DC bus voltage
K_{droop}	Generator droop gain
$\omega_{m,ref}$	Desired propulsion rotor speed
P_{Gi}	Generated power of i^{th} generator
$P_{Gi,ref}$	Reference value for electrical power of i^{th} generator
$P_{IM,ref}$	The reference power of induction motor
I_r	Rated continuous current
T_k	Rated duration of short-time withstand current
I_{inrush}	Inrush current
$I_{SC,max}$	Maximum short-circuit current
$I_{inrush,max}$	Maximum inrush current
P_{Lj}	Real power of j^{th} load
P_{Gi}^{min}	Minimum generated power of i^{th} generator
P_{Gi}^{max}	Maximum generated power of i^{th} generator
V_{min}	Minimum bus voltage for tolerance limit
V_{max}	Maximum bus voltage for tolerance limit
$Rr_{i,max}$	Maximum ramp rate of the power of i^{th} generator
E_{min}	The minimum stored energy
E_{max}	The maximum stored energy

configuration and mission evaluations where only steady-state operating conditions are of interest, while the term "transient performance criteria" refers to specifications that provide the guidelines for real-time ship-wide operation and the requirements for monitoring, control, protection and load managements. As an example, a fuel consumption problem is one of the primary steady-state criteria for economic operation and mission scheduling. As the operational status of the ship varies under different missions, it is important to plan and schedule in advance based on the ship's configuration to determine the potential fuel consumption and optimize the fuel efficiency. On the other hand, system stability is typically connected with transient behavior. Relevant system states need to be continuously monitored and tuned by the control system to maintain the ship-wide stability when encountering system changes or disturbances.

In order to evaluate the performance of a system, both steady-state performance criteria and transient behavior of the power system should be considered in design specifications. Some aspects of the system behavior are targeted under transient performance analysis, whereas others are targeted in steady-state analysis. There are also some performance aspects that cover both transient and steady-state behaviors. It is important to note that design specification can take a form of a function of time that need to be minimized or maximized throughout a specified period of system operation. Typically, a function that reflects a "cost" is minimized while a function reflecting a system utilized is maximized. Alternatively, a specification can take the form of a set of constraints on the values of some of the system parameters and variables within a certain system's operational domain. In the

following, we discuss in detail these specifications as categorized into transient performance criteria and steady-state performance criteria.

2.2.1 Transient Performance Criteria

The transient response of a system mainly occurs after any significant changes in the system operating setting and conditions such as reconfiguration switching, battle damages or faults in the system. The following is a list of common specifications for SPS transient analysis:

- System Stability
- Voltage Performance:
  - Notional Bus Voltage
  - Voltage Tolerance
  - Voltage Ripple and Noise
- Power Ramp Rate:
  - Main Generators
  - Auxiliary Generators
  - Ship Propeller
- Droop Gain Ramp Rate
- Ship Propulsion Rotor Speed

- Ship Induction Motor (IM) Electrical Power
- Electrical Power of Generator
- Current Specifications
- Load Input Impedance

The above-mentioned transient specifications and their impacts on the ship design are discussed in detail in the following sections.

2.2.1.1 System Stability

A power system is stable if the effect of any perturbation caused by a disturbance diminishes over time within its operation, and the system returns to its original operating behavior. Confidence in system stability analysis is bounded by the model accuracy on which the analysis is based. Stability is generally coupled to other important system's behavioral properties, and essentially all system performance criteria depend on it as a pre-condition [97, 108, 109].

In the MVDC SPS, loads are usually fed via high-bandwidth power-electronic converters directly connected to the MVDC bus. Because the converters aim to maintain the load power at a constant level, they will present a constant power load (CPL) behavior even under fast variations of voltage and/or current. The CPLs are seen by the system as negative incremental resistances, which may yield voltage instability in the MVDC. The stability problems in DC systems are mostly related to higher-frequency dynamics, unlike the AC systems. Another major difference is that there is no need for phase angle synchronization

for torque angle stability of the generators. A more comparative stability discussion of different ship power system architectures (AC, DC and hybrid) is given in the ESRDC stability report [97]. This study shows that stability is a design consideration, so any of the power distribution architectures do not have an inherent advantage over the others for the stability purpose.

There are many approaches for the system stability, including external stability (input to state, input to output, small gain, etc), or internal stability. However, two of the most important approaches are through Lyapunov's theorems. The first method, or Lyapunov's direct method [72], involves the construction of a Lyapunov function which allows the magnitude of a perturbation that the system can tolerate at the operating point to be determined.

The second approach, called Lyapunov indirect method, or small signal method [11], analyses the system in the form of (2.2). The small signal stability is determined through linearization of the system and computing the eigenvalues of the state matrix of the linearized Average Value Model (AVM) of the system. However, this approach only guarantees local stability of the system; therefore, a large number of operating points are studied to build a confidence in the system's stability. The effects of 'large' pulse loads, as common in electric ships, may pose considerable challenges on the main assumptions in the small signal method, especially when dealing with a linearized model during or just after the operation of a very large pulse load [45]. Therefore, it will be necessary to develop and derive more sophisticated large-scale perturbation nonlinear stability techniques.

Another useful approach for the ship power DC distribution system is generalized immittance based stability analysis, developed by the ESRDC members [97, 99, 98]. This

is a frequency domain stability technique which accommodates several operating points and uncertainty in a single analysis. The principal characteristic of this approach is that a component impedance/admittance is expressed by a bounded set of values including all possible behaviors, not by a single value at a specific frequency. Another stability analysis for MVDC distribution systems on ships is presented in [91, 92] by using passivity-based stability criterion. This method uses an impedance measurement technique for the system bus to check whether the system is passive or not. Therefore, if this method guarantees the passivity of the bus impedance, the stability is also ensured. A comprehensive survey of different stability criteria for DC power distribution systems is given in [83].

2.2.1.2 Voltage Performance

2.2.1.2.1 Notional Bus Voltage

The system DC bus voltage is mainly determined by the propulsion motor voltage, desired generator voltage, load considerations, converter design, standard cable ratings, efficiency, and arc fault energy [4]. Note that power quality is represented by bus voltage deviation from the bus voltage reference. In the model used in this research, the preferred rated voltage is $5\ kV$. The following cost function represents the voltage specification:

$$Cost_{vol} = \sum_{k=1}^{N} \left(v_{dc}(k) - v_{dc}^{ref} \right)^2 \tag{2.3}$$

where $v_{dc}^{ref} = 5\ kVDC$ and $v_{dc}(k)$ represent the state variable defined in the mentioned model (2.2) at sample time k. N is the final time step. The objective of the controller is to minimize the above cost function in order to maintain the bus voltage close to the reference value.

2.2.1.2.2 Voltage Tolerance

The voltage tolerance is a constraint type specification that identifies the maximum allowable variation in the DC voltage measured at the output of a component. As specified in [4], the steady-state (continuous) DC voltage tolerances limits should be $\pm 10\%$. Accordingly, by assuming the reference DC voltage v_{dc}^{ref} as the base value, the following voltage tolerance constraint (in per unit) is typically used:

$$0.9 < v_{dc}(k) < 1.1 \tag{2.4}$$

2.2.1.2.3 Voltage Ripple and Noise

When DC is produced from an AC/DC rectifier, it is natural that the DC level varies directly based on the voltage on the AC side. This produces a varying voltage about the DC level, which corresponds to the ripple. If a pulse width modulated rectifier is used to produce the DC voltage, a high-frequency waveform resulting from pulse-width modulation (PWM) switching is superimposed on the DC and AC sides and is defined as noise. Noise can also come from the loads that are connected to the DC bus. The acceptable RMS value of voltage ripple and noise should not exceed 5% in per unit voltage [4].

2.2.1.3 Power Ramp Rate (PRR)

The health of the electric ship power system is adversely affected by high power loads, particularly, without the presence of the energy storage systems or stabilizing control methods. In case of large pulse-type loads, short-time power demand may significantly exceed the power rating of all the installed generators. The electrical power ramp rate for

the generators (MTGs and ATGs) and the ship propulsion motor should be considered as one of the specifications and requirements for the SPS to protect and extend the life cycle of the generators and the induction motor. The proposed cost functions for the power ramp rate of MTGs, ATGs, and propeller are described below.

2.2.1.3.1 Main Generator PRR

Since extreme power ramping has a negative impact on the life-span of gas turbine and generator, considering electrical power ramp rate of the main generator is one of the important design requirements. A proposed measure for the power ramp rate of MTG is as follows:

$$MTG_{PRR} = \sum_{k=1}^{N} \left(P_{MTG}(k) - P_{MTG}(k-1)\right)^2 \tag{2.5}$$

where P_{MTG} is MTG output power. The objective of the controller is to minimize the above cost function. In so far as this specification affects the life cycle of the generator in the long period time, it can be also considered as a steady-state specification.

2.2.1.3.2 Auxiliary Generator PRR

Electrical power ramp rate of the auxiliary generator is also considered as one of the important requirements to limit burden on the generation source and also limit the wear of the machine and increase its expected life. A proposed measure for the power ramp rate of ATG is as follows:

$$ATG_{PRR} = \sum_{k=1}^{N} \left(P_{ATG}(k) - P_{ATG}(k-1)\right)^2 \tag{2.6}$$

where P_{ATG} is ATG output power. The objective of the controller is to minimize the above cost function.

2.2.1.3.3 Ship Propeller Electrical PRR

Ship propeller electrical power ramp rate should be considered as one of the design requirements to protect and extend induction motor life cycle. Component wear is reduced by penalizing power ramp rate. A proposed measure for the power ramp rate of the ship propeller is as follows:

$$Prop_{PRR} = \sum_{k=1}^{N} \left(P_{IM}(k) - P_{IM}(k-1)\right)^2 \tag{2.7}$$

where P_{IM} is ship propeller electrical power. The objective of the controller is to minimize the above cost function.

2.2.1.4 Droop Gain Ramp Rate

The generator droop gain affects the DC bus voltage. Therefore, droop gain can be used as a control input to indirectly control the output power of primary sources of generation. It is used to determine the power share between energy sources. Droop gain ramp rate is one of the system specifications that should be met to support power quality. Meeting this specifications will also prevent large and sudden changes in demand. A proposed droop gain ramp rate measure can be defined as follows:

$$Droop_{rate} = \sum_{k=1}^{N} \left(K_{droop}(k) - K_{droop}(k-1)\right)^2 \tag{2.8}$$

The objective of the controller is to minimize the above cost function to guarantee power quality.

2.2.1.5 Ship Propulsion Rotor Speed (SPRS)

Ship propulsion rotor speed is another important specification for the SPS which should be maintained in the desired ship velocity. The specification of ship propulsion rotor speed is defined by the following function:

$$Cost_{SPRS} = \sum_{k=1}^{N} \left(\omega_m(k) - \omega_{m,ref}\right)^2 \tag{2.9}$$

where ω_m is propeller rotor speed and is defined as a state variable in the mentioned model. The objective of the controller is to minimize the above cost function to maintain the propeller rotor speed close to the desired value. There is also another performance requirement named "battle speed" which represents the maximum attained sustained speed in case of full engagement of weapons and sensors [27].

2.2.1.6 Ship IM Electrical Power

Load-following performance can be obtained by considering the tracking term of ship propeller electrical power as a specification to be met. A proposed structure is as follows:

$$Cost_{IM-power} = \sum_{k=1}^{N} \left(P_{IM}(k) - P_{IM,ref}\right)^2 \tag{2.10}$$

where P_{IM} is ship propeller electrical power. The objective of the controller is to minimize the above cost function. If there is any other important load, its power can be added in the cost function in the same way with tuning weighting factors which specify the priority of loads tracking in the controller.

2.2.1.7 Electrical Power of Generator

Fuel efficiency is considered in terms of deviation of generator from its optimal setting. Electrical power of the generator can be considered as one of the objectives in order to work at the most efficient point. It is assumed that an efficiency curve for a generator is known. The specification of electrical power of the generator is defined by the following function and the objective is to minimize the function.

$$Cost_{Gen-power} = \sum_{k=1}^{N} \left(P_{Gi}(k) - P_{Gi,ref}\right)^2 \tag{2.11}$$

$P_{Gi,ref}$ can be also defined as a control input in the system to manage the generator to operate at the most efficient point. In so far as this objective affects the fuel efficiency, it can be also considered as a long-term objective or steady-state specification.

2.2.1.8 Current Specifications

2.2.1.8.1 Rated Continuous Current (I_r)

The rated continuous current is the continuous current under specified conditions of use and behavior.

2.2.1.8.2 Rated Short-Time Withstand Current (I_k)

The rated short-time withstand current of the MVDC equipment should be more than or equal to the maximum expected short-circuit current [4]. Characteristics of the MVDC system define the short-circuit current and the short-time withstand current.

$$I_k \geq I_{SC,max} \tag{2.12}$$

where $I_{SC,max}$ is the maximum expected short-circuit current.

2.2.1.8.3 Rated Duration of Short-Time Withstand Current (T_k)

T_k is defined as the intervals of time for which the system can carry a current equal to its rated short-time withstand current. This criterion is determined by the time delays in the system protection coordination. For the MVDC systems with traditional switchgear, historic values of 0.5 s, 1 s, 2 s, and 3 s should be used. For the new designs with fast power electronics, rated duration values of 0.0001 s, 0.001 s, 0.01 s, 0.05 s, 0.1 s, and 0.2 s should be used according to [4].

2.2.1.8.4 Load Inrush Current (I_{inrush})

The connection of any load or power source must not cause excessive inrush current in the system. The connected load shall connect to the bus in a manner that minimizes the disturbance of the MVDC bus voltage. The amount of inrush current is determined by how the load is brought on to the MVDC bus [4]. The inrush current (I_{inrush}) needs to be designed for the system so that the capacity is not exceeded over the life of the ship.

$$I_{inrush} \leq I_{inrush,max} \tag{2.13}$$

where $I_{inrush,max}$ is defined as maximum acceptable inrush current.

2.2.1.8.5 Load and Source Current Ramp Rate During Disconnection

The load will ramp its current to a low value before disconnecting from the MVDC bus. The power source will ramp its supply current to a low value before disconnecting from the

MVDC bus [4]. The normal current ramp rate must not exceed the specified limit defined by a system designer.

2.2.1.8.6 Load Input Current Ramp Rate During Operation

A connected load cannot draw more power from the DC bus that is allowed by the load input current ramp rate. The system designer should establish the MVDC bus requirements to match the load current ramp rate specification [4].

2.2.1.8.7 Load or Source DC Ripple Current

Connected loads containing solid state power converters will draw mostly DC current from the MVDC bus. The amount of ripple current depends on the nature of the power conversion and the amount of internally provided filtering. The maximum tolerable amount of load ripple current should be specified by a system designer.

2.2.1.9 Load Input Impedance

Loads connected to the MVDC bus are predominately solid state power converters, which induce negative input impedance and can impact overall system stability. Input impedance data should be provided for the system design and analysis [4].

2.2.2 Steady-State/Long Term Performance Management

Steady-state performance mainly occurs when the system settles down on the operating points and the steady system continues working normally. The nature of a ship's mission will determine priority and importance of providing power to each load. Operational Conditions,

based on performance level of the different mission systems such as mobility, should be defined. For the systems in combat mode and other missions, the performance levels should be translated and quantified into electric load requirements, Quality of Service (QoS), Mean Time Between Service Interruption (MTBSI) and acceptable performance degradation in higher sea-states. For mobility specification, a speed profile should be specified at a given operationally significant sea-state. There are three different modes of operation as mission requirements: Surge to Theater, Economical Transit and Operational Presence [49].

Surge to Theater: This mode governs the allowed maximum number of refueling with only self-defense capability, knowing the ship is transiting at a given distance at maximum design speed of the corresponding sea state. It is assumed that refueling occurs when 50% of the whole fuel capacity is consumed. The ship should also arrive in theater with a tank not less than 50% full. The goal in this mode is to minimize the dependency on replenishment ships to arrive at a theater of operations, which must happen as fast as possible. A Surge to Theater Operational Condition should be defined to determine environmental conditions (sea-state and temperature), and also to enable a prediction of electrical load and quality of service requirements.

Economical Transit: Similar to the traditional Endurance Speed and Endurance Range, in this mode, when the ship is traveling at speed at least equal to the endurance level, it must be able to reach the endurance range. In this mode, all of the fuel capacity, minus tail pipe allowances, are permitted to be consumed. An Economical Transit Operational Condition needs to be defined to calculate fuel requirements.

Operational Presence: Operational presence specifies the minimum time that a ship, given a speed-time profile and mission system capability, should be capable of conducting one or more missions, such that at most 1/3 of the fuel capacity is consumed. In order to calculate fuel requirements, an Operational Presence should be defined and used.

In the following, some of the most important steady-state specifications are given:

- Quality of Service (QoS) Metrics
- Availability
- Fuel Minimization/Efficiency Metrics
- Component Efficiency
- Survivability
- Operability and Dependability

2.2.2.1 Quality of Service

Quality of Service (QoS) is the ability of the power system to reliably provide electrical power to loads with the required power continuity [50]. It is considered one of the most important performance criteria for a ship system design, especially shipboard power system design. For the purpose of this research, the review is based on IEEE 1662-2008 [3] and IEEE 1709-2010 [4]. From the load's perspective, QoS is measured by a Mean Time Between Service Interruption (MTBSI). Also, a failure is defined as any interruption of service or abnormal system status that prevents a mission system from following its mission. According to the definition of failure, all the interruptions in service will not result in a QoS

failure. QoS is known as one of the reliability metrics. Reliability is the measure of service continuity in equipment loads under normal operating conditions. Mean time between failures and mean time to repair for combinations of equipment are the major metrics for reliability [26]. In order to design a system to achieve a particular MTBSI, QoS does not account for survivability events such as battle damage, flooding, or fires. QoS does account for equipment failures, training and normal system operation transients [50].

As defined in [4], there are four categories of loads mainly based on the maximum tolerable duration of power interruption for each load. Two time constants, t_1 and t_2, are used to define the reference time scale for the loads. "t_1" represents "Reconfiguration Time" which is defined as the maximum time to reconfigure the distribution system without bringing online any additional generators. "t_2" represents the "Generator Start Time" which is defined as the time to start and bring online the slowest generator set in the power system. t_1 can be on the order of milliseconds, $0.01\ s \leq t_1 \leq 2\ s$. t_2 is on the order of minutes, $60\ s \leq t_2 \leq 300\ s$ [4, 50].

The four QoS categories for loads are defined as follows [50]:

- Uninterruptible Loads: Loads that cannot withstand a power interruption of duration t_1.
- Short-term Interrupt Loads: Loads that can withstand power interruptions of duration t_1 but cannot withstand power interruptions of duration t_2.
- Long-term Interrupt Loads: Loads that can withstand power interruptions of duration t_2.

- Exempt Loads: Loads that can also withstand power interruptions of duration t_2. It is common that only a portion of the propulsion load is assigned as Exempt Loads to prevent the installation of excess generation capacity as for IPS configurations, enough redundancy in generation is not available to assure the ship could achieve its maximum speed with any one generator out of service.

The numerical formulation and calculation of QoS metric can be found in [69, 111, 41, 51, 50]. To calculate QoS rating, a few elements need to be defined:

- The fraction of time that the ship will be in an operational mode i is represented by $f_{om}(i)$.

- Mission QoS model for each operational mode: This model returns 1 when QoS failure happens for a given set of power interruptions to one or more mission loads and returns 0 otherwise. This model is denoted as $q_{om}(i, pi(k))$ where i is the operational mode and $pi(k)$ is a vector of power interruptions for the k^{th} mission load.

- The concept of operation for the ship which determines which power components are online and in what configuration for each operational mode: $p_{om}(i, j)$ gives the fraction of time that power component j in operational mode i is online.

- Power system fault effects, determined for each failure of a power system element j, are defined by a vector of power interruptions for each of the k mission loads, represented by $pi(j, k)$.

- Component reliability model $r(j)$ that provides Mean Time Between Failure (MTBF) for each power system component j where time is measured if the component is on.

Then, the fraction of time that a QoS failure will happen due to the power system faults of component j is given by:

$$f_{qos} = \sum_{i=1}^{n} f_{om}(i) p_{om}(i,j) q_{om}(i, pi(j,k)) \tag{2.14}$$

where n is the total number of operational modes. The fraction of time that the component j is on is given by:

$$f(j) = \sum_{i=1}^{n} f_{om}(i) p_{om}(i,j) \tag{2.15}$$

Now the MTBF of component j based on real-world time is given by:

$$r_c(j) = \frac{r(j)}{f(j)} \tag{2.16}$$

The QoS failure rate $QoS(j)$ of power system component j is represented by:

$$QoS(j) = \frac{r_c(j)}{f_{qos}(j)} \tag{2.17}$$

Therefore, the total QoS of the system due to all system component failures can be derived as:

$$QoS = \sum_{j=1}^{m} \frac{r_c(j)}{f_{qos}(j)} \tag{2.18}$$

where m is the total number of power system components. With this definition, QoS is now represented in terms of three factors, namely meantime-between-failure (MTBF) values of power components, mission duration and power interruption events.

2.2.2.2 Availability

Availability is the probability that the system will be able to deliver the proper service or perform its mission profile when needed at an arbitrary point in time. Availability is mainly affected by how often failures happen or maintenance is needed (reliability), and how quickly corrective maintenance can be performed (maintainability). Therefore, it is a function of how often a system is unusable and how much time it takes to restore it [103, 21].

There are many factors that specify the level of availability. The basic factors that define availability can be categorized as failures, maintenance and resources. Accordingly, two measures of availability are determined as follows based on [103]: inherent availability and operational availability.

2.2.2.2.1 Inherent Availability

In this category, only the impact of design on availability is considered. The steady state equation for inherent availability can be expressed as:

$$A_i = \frac{MTBF}{MTBF + MTTR} \tag{2.19}$$

where MTBF is mean time between failures and MTTR represents the mean time to repair which is a function of maintainability [103].

2.2.2.2.2 Operational Availability

In this category, the impacts of design and the support system on availability are being considered. The steady state equation for operational availability can be expressed as:

$$A_o = \frac{MTBM}{MTBM + MDT} \tag{2.20}$$

where MTBM is the mean time between maintenance and MDT represents the mean downtime [103]. Availability is calculated based on uptime and downtime. Uptime is the time when the system was able to perform all the required services during a specified calendar interval. The Total Time represents the time when the system was supposed to be up during a specified calendar interval. The operational availability can be also expressed based on Uptime and Total Time [103] as follows:

$$A_o = \frac{Uptime}{Total\ \ Time} \tag{2.21}$$

More information and explanations about the impacts of reliability and maintainability metrics on operational availability are given in [103] in detail.

2.2.2.3 Fuel Efficiency

The fuel optimization problem is naturally a static optimization problem since fuel cost savings would be meaningful when considered over a long period of operation. Fuel consumption metric has a significant role when it causes the reduction of operation cost and subsequently preserving fuel for emergency mission conditions. There are two main representations for the fuel consumption function.

Generally, the generator fuel consumption function is decreasing with increasing produced power. Fuel consumption mainly depends on the power sharing between the generators and the total generated power [65]. The fuel consumption-produced power curves of different generators are shown in [65, 13]. The first method to formulate fuel cost function is presented in [69] and [13], where the curves are sufficiently approximated by second-order polynomials:

$$SFC_i(P_i) = a_i P_i^2 + b_i P_i + c_i \tag{2.22}$$

where SFC_i is the Specific Fuel Consumption (SFC) representing hourly consumption per unit of power, P_i is the power produced by the i^{th} generator. a_i, b_i and c_i are the coefficients of second order polynomial function based on each generator's fuel consumption-produced power curve [65, 13]. Moreover, due to additional fuel consumption and life cost of the prime mover during start-up, a fixed amount of fuel $C_{startup}$ can be considered for each start-up. Also, we can consider generator start/stop constraint due to resulting increased fuel consumption and maintenance cost. It can be formulated as a constraint as follows:

$$t_k - t_{i,s} \geq T_{i,min} \tag{2.23}$$

where t_k is the examined time instant, $t_{i,s}$ is the time instant at which the i^{th} generator lastly started or stopped operating and $T_{i,min}$ is the minimum permissible period of the i^{th} generator's start/stop. In order to obtain fuel cost minimization [65], we have:

$$Fuel_{cost} = \sum_i Cost_i \cdot P^*_{i,t_k} \cdot SFC_i(P^*_{i,t_k}) \tag{2.24}$$

where $Cost_i$ is the cost of the consumed fuel by the i^{th} generator. P^*_{i,t_k} is the dispatched power to the i^{th} generator (in p.u.) at $t = t_k$. $SFC_i(P^*_{i,t_k})$ is the specific fuel consumption defined in (2.22).

The second general formulation of fuel cost function is as follows [40, 107]:

$$\zeta_i(P_i) = \zeta_{i,0} + \frac{\zeta_{i,2} - \zeta_{i,0}}{1 - e^{-m_i}} \left(1 - e^{\frac{P_i - P_{i,min}}{P_{i,max} - P_{i,min}}}\right) \tag{2.25}$$

where $\zeta_i(P_i)$ represents the specific fuel consumption for the i^{th} generator. $P_{i,min}$ and $P_{i,max}$ are the minimum and the maximum generation capacity of the i^{th} generator, respectively. m_i is the exponential parameter. $\zeta_{i,0}$ represents the specific fuel consumption at the lowest power setting, and $\zeta_{i,2}$ represents the final specific fuel consumption at rated power. ζ_0, ζ_2 and m are determined as functions of the maximum power rating of the turbine. The exponential parameter m must be determined by minimizing the following index:

$$\Upsilon = \sqrt{\sum_{k=1}^{n} \left(\zeta(P_k) - \zeta_{data,k}\right)^2} \tag{2.26}$$

A task that can be accomplished by solving:

$$\frac{\partial \Upsilon}{\partial m} = 0 \tag{2.27}$$

This nonlinear least squares problem is determined numerically, and the results for various turbines are given in [40]. The information on different turbines was obtained from the handbook of each gas turbine. So, the SFC function is different for each generator (MTGs and ATGs), represented by the mentioned equations and SFC-generated power curves. The specific fuel consumption for seven different turbines using this approach and the values of ζ_0, ζ_2 and m for seven turbines are given in [40]. Also, the specific fuel consumption of two

gas-turbine generators is given in [12] which indicates that a generator SFC decreases as the percent of rated load increases.

2.2.2.4 Component Efficiency

In order to meet economic constraints associated with the particular mission of the SPS, MVDC power systems are expected to be efficient. The system efficiency should be calculated for the range of operating conditions and missions. The efficiency calculations of the MVDC system may include different components of a ship such as generators, converters, storage devices, transformers and cables. It is worth mentioning that the main part of total losses is caused by converter losses, so special consideration should be given through reducing the losses in their design, selection and application. Thus, to develop the overall system efficiency, the specific component efficiencies are required. As an example, the propeller efficiency can be defined as follows [63]:

$$E_{prop} = \left| \frac{J_e.K_T}{2\pi.K_Q} \right| \tag{2.28}$$

where torque coefficient (K_T) and thrust coefficient (K_Q) are both the functions of advance coefficient (J_e):

$$J_e = \frac{v_s}{N_r.D_{prop}} \tag{2.29}$$

where v_s is velocity of the ship, N_r is the shaft rotational speed and D_{prop} is the propeller diameter. Therefore, propeller efficiency significantly depends on torque coefficient, thrust coefficient, propeller diameter, shaft rotational speed and velocity of the ship [63]. In many applications, component efficiency should be calculated at the following load points: 10%, 25%, 50%, 75%, 90% and 100% based on a 1.0 per unit voltage in each case [4].

2.2.2.5 Survivability

Survivability is defined as the capability of a system to deliver power in spite of multiple simultaneous faults caused by hostile or natural disruptions. The survivability of the shipboard power system is critical to the mission of a ship, especially under battle conditions. Survivability is related to the continuation of the generation and distribution of power from the power sources to the loads. Under conditions where the power system cannot serve all loads - due to damage, equipment failure or unavailable parts of the SPS due to attack - emergency control actions should be taken for the ship to survive. In general, the survivability response is shedding the appropriate loads in the order of their priorities. Survivability also entails restoring power to the shed loads if there is sufficient capacity and connectivity, and if the load can be re-energized with minimal safety risk [4].

Survivability for ship designs will likely be defined by two measures: Design Threats and Design Threat Outcomes. A Design Threat is a threat to the ship where a Design Threat Outcome has been defined. The design threat outcome is a metric for total ship survivability and is defined as the acceptable performance of the ship in terms of the aggregate of susceptibility, vulnerability and recoverability when exposed to a design threat [51]. Design Threat Outcome definitions could include the following statements [41]:

- Ship will likely be lost.
- Ship will likely remain afloat and not be able to accomplish one or more primary missions for a period of time exceeding one day.

- Ship will likely remain afloat and be able to accomplish all of its primary missions following restoration efforts not more than two hours using only organic assets.
- Ship will likely remain afloat and would likely be able to accomplish all of its primary missions without interruption.
- The threat weapon is not considered an important threat because the probability that the threat weapon would have been defeated before striking the ship is greater than 98%.

Note that the term "likely" should be defined as a particular probability of occurrence. An appropriate choice would be to define "likely" as a probability of occurrence more than 86% [41].

So the three principal disciplines of survivability are susceptibility (avoiding being hit), vulnerability (withstanding a casualty) and recoverability (recovering from damage) [31], which are explained in brief here.

Susceptibility: A measure of the capability of the ship, the crew and the mission critical systems, to avoid and/or defeat an attack. This is a function of operational tactics, countermeasures, signature reduction and self-defense system effectiveness.

Vulnerability: A measure of the capability of the ship, the crew and mission critical systems, to tolerate the initial damage effects of conventional, CBR, or asymmetric threat weapons, or accidents, to carry on performing assigned primary warfare missions, and to protect the crew from serious injury or death.

Recoverability: A measure of the capability of the ship and the crew after initial damage effects, regardless of the cause, to take emergency actions to contain and control damages, minimize personnel casualties, prevent loss of a damaged ship, and restore and maintain primary mission capabilities.

One way to evaluate survivability P_S for different control approaches is represented by the following equation [86]:

$$P_S = 1 - (P_X.P_V).(1 - P_R) \tag{2.30}$$

where P_X, P_V and P_R are susceptibility, vulnerability and recoverability probabilities, respectively. A control action should be chosen when P_S is maximized as a metric.

Another survivability index of a shipboard power system refers to the power supply range and energy which a power system can provide after an attack or natural fault. This index demonstrates the percentage of the load nodes that can be connected to the power supplies after an attack which is defined as follows [61]:

$$P_s = \frac{\sum_{i=1}^{m} E_i}{M} \times 100\% \tag{2.31}$$

where M is the total number of nodes in the grid, m is the number of supply area and E is the number of nodes that can be connected to the power sources.

A twofold survivability metric is also presented in [28, 29] to measure two separated issues. In the case of damage, in the first metric, the maximum value of all loads that can be serviced is calculated by considering their priorities to show an overall production/distribution ability. The overall survivability score is the sum of the weighting of the load times the amount of power provided to that load. In the second metric, an indication

of the severity of the effect of lost loads is calculated by determining the highest priority load that cannot be serviced while satisfying all higher priority loads. The survivability tier score represents the highest priority load that is not fully satisfied. This survivability metric can be measured for one or several blasts (faults). For multiple blasts, these two scores are averaged over a number of blasts [29]. A comparative study between a ring bus topology and a breaker-and-a-half topology is investigated in [29].The effects of topology on weight, volume, fuel usage (efficiency) and survivability of an electrical distribution system is considered further. In this study, the total weight and volume of the system include weights and volumes of the electrical distribution system including generators, gas turbines, converters, and main bus cabling. Based on this comparative analysis, the ring bus is heavier and larger, but it is more survivable. Fuel efficiency is the same in both topologies [29]. In another study [38], different possibilities for MVDC architectures are assessed from a fault performance perspective by investigating survivability, size and weight. During fault events, each of the MVDC architectures is evaluated based on five system design criteria: reliability, speed, performance, economics and simplicity. According to this study, the breaker-less topologies are less survivable. Moreover, survivability of the system is achieved at a price of high size and weight [38]. Thus, naval architecture considerations (e.g. stability, survivability and space) and ship missions determine physical size constraints. For example, large power demand requires a major design consideration on the physical size of power generation and system equipment. For warships, a greater fraction of generated power is dedicated to combat systems [68]. One crucial objective in the development of the smart ship systems design (S3D) environment is to enable estimating the size and weight

requirements for different devices of a naval vessel with respect to factors such as rated power, bus voltage and system mass [94].

Energy Storage Modules: When there exists sufficient flexibility between prime movers and there is no pulsed load available, an energy storage module is not necessary for the system to guarantee survivability or quality of service [48]. In the shipboard power system, weaponry loads including electromagnetic launch systems, electromagnetic guns and free electron lasers are known as high power pulsed loads. These loads draw very high short-time current from the system which can drop the voltage in the whole microgrid and drift the frequency for a short period of time. In such situations, due to the size and weight constraints, it is infeasible to add more conventional generators to support the system for high power loads. Therefore, an Energy Storage Module (ESM) needs to be incorporated into the system to compensate power peaks. The application of an ESM is not just limited to support high power loads and can be also used in other certain design situations to improve power quality by providing backup power for uninterruptible and short-term interruptible loads [48, 80]. Thus, using energy storage modules may prove economical by reducing fuel consumption, improve power quality and reduce the total cost. For the U.S. Navy combatants, an ESM is mainly used to enhance survivability and enable high power pulsed loads [64]. For supporting pulsed loads, the existing generators must be oversized without using an ESM, which is a problem considering weight and size constraints. Another benefit of ESMs is their important role in the Ship Energy Efficiency Management Plan (SEEMP). The presence of ESMs significantly improves the flexibility of SEEMP by breaking the

conventional dependency between demand side and generation side for the stability purpose. By using the ESMs, the excess energy does not need to be dissipated through dumping resistors for the stability of the power system and can be partially or fully stored in the ESMs, thus decreasing, the total cost [64]. Moreover, energy storage systems may be used to restart a dark ship system. A dark ship condition is when there are no online generators, but energy storage modules are available for startup and control system [46].

Three important parameters for comparing energy storage systems are capacity, rate and cycle. Capacity represents the total amount of energy (J) that can be stored in the energy storage system. Transfer rate determines how fast that energy can be transferred (energy per time). The cycle represents the reversible process of charging and discharging the ESM. The ESM's cycle life is determined by the number of times an ESM can be charged and discharged [68]. Energy storage modules can include different technologies such as batteries, flywheels and ultra-capacitors [68, 52, 67]. Based on the specific application, the power rating and energy capacity of an energy storage system fall into the following categories [48]:

- Low Power ($\sim 250kW$): Provide backup power to uninterruptible loads for 2 to 10 s. In this case, energy storage modules need to be distributed.

- Medium Power ($\sim 500kW$): Provide backup power for uninterruptible and short-term interruptible loads for 5 to 10 min. In this case, energy storage modules can be either centralized or distributed.

- Low Power ($\sim 250kW$): Provide emergency starting for power generation modules in a dark ship condition for 15 to 30 min.

- High Power ($\sim 30MW$): Provide load leveling for pulse power loads for seconds.

- High Power ($\sim 30MW$): Provide standby power for pulse power loads for 5 min.

For the short term applications (1 s - 1 min), the flywheel can be used as a reliable energy storage solution. The flywheel also has the capability to work under a wide range of temperatures which makes it feasible to be utilized in a harsh environment like shipboard power systems. On the other hand, ultra-capacitor has the capability to provide very high power density with low losses. Batteries as a mature technology are also known as a convincing and effective energy storage solution due to their reliable performance and long history in the market [52]. A hybrid combination of aforementioned energy storage technologies and its advantages along with a study on optimal combination/sizing of the system are provided in [52]. This study shows that the combination of flywheel and battery yields better performance over the other combinations. Although the combination of the three above-mentioned elements achieves similar performance to the combination of flywheel and battery, this solution is not a preferred option because of weight and size limitation in the shipboard power system environment [52]. For design and operation of a battery energy storage system, [66] presents a battery capacity decision procedure according to the specific fuel consumption of generators. It is shown in [66] that an onboard battery ESM can be considered as a practical solution to increase fuel efficiency, reliability and the quality of power.

2.2.2.6 Operability and Dependability

Operability is a metric which quantifies the performance of SPS during a specific scenario or event. Operability determines the contribution of the performance of SPS to the mission effectiveness in that given scenario. Suppose that there is a load i in total loads I. $o_i(t)$ is defined as the operation status of load i at time t. Generally, it is a binary function which takes 1 when load i is operating and 0 when load i is not operating. However, for some cases, it can also get partial operation like $o_i(t) = 0.7$. In addition, $w_i(\theta, t)$ is a time-varying weight function which specifies the importance of load i for the specific event $\theta \in E$. E indicates a set of all possible events. A more detailed explanation about weight functions is given in [34, 35]. The operability metric is calculated as follows [35]:

$$O(\theta) = \frac{\int_{t_0}^{t_f} \sum_{i=1}^{I} w_i(t,\theta) o_i^*(t) o_i(t) dt}{\int_{t_0}^{t_f} \sum_{i=1}^{I} w_i(t,\theta) o_i^*(t) dt} \tag{2.32}$$

where $o_i^*(t)$ denotes the commanded operation status of load i which takes value in $[0, 1]$. t_0 and t_f represent the time when the specific event happens and when it ends, respectively. The operability metric $O(\theta)$ also takes value in the range $[0, 1]$.

Since the system should work well over a wide range of threat scenarios, another important metric named dependability is defined as an extension of operability metric. Unlike operability that only considers one particular event, the dependability metric works with the entire set of possible events E to obtain a balanced design. Two concepts are defined: average system dependability and minimum system dependability. Average system dependability is the mean operability over a set of considered events, and minimum system

dependability is the worst case of operability over a set of considered events. Let the probability density function $f_\theta : E \to [0, \infty)$:

$$\int_E f_\theta(\theta) d\theta = 1 \tag{2.33}$$

Then, the average system dependability ($\bar{D}_s$) is formulated as [35]:

$$\bar{D}_s = \int_E O(\theta) f_\theta(\theta) d\theta \tag{2.34}$$

and the minimum system dependability ($D_{s,min}$) is formulated as [35]:

$$D_{s,min} = \min_{\theta \in E} O(\theta). \tag{2.35}$$

Therefore, the operability and dependability metrics specify to what degree the system can withstand different particular events and measure the performance of SPS by the continuity of service to the system loads with regard to a hostile disruption. Both of these metrics are used when we want to evaluate the ability of a ship to follow its mission.

2.2.3 Constraints and Operating Regions

Since all system variables, including states and control inputs, are required to stay within their own pre-specified operation range to guarantee safe operation of SPS, the system constraints need to be defined to represent hardware limitations as well as operational requirements. Here, some of the most important system's constraints and operating conditions are described briefly:

- Power generation limits: There are limitations on the power values of the main generators as well as the auxiliary generators.

- Low load constraint P_{Gi}^{min} (known as a technical minimum): To avoid possible damage and decrease the maintenance costs, the generated power should not be lower than a known value. This level is defined by the manufacturer.
- High loading constraint P_{Gi}^{max}: The generator power should not go above a certain level for longer than a specified time interval since the mechanical and thermal losses will increase and blackout prevention capability is limited.

Therefore, the following operating conditions need to be considered for the generators (MTGs and ATGs):

$$P_{Gi}^{min} \leq P_{Gi} \leq P_{Gi}^{max},\ i = 1, ..., NG \tag{2.36}$$

where P_{Gi} represents the output power of i^{th} generator and NG is the total number of generators in the system.

- Power balance conditions: The following constraints guarantee that the generated power is balanced by consumption:

$$\sum_{i=1}^{NG} P_{Gi} \geq \sum_{j=1}^{n} P_{Lj} \tag{2.37}$$

where n is the number of loads and NG is the total number of generators in the system. P_{Lj} represents the power consumption of j^{th} load.

- There are also operational limitations on the power values of the ship propulsion motors.

- Generator droop gain takes its values in an interval.

- Bus voltage tolerances limits:

$$V_{min} < v_{dc}(k) < V_{max} \tag{2.38}$$

- Ramp rate constraint: A high change rate in the generator loading must be avoided to eliminate any mechanical stress and/or damages [65].

$$\frac{|P_{Gi}(k) - P_{Gi}(k-1)|}{t_k - t_{k-1}} \leq Rr_{i,max} \tag{2.39}$$

where $Rr_{i,max}$ represents the maximum rate of change of the produced power by the i^{th} generator, t_k refers to the current examined time instant and t_{k-1} is the previous examined time instant. The value of $t_k - t_{k-1}$ should meet the acceptable sampling time range to accurately sample the system.

- Blackout prevention constraint: It specifies the maximum allowed continuous loading of the generators where the system is blackout-proof.

- Energy Storage (ES) constraints: Energy storage devices are sometimes used in the system to make sure there is a balance between power sources and load demand, especially when the pulse loads are in operation. The minimum stored (or storage) energy, denoted as E_{min}, is defined by reserved adequacy and reliability criteria. On the other hand, the maximum stored energy, or E_{max}, is set by considering technical specifications. The ES energy, or simply E_S, should also comply to the following specifications and requirements at the end of each time interval [102].

$$E_{min} \leq E_S \leq E_{max} \tag{2.40}$$

- Generator start/stop condition: Frequent start/stop of the generators will increase fuel consumption and maintenance cost.

In Fig. 2.3, a better description for some of the required operating constraints along with their relationship to system performance is illustrated.

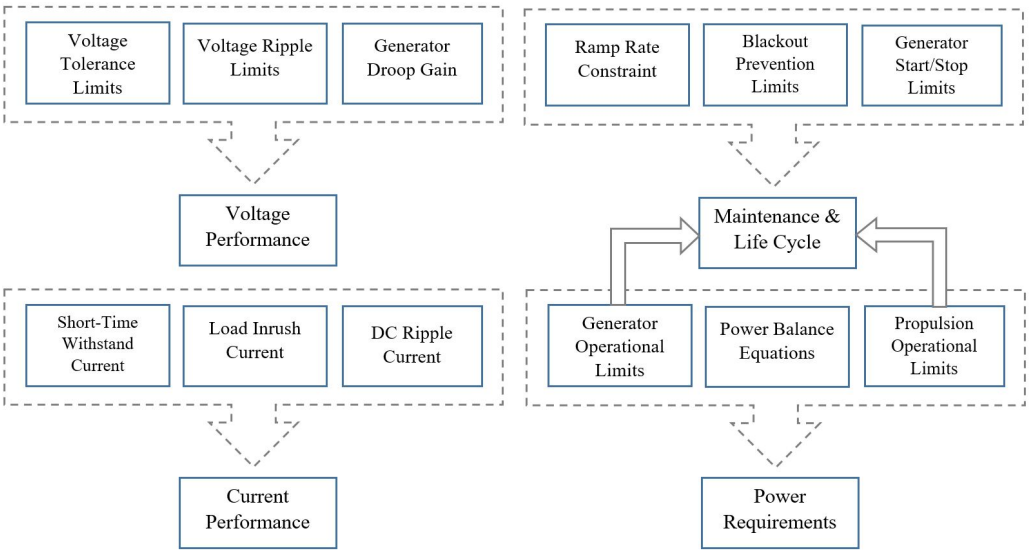

Figure 2.3: Summary of required constraints and their relationship to system performance

2.2.4 System Specification in a Distributed Control Setting

Design specifications and requirements of the MVDC SPS can be decomposed to be formulated in a distributed manner. The aim of this section is to express the importance of specifications' properties and also how to deal with their priorities in a distributed manner to follow a ship's mission. There are few research works in this field that deal with formulating specifications as the objective functions in distributed control for the SPS [16, 55, 8]. In the distributed control architecture, the centralized control problem is

partitioned into several smaller local control modules which compute their own optimization problems in the separate processors and exchange data efficiently to achieve a closed-loop objective [101]. In this case, the communication network can be part of the control design in the optimization problem. The resulted distributed control structure brings out several significant advantages including a higher robustness and good error tolerance characteristics, higher system flexibility and less computational complexity as well as a good overall system performance [10]. Reliability and maintainability could also be improved when compared with the centralized controller.

In a distributed control structure, in addition to considering the local specifications, constraints and stability criteria for each subsystem, there is also a convergence stability specification and a coupling constraint for the coordinator. All of these specifications and constraints should be met to achieve a closed-loop stability. Therefore, a convergence study should be considered in the distributed control. The centralized and distributed architectures are shown in Fig. 2.4. The local optimization problem is solved based on its own local state variables x_i, coordination parameters and the latest interaction variables z obtained from other subsystems with respect to subsystem's states and inputs constraints. The coordination vector is $[\lambda_i^T \ z_i^T]^T$ for $i = 1, 2, \ldots, M$. Various algorithms exist for updating coordination parameters with different convergence rate [20, 57, 39]. The maximum coordination error tolerance value ϵ is defined as a stopping criterion, which, preferably, needs to be close to zero to achieve an optimal solution.

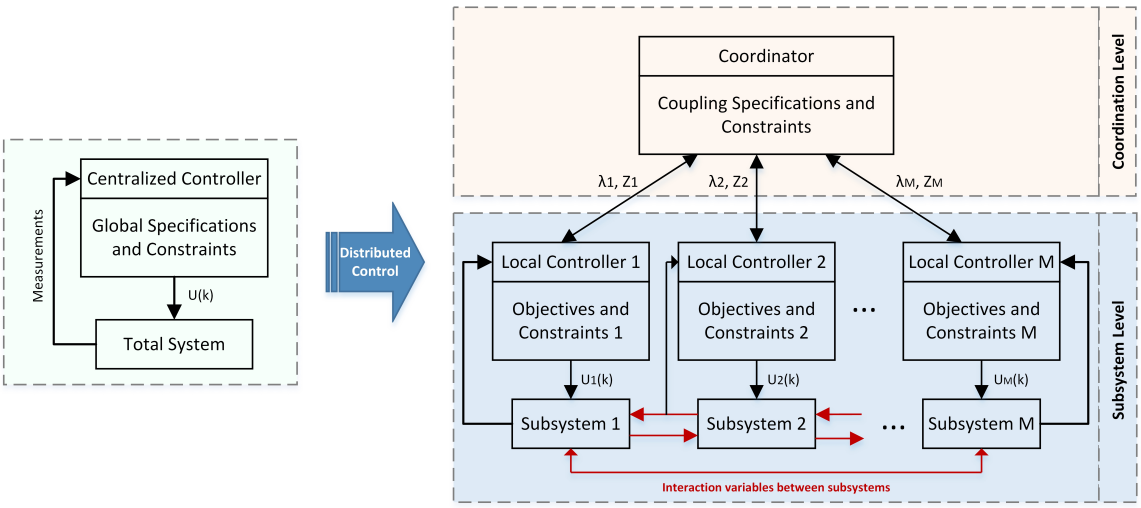

Figure 2.4: Centralized and Distributed Control Specifications Scheme

2.2.5 Applications

As previously discussed, the transient and steady-state system specifications and performance metrics reviewed and summarized in this chapter can be directly applicable to different aspects of shipboard power system design including control, simulation, verification, testing, protection and optimization. In Fig. 2.5, a general overview of presented specifications and performance criteria is illustrated for better description and understanding. In the following discussion, four representative examples are presented that show how the discussed specifications, both in the time frame of transient and steady-state, can play an important role in the existing and future electric ship power system design and analysis practices.

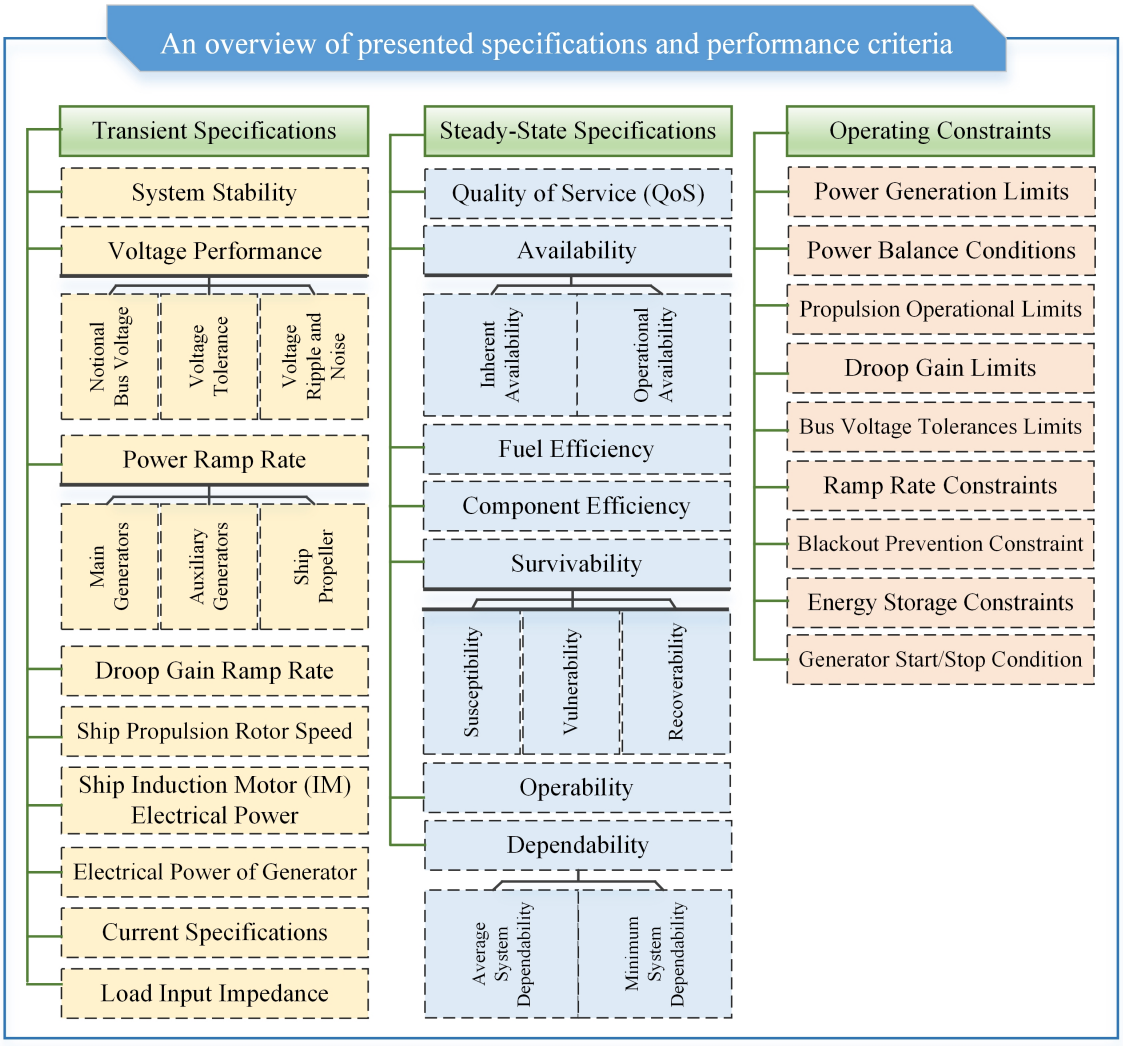

Figure 2.5: An Overview of Presented Specifications and Performance Criteria

2.2.5.1 Set-Based Design Methodology

It is necessary to seek a design solution which satisfies multi-objective performances simultaneously. Since the traditional point-based design method is highly iterative, it can be inefficient in multidisciplinary design optimization problems [58, 110]. Set-Based Design (SBD) is a complex design methodology which offers improvements over the point-based design method. It allows more of the design effort to proceed concurrently, deferring detailed specifications until tradeoffs are more fully understood [93]. The set-based design is anticipated to have the greatest benefit to the Navy ship design. The basic concept of set-based design is to use sets of values for the design variables, instead of points [58]. There are four main features for the set-based design outlined in [93]:

1. defining broad sets of design parameters,

2. delay narrowing the sets to have more tradeoff information available when making decisions,

3. narrowing the sets gradually until an optimum solution is revealed and

4. increasing the level of detail or design fidelity as the sets narrow.

In the set-based design methodology, delaying decisions and working with sets imply that decisions are better informed and uncertainty is better handled during the ship design process [58]. To have a better understanding of a set-based design method, a general multidisciplinary optimization problem is defined as follows:

$$\min_{z \in \chi} f_i(z), \qquad i = 1, 2, ..., p \tag{2.41}$$

subject to

$$g_i(z) \leq 0$$

where (2.41) denotes a multidisciplinary problem which includes p disciplines. Each discipline has one objective function, denoted by $f_i(z)$ for $i = 1, 2, ..., p$, that depends on the values of design variables z. The goal of the optimization algorithm is to minimize objective function (2.41) with respect to constraints on design variables. As mentioned before, one of the features of SBD method is to describe design parameters by sets which change while the design progresses. Accordingly, the allowable ranges of design variables can be described as the set of values between the upper bound z_{UB} and lower bound z_{LB}:

$$z_i \in [z_{LB}, z_{UB}], \qquad i = 1, ..., l.$$

The design space, denoted by χ, is defined by the bounds on the design variables. In the SBD method, the bounds on the design variables change during the optimization. A comprehensive design guideline on applying four SBD principles along with mathematical statements are presented in [58] for a ship multidisciplinary design optimization application. The system objective function for a ship design problem is composed of a sum of terms that represents a multi-objective problem. Therefore, the presented specifications, cost functions and operating constraints provided in this chapter can be easily taken into the account in defining design criteria and requirements for such set-based design methodology for the multi-objective design practices.

2.2.5.2 Model-based Power Management System (PMS) Design

For quite a long time, the on-board ship power/energy control and management relied heavily on rule-based control strategy and the experience of trained operators. However, going forward, the development of a more intelligent PMS becomes an immediate requirement to ensure secure, efficient and reliable ship design and operation. A model-based ship-wide operation management system that coordinates dynamic interactions of on-board components and manages real-time power system operations is envisioned to provide improved reliability, power quality and system economy over a wide range of operating scenarios [82, 89, 115]. More specifically, as pointed out in [9, 87], there exists several layers of control loops from high-speed power electronic controllers, to ship-wide operation management such as reconfiguration, load management, fault isolation and self-restoration, to steady-state based economical dispatch. The overall design of such management solutions need to take into consideration a series of different design criteria for the future PMS system. Therefore, the proposed specifications provided in this chapter become a natural aid for such operation management design practices - it provides proper references and guidelines for operation and optimization functions within the time scale of interest.

2.2.5.3 Dynamic Security Assessment

Real-time security assessment, among other dynamic monitoring and analysis, has always been a critical part of ship operation as it monitors the operating status of the ship, accurately evaluates the security margin and helps the operators identify violations that may jeopardize the integrity of the system and take steps to reduce the risk of system

instability [74, 81]. The development of dynamic security assessment tools requires clear identifications of transient security limits/region of specified operating conditions under a list of selected contingencies [33]. Criteria provided in this chapter would be a proper fit for this design purpose as it provides comprehensive details of system transient characteristics that need to be kept track of in real-time.

2.2.5.4 Mission Definition and Analysis

One of the arguably most impactful design practices in early-stage ship design is the mission-level analysis and evaluation. A mission involves a set of functions which define basic operations required for mission success (e.g., steering, power generation, high energy radar, etc.), a set of standards which define overall mission domain performance (e.g., total operation cost, surge speed, range, etc.) and time specifications which can be either exact or approximate (e.g., start time, duration, etc.) [7]. A mission can also include a set of mission segments which provide additional details for one leg or part of the overall mission, in which each mission segment belongs to a specific operational state. Therefore, it is apparent that the definition and creation of a mission profile would inevitably require specialized knowledge and specifications that can support the appropriate analyses. Therefore, the specifications and design criteria provided in this chapter play an important role on the mission-level to provide the necessary mission-related information and refine the ship performance evaluation for a given mission.

2.3 Conclusion

In this dissertation, the system under consideration is a nonlinear MVDC shipboard power system. This chapter provided a complete description about the MVDC model and its formulations used in this work. Shipboard power systems are going through fundamental transitions to provide reliable and abundant power supply to the future general of all-electric fleets. With the DC distribution bus and power conversion in the center of this transition to achieve improved power density and efficiency, MVDC is envisioned as the obvious choice for the on-board power generation and distribution. Realizing the lack of supporting documentation for this transition, this chapter also provided a comprehensive illustration of important transient and steady-state design requirements and specifications to facilitate the design and development of the latest MVDC SPS. The information summarized in this chapter is expected to contribute to the understanding, evaluation, design and improvement of the shipboard power systems.

CHAPTER III

CENTRALIZED MODEL PREDICTIVE CONTROL OF AN MVDC SPS

In this chapter, we propose two centralized model predictive control for the nonlinear MVDC shipboard power system management. At first, an MPC-based controller is designed to control the MVDC ship power system when dealing with a high power pulsed load such as free electron lasers under battle conditions. The nonlinear MPC also guarantees asymptotic stability of the closed-loop system by including a final cost in the objective function and a terminal inequality constraint. Second, an MPC-based algorithm is proposed to address the reconfiguration problem of the MVDC system in the abnormal conditions. The results of this chapter have been published in [115, 114]. Before presenting the main results of this chapter, the basics of model predictive control approach are explained in the following section.

3.1 Model Predictive Control

Model Predictive Control (MPC) is an effective model-based approach which uses the system model to predict the future state variables and generates an optimal control sequence over the prediction horizon h by optimizing an objective function subject to the system and operating constraints. Only the first element in the optimal control sequence is applied to the system at instant k, and the remainder is discarded [23, 76, 104]. MPC enables us

to go one step further than optimal control by incorporating a model of the system that allows the impact of control actions to be predicted forward for some finite amount of time. Therefore, in this method, the future effects of control decisions are considered as part of the optimization problem. MPC can handle the cost function in any form including nonlinearities or several control objectives, as well as different constraints. The presence of the system model is an essential condition for the development of the predictive control. The basic structure of the MPC is depicted in Fig. 3.1.

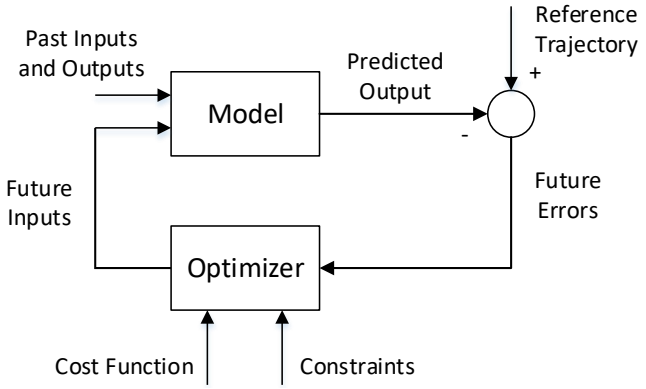

Figure 3.1: Basic Structure of MPC [23]

The overall objective function for a nonlinear MPC is as follows:

$$J = \sum_{k=0}^{N-1} L(x(k+1), u(k)) \tag{3.1}$$

where L denotes a nonlinear function with respect to x and u, and N is the final time step. In every time step k, predictions and optimal control sequence are computed over a finite prediction horizon h. So the following cost function is minimized in every time step k:

$$J_k = \sum_{i=1}^{h} L(x(k+i), u(k+i-1)) \tag{3.2}$$

subject to state constraints $\Psi(x(k)) < 0$, control inputs constraints and the system's dynamic constraints (2.2). Typically, an objective function that reflects a "cost" is minimized while a function reflecting a system utilized is maximized. Here, the following set-point cost function is used:

$$L(x(k), u(k-1)) = \|(x(k) - x^*(k))\|_Q^2 + \|u(k-1)\|_R^2 + \|\Delta u(k-1)\|_{R^*}^2 \qquad (3.3)$$

where $\|\cdot\|$ denotes the Euclidean norm. Q, R and R^* are weighting matrices. $\Delta u(k)$ denotes the changes in the control inputs and $x^*(k)$ is the desired value of state variable vector in time step k. Note that the MPC controller solves the optimization problem over prediction horizon h in each time step k. The objective of the MPC controller is to meet desired performance by driving system states to the defined $x^*(k)$ while minimizing the cost of control inputs as well as the variations in control inputs $\Delta u(k)$ using a permissible trajectory defined by the state and control constraints. Using the computed optimal control sequence, the first element of the control sequence, $u^*(k)$, is given to the system at time k and the rest are discarded.

To efficiently handle uncertain load conditions, the Autoregressive Integrated Moving Average (ARIMA) prediction method is used to predict load changes in the system with a predefined T_d delay. The ARIMA prediction is a time series method in the generalization of an Autoregressive Moving Average (ARMA) method which is widely used in uncertainty forecasting [19, 60].

In this research, we use two methods to solve nonlinear optimization in the MPC controller. The first method is a Tree Search Algorithm [70] which is mainly used for the

discrete control inputs to find an optimal solution. In this method, the trade-off between optimality and the size of discretization of control inputs is an important factor to be considered. Using this algorithm, the controller finds the optimal combination from the set of discrete inputs that minimizes (or maximizes) the objective function subject to state and input constraints. The second method is *fmincon* solver in MATLAB which is used for a nonlinear multivariable optimization problem. This solver includes four optimization algorithms: interior-point (default), trust-region-reflective, SQP, and active-set which can be chosen by setting *options* in the *fmincon* function. Note that *fmincon* is a gradient-based method that is designed to work on problems where the objective and constraint functions are both continuous and have continuous first derivatives.

In the next section, the closed-loop stability of the nonlinear MPC for an MVDC SPS system with continuous control inputs is achieved by adding a terminal cost and an additional terminal state inequality constraint.

3.2 Stability Analysis

This section presents a nonlinear MPC approach that ensures the closed-loop stability of the considered MVDC SPS system. Based on the method introduced in [30], the objective function includes a finite horizon cost as well as a terminal cost subject to state and input constraints, system dynamics (2.1) and an additional inequality constraint on terminal state. The terminal state inequality constraint guarantees that the system state will lie within a predefined terminal region at the end of the finite prediction horizon. Based on this method,

we first obtain the Jacobian linearization of the nonlinear MVDC system (2.1) around the reference values, leading to the following linear model:

$$\dot{x}(t) = Ax(t) + Bu(t) \tag{3.4}$$

Then, the considered optimization problem setup with guaranteed stability is as follows:

$$J(x,u) = \int_t^{t+T_p} \left(\|x(\tau)\|_Q^2 + \|u(\tau)\|_R^2\right) d\tau + \|x(t+T_p)\|_P^2 \tag{3.5}$$

or, if the objective is reference tracking,

$$J(x,u) = \int_t^{t+T_p} \left(\|x(\tau) - x_{ref}\|_Q^2 + \|u(\tau)\|_R^2\right) d\tau + \|x(t+T_p) - x_{ref}\|_P^2$$

subject to system's dynamic constraints, state constraints, control input constraints and an additional finite state constraint ($x(t+T_p) \in \Omega$) which requires the states at the end of the finite horizon to be in an assigned terminal region Ω. Q and R are symmetric positive-definite weighting matrices which are selected for desired performance. T_p is a finite prediction horizon and P is a symmetric and positive-definite terminal penalty matrix.

In this method, the terminal penalty matrix, P, and the terminal region, Ω, are calculated offline to be used in the objective functions and constraints of the online MPC optimization problem. We determine a linear state feedback $u = Kx$ such that $\bar{A} = A + BK$ is asymptotically stable. Then, a terminal penalty matrix P of the terminal cost is determined based on the solution of the following Lyapunov equation:

$$(\bar{A} + \kappa I)^T P + P(\bar{A} + \kappa I) = -Q^* \tag{3.6}$$

where P is a unique positive-definite and symmetric matrix, $Q^* = Q + K^T RK$, and a $\kappa \geq 0$ is chosen such that:

$$\kappa < -\lambda_{max}(\bar{A}), \tag{3.7}$$

where $\lambda_{max}(\bar{A})$ denotes the largest real part of the eigenvalues of the matrix $\bar{A}$. So, by choosing a constant κ satisfying (3.7) and solving Lyapunov function (3.6), we determine a unique terminal penalty matrix P.

The second step is to determine a terminal region Ω. We are looking for a neighborhood of the origin, Ω_α, defined as

$$\Omega_\alpha := \{x \in R^n | x^T Px \leq \alpha\} \tag{3.8}$$

for some constant α. Note that the linear feedback controller should satisfy the constraints in Ω_α. The following optimization problem should be solved for several iterations until the maximum value is non-positive:

$$\max_x \ \left\{x^T P\phi(x) - \kappa \cdot x^T Px | x^T Px \leq \alpha, Kx \in U\right\} \tag{3.9}$$

with

$$\phi(x) = f(x, Kx) - \bar{A}x. \tag{3.10}$$

If there exists a suitable value for α, the region Ω_α is used as a terminal region in the online MPC optimization problem. Accordingly, the new optimization problem setup includes the terminal inequality constraint. Note that both the terminal cost and terminal constraint are computed offline and even though the design process starts with linearization, the operation, prediction, and optimization of the MPC does not rely on linearization. The complete discussion on the terminal cost and terminal inequality constraint can be found in [30].

3.3 Centralized MPC for a Nonlinear MVDC Shipboard Power Systems under a High Power Pulsed Load

The health of the electric ship power system is adversely affected by high power loads, particularly, without the presence of any appropriate control methods. In case of large pulsed-type loads, short-time power demand may significantly exceed the power rating of all the installed generators. In the shipboard power systems, war specific loads such as electromagnetic guns or free electron lasers that draw very high short time current are known as pulsed loads. Such current behaviors can potentially cause the system voltage to drop in the entire microgrid, or shut down the propulsion system, or perhaps throw the underlying loads themselves offline.

To efficiently manage stressful pulsed loads in the SPS, we implemented an MPC controller for the nonlinear MVDC SPS described by (2.2). The goal of optimization problem is to meet voltage performance by maintaining it in the desired value and minimize the changes of the control inputs Δu with respect to states and control inputs constraints. Therefore, the objective function is defined as follows:

$$J(x,u) = \sum_{k=0}^{N-1} \left(q \cdot (v_{dc}(k) - v_{dc}^{ref}(k))^2 + \|\Delta u(k)\|_{R^*}^2 \right) \tag{3.11}$$

subject to control inputs and states constraints and system's dynamic constraints (2.2). q is the weighting factor for the voltage tracking objective. In this case study, the reference voltage v_{dc}^{ref} is 5 kV DC. The control inputs are the droop gain and the power reference for each generator (MTG & ATG). The droop gain control is applied to determine the power share between energy sources. It has indirect impacts on the output power of generators and can control DC bus voltage to improve the power quality on the microgrid. Here, the

control inputs are continuous and the nonlinear optimization method used in the MPC is *fmincon* solver in the MATLAB.

3.3.1 Simulation Results

This section provides the simulation results of two case studies with different prediction delays to validate the proposed MPC method when we have a square pulsed load with 2 MW amplitude in the system. The system under consideration is a nonlinear MVDC SPS model described by (2.2). In the simulation results, a comparison is presented for different cases of prediction, namely, no prediction, perfect prediction, and ARIMA prediction with different prediction delay values. To quantify the effectiveness of the proposed control approach, we introduce the following Improvement Factor (IF):

$$IF = \frac{1}{N}\sum_{k=1}^{N}\frac{\|v_{dc}(base\ line) - v_{dc}(no\ prediction)\|}{\|v_{dc}(base\ line) - v_{dc}(ARIMA)\|} \tag{3.12}$$

which $v_{dc}(base\ line)$ is the value of DC bus voltage when we have perfect prediction of a pulsed load event. $v_{dc}(no\ prediction)$ and $v_{dc}(ARIMA)$ are the values of DC bus voltage when we have no prediction and ARIMA prediction of a pulsed load event in the MPC controller.

The control inputs are chosen as the droop gain and the power reference for each generator. The control inputs constraints are as follows:

$$0.01 < K_{droop_1} < 0.09$$

$$0.01 < K_{droop_2} < 0.09$$

$$21.15 \times 10^6 < P_{ref_{Gen1}} < 25.85 \times 10^6$$

$$2.97 \times 10^6 < P_{ref_{Gen2}} < 3.63 \times 10^6$$

The nominal values (initial values) for the power references in main and auxiliary generators are set at 23.5 MW and 3.3 MW, respectively, but this setting can be changed. The weighting factor for the voltage tracking objective in (3.11) is defined as $q = 1$. The weighting matrix R^* minimizing changes in the four control inputs is defined as follows:

$$R^* = \begin{bmatrix} 10 & 0 & 0 & 0 \\ 0 & 5 & 0 & 0 \\ 0 & 0 & 0 & 0 \\ 0 & 0 & 0 & 0 \end{bmatrix}$$

The objective of the MPC controller is to meet voltage performance requirement of maintaining the bus voltage in 5 kV DC as well as having minimal variations in the control inputs. The simulation is done on a PC with Core i7-7700K CPU and 32.0 GB of RAM running on MATLAB R2016a. The horizon for the MPC controller is 2. The sampling time T_s is $0.01s$, the control interval T_c is $0.1s$ and v_{dc}^{ref} is 5 kV. Here, *fmincon* solver in the MATLAB is employed for the nonlinear optimization problem in the MPC controller.

The following two subsections present the results of applying the MPC controller under no prediction, perfect prediction and ARIMA prediction with two different prediction delays.

3.3.1.1 Case I

In this case, the prediction delay T_d in the ARIMA prediction is set to $10\ T_s$. The pulsed load starts at $t = 2\ s$ with $2MW$ amplitude and $2\ s$ duration as depicted in Fig. 3.2. The control inputs are shown in Fig. 3.3 for this case with three different predictions. Fig. 3.4 depicts the bus voltage of the MVDC system. In these figures, the red line shows the results

when no pulsed load prediction is used. The green and blue lines show the results for ARIMA and perfect prediction of a pulsed load event in the MPC, respectively. Perfect prediction (base line) represents the results when MPC has complete information of the pulsed load event including amplitude, start time and end time for the prediction. In this case, the improvement factor described in (3.12) is 4.0899. Fig. 3.5 shows the output power of generators for ARIMA prediction.

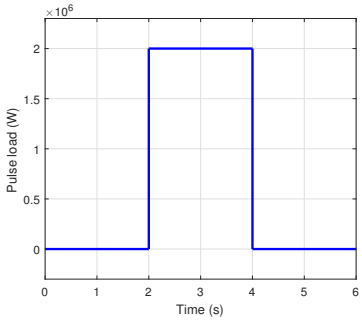

Figure 3.2: Pulse Load with 2 MW Amplitude

3.3.1.2 Case II

In this case, the prediction delay T_d in ARIMA prediction is set to $30\ T_s$. The pulsed load starts at $t = 2\ s$ with $2MW$ amplitude and $2\ s$ duration. Fig. 3.6 shows the control inputs for this case with three different predictions. Fig. 3.7 depicts the bus voltage of the MVDC system. Since there is more prediction delay in this case, the larger error is observed in the bus voltage near the start time and end time of the pulsed load (2s and 4s) in comparison with the previous case. These changes are obvious in the Fig. 3.7. In this case, the improvement factor is 1.6739.

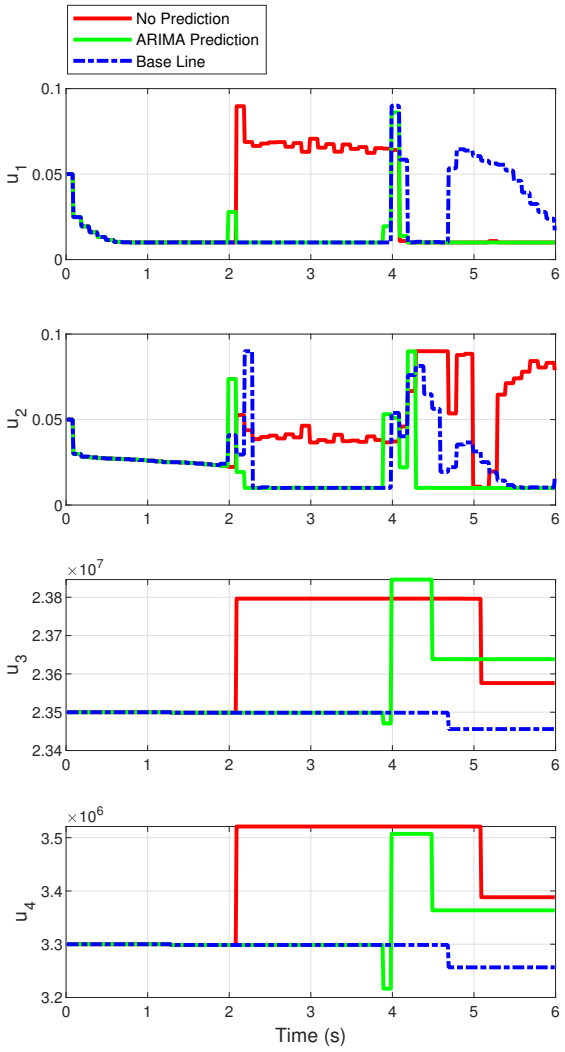

Figure 3.3: Control Inputs of Case I: $u_1 : K_{droop1}$, $u_2 : K_{droop2}$, $u_3 : P_{ref_{Gen1}}$, $u_4 : P_{ref_{Gen2}}$

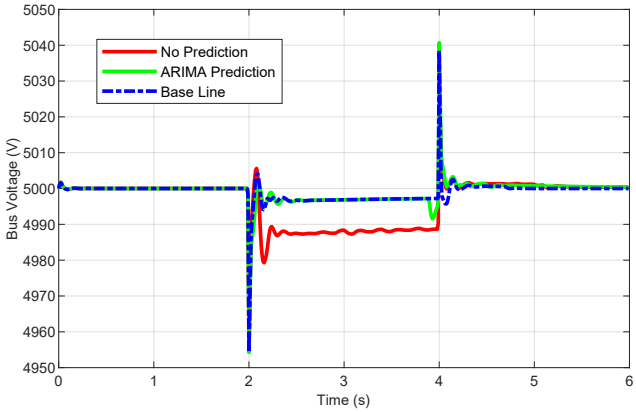

Figure 3.4: DC Bus Voltage (V) of Case I

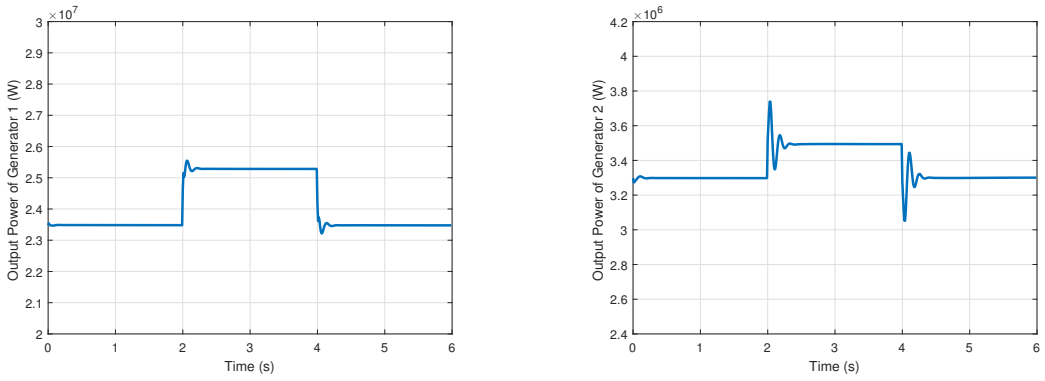

(a) Output power of generator 1

(b) Output power of generator 2

Figure 3.5: Output power of generators of Case I (ARIMA prediction)

A summary of the simulation outcome for these two cases is shown in the Table 3.1. Accordingly, the simulation results verify the effectiveness of the presented MPC-based controller to mitigate the effects of a high power pulsed load event in the MVDC SPS.

3.3.1.3 Stability Analysis Discussion

The stability guarantee, as described in Section 3.2, is added to the simulation to compare the performance of approaches. The objective function is extended to include terminal cost and an additional terminal state inequality constraint. The terminal penalty matrix, P, is obtained based on the solution of the Lyapunov equation (3.6) and linearization of (2.1).

At first, the Jacobian linearization of the nonlinear MVDC system (2.1) is obtained, and then, a linear state feedback $u = Kx$ is designed such that $\bar{A} = A + BK$ is asymptotically stable. This linear state feedback is just used to find a terminal penalty matrix, P, and a terminal region offline. Based on $\lambda_{max}(\bar{A})$ and the condition (3.7), we choose a constant

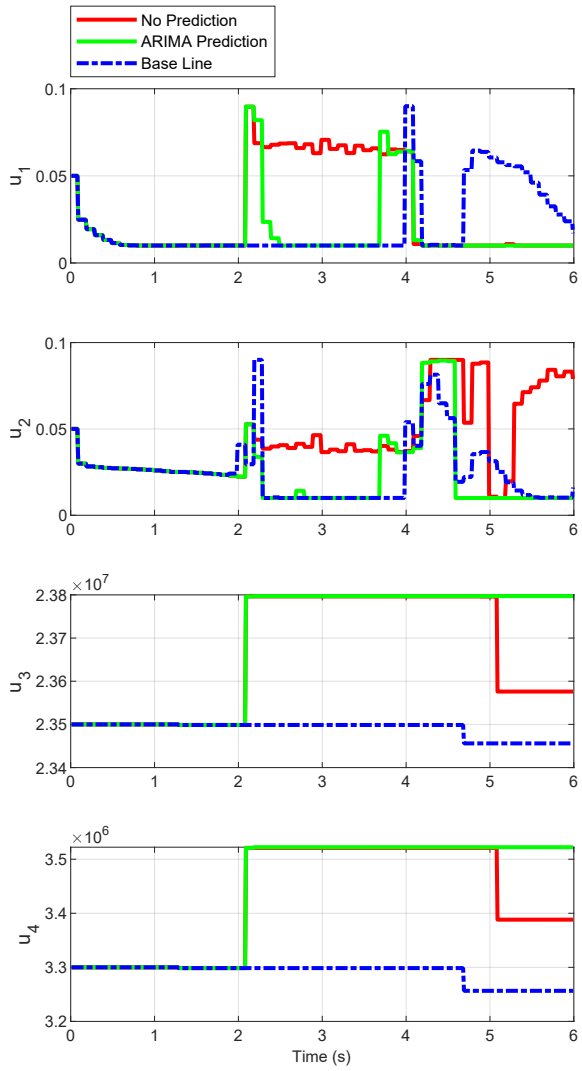

Figure 3.6: Control Inputs of Case II: $u_1 : K_{droop1}$, $u_2 : K_{droop2}$, $u_3 : P_{ref_{Gen1}}$, $u_4 : P_{ref_{Gen2}}$

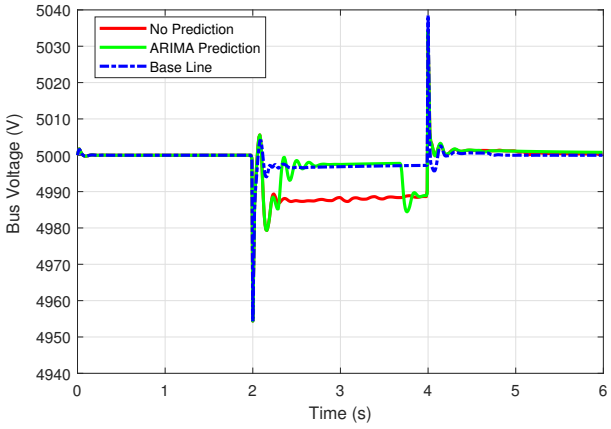

Figure 3.7: DC Bus Voltage (V) of Case II

Table 3.1: Simulation Information

	Case I	**Case II**
Sampling Time (T_s)	$0.01\ s$	
Control Interval (T_c)	$0.1\ s$	
Reference Bus Voltage	5 kV	
Pulse Load Amplitude	2 MW	
Prediction Delay (T_d)	$10\ T_s$	$30\ T_s$
Improvement Factor	3.9768	1.8938

κ which yields the unique solution for the Lyapunov equation (3.6). Then, the following optimization problem

$$\max_{x} \ \left\{x^T P\phi(x) - \kappa.x^T Px | x^T Px \leq \alpha, Kx \in U\right\}$$

is solved by reducing α from α_1 until the optimal value is nonpositive, where α_1 is the largest possible value such that $Kx \in U$ for all $x \in \Omega_{\alpha_1}$. Finally, an $\alpha = 0.024$ is obtained from this process which specifies a region Ω_α in the form of (3.8) in which the following inequality is satisfied:

$$x^T P\phi(x) \leq \kappa x^T Px \tag{3.13}$$

The region Ω_α can then serve as a terminal region in the online MPC optimization problem. Here, the output simulation signals are almost similar to the previous section and the response will not be repeated for the sake of brevity. However, it is observed that for the case of no prediction, the stability guarantee improves the performance of the system. Even

though the MPC controller can work without the added stability constraints, there is no guarantee that the controller will perform suitably with any initial condition or different sampling time or control interval. There is no significant difference in terms of computation time between controllers with stability guarantee and without it; however, the latter case usually requires longer prediction horizons. In general, it is recommended to impose stability conditions to the controller to guarantee the stability of the closed loop system under different conditions.

3.4 Reconfiguration of MVDC Shipboard Power Systems: A Centralized MPC Approach

Since a shipboard power system does not have any external generation support in case of an emergency, survivability is critical to the mission of a ship, especially under battle conditions. In a ship power system, the priorities of the loads are defined according to the missions of the ship. In order to serve the vital loads and maintain a proper power balance without excessive generation, the capability to perform a fast reconfiguration of the remaining system is critical under abnormal conditions. The objective in the reconfiguration problem can include the minimization of network loss, the minimization of load balancing index, and maximizing power delivered to the loads. The minimization of the distribution system's losses is a common objective in the terrestrial power systems. However, the network loss is considered very small in the ship power systems; therefore, the loss minimization is not a big issue in these systems [78].

In this section, an MPC-based reconfiguration method is proposed for a nonlinear Medium-Voltage DC Shipboard Power System. By applying the proposed MPC approach,

the reconfiguration is formulated as an optimization problem with respect to operating constraints and also the priorities of loads. According to the missions of the ship, the loads are categorized as vital loads, semi-vital loads, and non-vital loads by the appropriate weighting factors. The main goal is to maximize the power delivered to the loads with respect to power balance and generation limits. The proposed reconfiguration algorithm allows for a ship's survival through abnormal scenarios such as battle conditions, in which damage and equipment failure limit the total number of serviceable loads. The simulation results of three cases with the use of a nonlinear MVDC SPS model are given to illustrate the effectiveness of the proposed method.

3.4.1 Main Results

In this research, the general dynamics of a nonlinear MVDC system which is described in (2.2) is considered. This section aims to present a reconfiguration method based on model predictive control to maximize the utility of the mentioned MVDC system. The control inputs are defined as M circuit breakers that determine the status of each generator and load. The status of breakers can be either closed "0" or open "1"; so there exists 2^M position possibilities for the breakers. If an abnormal operation is detected, the optimization problem is solved to find the optimal control inputs (switch configuration to shed non-vital loads) which transfer the maximum weighted power without exceeding generators limits and violating other system constraints. By using the model predictive control approach, the validity of predicted states and proposed control inputs are checked with respect to the constraints. The proposed algorithm analyzes various control input sequences to identify

the best cost function and the associated control inputs. A tree search algorithm has been implemented to find the optimum control input (switching configuration). In this method, the controller finds the optimal combination from the set of discrete inputs that maximizes the objective function subject to state and input constraints. In the case study, the control inputs are the status of switches of generators and loads, so they are discrete variables. A sequence of valid control inputs can be obtained for each path in the search tree by optimizing the utility functions. Then, the control input $u^*(k)$ corresponding to the first element in the sequence is applied to the system at time k while the other control inputs are discarded.

3.4.1.1 Reconfiguration Algorithm

- **Step 1.** The status of generator and load switches are defined as control inputs. At first, it is assumed that all the breakers are closed by default. So, the status of all switches are "1."

- **Step 2.** Check the status of the system. Switches will stay unchanged under normal operating conditions.

- **Step 3.** If an abnormal operation is detected, solve the optimization problem to find the optimal switch configuration that transfers the maximum weighted power, yet does not exceed generator limits.

  - For every valid combination of switches, check the output of the system in the prediction horizon. Discard the combination if the predicted output violates

the constraints (the control solution that leads to system states violating the constraints are discarded).

– Choose the switch configuration that results in the best objective function over the prediction horizon. The cost function and constraints are defined as:

$$\max J = \sum_{k=0}^{N-1} \sum_{i=1}^{N_L} \rho_i \, S_i(k) P_{L_i}(k) \tag{3.14}$$

subject to system's dynamic constraints (2.2) and

$$\sum_{j=1}^{N_G} S'_j(k) P_{G_j}(k) \geq \sum_{i=1}^{N_L} S_i(k) P_{L_i}(k) \tag{3.15}$$

and

$$P_{G_j}^{min} \leq P_{G_j}(k) \leq P_{G_j}^{max} \tag{3.16}$$

with

$$i = 1, 2, \ldots, N_L$$

$$j = 1, 2, \ldots, N_G$$

$$0 \leq k \leq N - 1.$$

- **Step 4.** Apply the first element of the optimal control vector and discard the rest.

- **Step 5.** Repeat steps 2–4.

N_L is the total number of loads. ρ_i is the weighting factor for the i^{th} load by considering the load priority during a particular mission. S_i is the switch status corresponding to the i^{th} load and S'_j denotes the switch status corresponding to the j^{th} generator. P_{L_i} is the power consumption of the i^{th} load and P_{G_j} is the output power of the j^{th} generator. N_G is the total

number of generators. Here, the constraints are the power balance equations (3.15), the power generation limits (3.16) and the system dynamic equation (2.2). Note that the MPC controller solves the optimization problem over prediction horizon h in each time step k. Accordingly, this reduces the right-hand side of the equation (3.14) to the summation of objective terms from $k+1$ to $k+h$ at each specific time step k.

Remark 1: The objective term $\|S(k) - S(k-1)\|_P$ with weighting factor P can be included in the objective function (3.14) with minus sign to minimize the changes of control inputs. In other words, frequent changes of switches in the system can be avoided by considering this term in the objective function. Other system's goals such as bus voltage tracking can be also included in the objective function by defining proper weighting factors.

3.4.2 Simulation Results

This section provides the simulation results of three cases to validate the proposed reconfiguration method. Here, a nonlinear MVDC SPS model is considered which includes two generators $N_G = 2$, and three loads $N_L = 3$. The control inputs are the status of five switches for the generators and loads.

As long as the control inputs can only be '0' and '1' for a switch, they are considered as a binary value. In the normal case, the controller chooses '1 1 1 1 1' as control inputs, i.e., all of the switches are closed and the maximum power is delivered to the loads (maximum cost function). When there is shortage of energy, the optimal path (switch configuration) is selected to maximize the power delivered to the loads with respect to load priorities and operating constraints. Three scenarios are provided to demonstrate the effectiveness of

the proposed reconfiguration method. In all these cases, we consider the sampling time $T_s = 0.01s$, the control interval $T_c = 0.1s$ and the horizon $h = 1$. The loads are connected to the system at time $t = 5s$ when the power system reaches its steady state operating mode with bus voltage $v_{dc} = 5\ kV$. The MPC controller is available in the system after time $t = 6s$ (i.e., after the transition system response due to the connection of loads has passed) for each control interval T_c.

3.4.2.1 Case I. Changes in Load Demand

- Load 1: Vital load (20MW), Load 2: Non-vital load (5MW), Load 3: Semi-vital load (1.25 MW)
- Weighting factors of the loads: $\rho_1 = 1, \rho_2 = 0.1, \rho_3 = 0.5$
- Event: Changing power demand in load 1 from 20 MW to 22 MW gradually from time $t = 10s$ to $t = 30s$
- Power generation limits: $P_{G1}^{max} = 13.5MW, P_{G2}^{max} = 13.5MW$

The simulation results for case I are shown in Fig. 3.8. The status of control switches is indicated in Fig. 3.8(a). Sum of the output power of generators and sum of the delivered power to the loads along with the maximum total generation capacity are shown in Fig. 3.8(b). At time $t = 17.58\ s$, the generated power cannot satisfy the power balance and generation limits at the same time because of changes in power demand of load 1. In this time, the controller chooses (1 1 1 0 1) as control input and sheds the non-vital load 2 to satisfy the constraint equations (3.15) and (3.16), and also maximizes the objective function (3.14).

3.4.2.2 Case II. Changes in Load Demand

- Load 1: Vital load (20MW), Load 2: Non-vital load (5MW), Load 3: Semi-vital load (1.25 MW)
- Weighting factors of Loads: $\rho_1 = 1, \rho_2 = 0.1, \rho_3 = 0.5$
- Event: Changing power demand in load 1 from 20 MW to 26 MW gradually from time $t = 10s$ to $t = 30s$
- Power generation limits: $P_{G1}^{max} = 13.5MW, P_{G2}^{max} = 13.5MW$

The simulation results for case II are shown in Fig. 3.9. The status of control switches is indicated in Fig. 3.9 (a). Sum of the output power of generators and sum of the delivered power to the loads along with the maximum total generation capacity are shown in Fig. 3.9 (b). At time $t = 12.5\ s$, the generated power cannot satisfy the power balance and generation limits at the same time because of changes in power demand of load 1. In this time, the controller chooses (1 1 1 0 1) as control input and sheds the non-vital load 2. By increasing load 1 gradually to reach 26 MW, at time $t = 29.1\ s$, again the total generated power cannot satisfy the power balance and generation limits at the same time. At this time, the control input (1 1 1 0 0) is chosen to shed both loads 2 and 3 to satisfy the constraint equations (3.15) and (3.16), and also maximize the objective function (3.14).

3.4.2.3 Case III. Fault in Generator 2

- Load 1: Vital load (10MW), Load 2: Non-vital load (15MW), Load 3: Semi-vital load (1.25 MW)

- Weighting factors of Loads: $\rho_1 = 1, \rho_2 = 0.1, \rho_3 = 0.5$
- Event: There is a fault in the generator 2 at time $t = 10\ s$.
- Power generation limits: $P_{G1}^{max} = 13.5MW, P_{G2}^{max} = 13.5MW$

The simulation results for case III are shown in Fig. 3.10. The status of control switches is indicated in Fig. 3.10 (a). Sum of the output power of generators and sum of the delivered power to the loads along with the maximum total generation capacity are shown in Fig. 3.10 (b). At time $t = 10\ s$, the generated power cannot satisfy the power balance and generation limits at the same time because of the fault in generator 2. In this time, the controller chooses (1 0 1 0 1) as a control input and sheds the non-vital load 2 to satisfy the constraints.

Therefore, based on these three scenarios, the simulation results demonstrate the validity of the proposed reconfiguration algorithm for the MVDC SPS load management.

3.5 Conclusion

In this chapter, we first present a nonlinear MPC approach to control the MVDC shipboard power system under a stressful high power pulsed load. The optimization goal in the MPC is to meet voltage performance with minimal variations in the control input with respect to state and control inputs constraints. The closed-loop stability analysis is also considered in the MPC optimization problem by adding a terminal cost in the objective function and considering an additional terminal state inequality constraint. A terminal penalty matrix and a terminal region are defined offline. Simulation results demonstrate

the validity of the proposed MPC approach for the effective shipboard power system load management.

Second, a reconfiguration algorithm is proposed based on a model predictive control approach for a nonlinear MVDC shipboard power system. Here, the optimization goal in the MPC controller is to maximize the power delivered to the loads with respect to the system and operating constraints. Balanced power conditions, power generation limits and the priorities of loads are also considered in the MPC controller. The control inputs are defined as the status of switches for the generators and loads. A tree search algorithm has been used in the MPC optimization problem to find the optimum control input. In the simulation section, three different cases have been investigated to show the effectiveness of the proposed reconfiguration method.

Next, we propose a distributed power management architecture for the nonlinear MVDC SPS by considering the MPC method as a local controller. The results presented in this chapter based on centralized MPC are useful to design the distributed control structure with local MPC controllers.

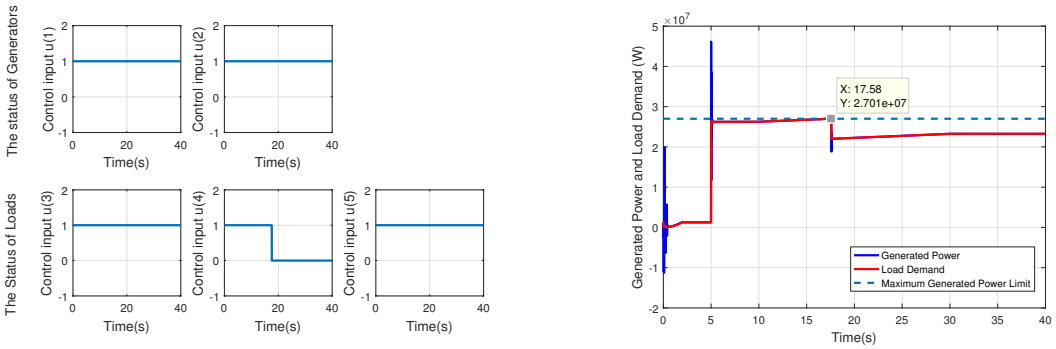

(a) (b)

Figure 3.8: Case I: (a) Control Inputs, (b) Generated Power and Load Demand

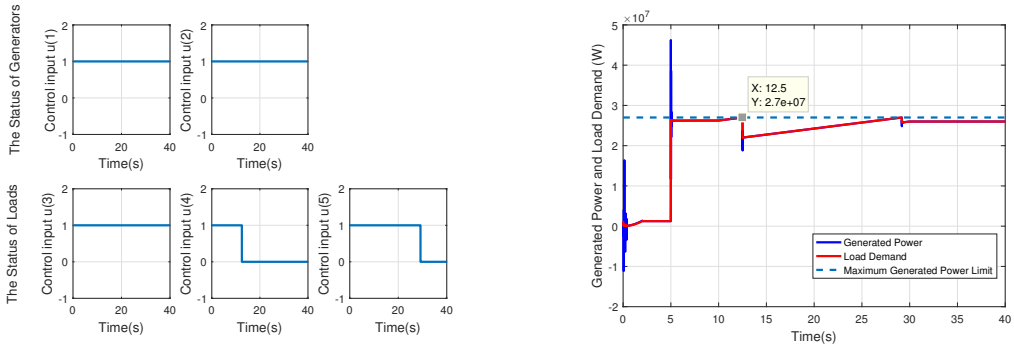

(a) (b)

Figure 3.9: Case II: (a) Control Inputs, (b) Generated Power and Load Demand

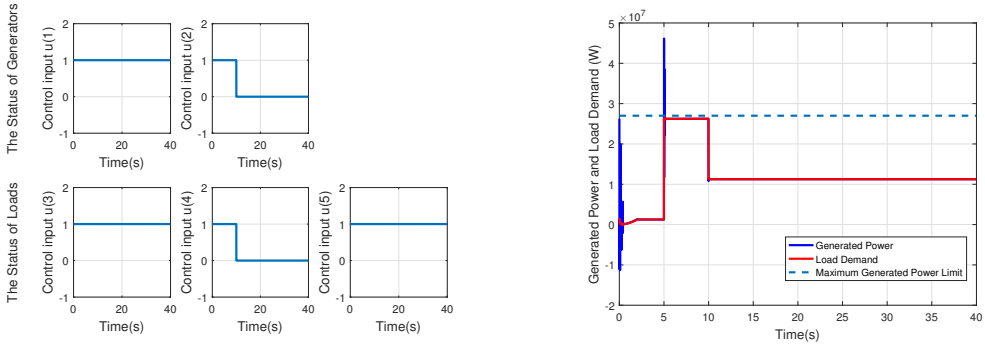

(a) (b)

Figure 3.10: Case III: (a) Control Inputs, (b) Generated Power and Load Demand

CHAPTER IV

DISTRIBUTED PREDICTIVE CONTROL STRUCTURE FOR AN MVDC SPS

In this chapter, a distributed control structure is presented for a nonlinear Medium-Voltage DC (MVDC) Shipboard Power System (SPS). The distributed control architecture has the advantages of less computational overhead, high flexibility, and a good error-tolerance behavior. In other words, the distributed structure has minimized the risk of total system failure, improved overall flexibility, and simplified the maintenance and further expansions of control systems. In the proposed framework, each subsystem is controlled by a local model predictive controller using local state variables and parameters, and also interaction variables from other subsystems communicated through a coordinator. The control inputs for each subsystem can be either continuous or discretized. For the MPC nonlinear optimization problems, the tree search algorithm and MATLAB *fmincon* solver are used when dealing with discrete control inputs and continuous control inputs, respectively. In the coordinator level, an optimization problem is iteratively solved to update a Lagrange multiplier vector to have a global optimal solution. The effectiveness of the proposed distributed control structure for a partitioned MVDC model is demonstrated by the simulation results. Performance analysis is accomplished by comparing centralized and distributed control methods on the global and partitioned models for both continuous

and discrete control inputs, and considering different specifications in the MVDC system. Two case scenarios are also provided to demonstrate the performance of distributed control structure for the MVDC system when we have a pulsed load or changes in the load demand. The results of this chapter has been partially published in [113].

4.1 MVDC System Model Formulations in the Distributed Structure

As mentioned in Chapter 2, the considered model in this research is a nonlinear MVDC shipboard power system which consists of one main turbine generator (MTG), one auxiliary turbine generator (ATG), one electrical driven propeller with variable speed drives (VSDs), four zonal service loads and one isolated pulsed load. The general dynamics of a global nonlinear MVDC system described in (2.2) in Chapter 2 is as follows:

$$\begin{aligned} x(k+1) &= f(x(k), u(k), k), \\ x(0) &= x_0. \end{aligned} \tag{4.1}$$

For the distributed control purpose, the global MVDC system can be partitioned into M subsystems as follows:

$$\begin{aligned} x_i(k+1) &= f_i\left(x_i(k), u_i(k), z_i(k)\right), \\ x_i(0) &= x_{i0}, \qquad i = 1, 2, \ldots, M \end{aligned} \tag{4.2}$$

where i represents the particular subsystem among M subsystems. x_i is the n_i dimensional state vector and u_i is the m_i dimensional control vector denoting the state variables and control inputs of the subsystem i, respectively. z_i is an r_i dimensional vector of interaction inputs for the subsystem i which is generated by the states of other subsystems:

$$z_i(k) = \sum_{j=1, j\neq i}^{M} h_{ij}(x_j(k)) \tag{4.3}$$

where the vector of interaction inputs z_i is a nonlinear combination of the states of the $M-1$ subsystems. For the i^{th} subsystem, $h_{ij}(\cdot)$ is a nonlinear function denoting the interaction input coming from the subsystem j, while $j \neq i$. In our case study, the global MVDC system is partitioned into two subsystems and the interaction inputs are currents. Complete system descriptions and performance analysis are given in the simulation results. The following section presents a full explanation of the proposed distributed control approach and coordination optimization formulations.

4.2 Distributed Model Predictive Control of an MVDC SPS

In this section, the distributed control and optimization algorithm are presented for the nonlinear MVDC shipboard power system described by (4.2). The distributed online control algorithm is composed of two main procedures: global and local. The Goal Coordination approach is used for interacting information between subsystems. The general distributed control structure is shown in Fig. 4.1. In the distributed structure, a model predictive control approach is applied to the local control level and each local MPC uses the dynamical model of its own subsystem described by (4.2).

4.2.1 Optimization and Problem Formulations

The optimization problem is to minimize J:

$$J = \sum_{i=1}^{M} \left(\sum_{k=0}^{N-1} g_i \left(x_i(k), u_i(k), z_i(k) \right) \right) = \sum_{i=1}^{M} J_i \tag{4.4}$$

subject to state constraints ($\Psi(x) \leq 0$), control inputs constraints ($U(x) \subseteq U$) and the subsystems' dynamic constraints (4.2). N is the final time step. $g_i(\cdot)$ is a nonlinear function

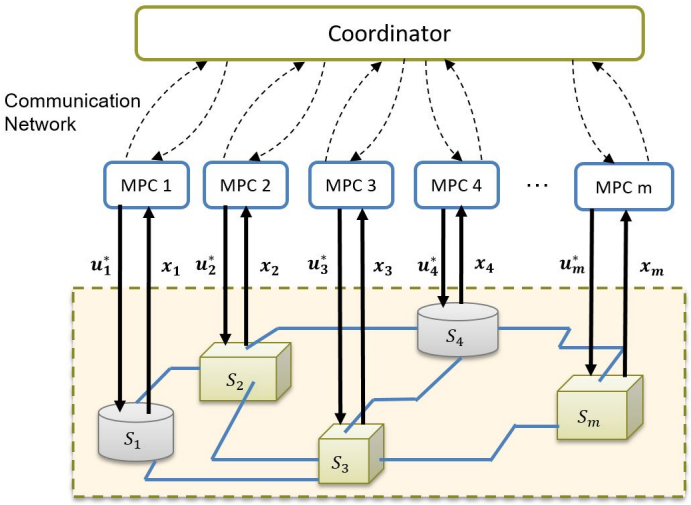

Figure 4.1: General Distributed Control Structure

describing the objective of i^{th} subsystem for $i = 1, \ldots, M$. Moreover, the coupling constraints are defined in (4.3).

The minimization of this optimization problem is equivalent to maximizing a dual function $\phi(\lambda)$ with respect to λ with:

$$\begin{aligned} \phi(\lambda) &= \min_{u} \;\; L(x, u, z, \lambda) \\ \max_{\lambda} \Big(\min_{u} \big(L(x, u, z, \lambda) \big) \Big) &= \max_{\lambda} \phi(\lambda) \end{aligned} \tag{4.5}$$

subject to equation (4.2) and the operating constraints. The Lagrangian function L is defined as follows:

$$L(x, u, z, \lambda) = J + \sum_{i=1}^{M} \sum_{k=0}^{N-1} \left(\lambda_i^T \left(z_i(k) - \sum_{j=1, j \neq i}^{M} h_{ij}(x_j(k)) \right) \right) = \sum_{i=1}^{M} L_i(x_i, u_i, z_i, \lambda_i)$$

with Lagrange multiplier vector λ_i. The Lagrangian function L is additively separable and can be decomposed into M independent sub-Lagrangian functions L_i:

$$L_i(x_i, u_i, z_i, \lambda_i) = J_i + \sum_{k=0}^{N-1} \left(\lambda_i^T z_i(k) - \sum_{j=1, j \neq i}^{M} \lambda_j^T h_{ji}(x_i(k)) \right) \tag{4.6}$$

where $h_{ji}(\cdot)$ is a nonlinear function denoting the interaction output of subsystem i to subsystem j. The optimization problem for each local MPC controller is to obtain the control inputs $(u_1, u_2, \ldots, u_M)$ to minimize the sub-Lagrangian functions, one for each subsystem subject to that subsystem's dynamical constraints (4.2) and the operating constraints for $\lambda_i = \lambda_i^*$. Therefore, instead of solving one centralized optimization problem, it is possible to have the problem of minimizing M sub-Lagrangian functions with the Lagrange multipliers $\lambda_i = \lambda_i^*$ obtained from the coordinator level. Note that each local MPC solves the local optimization problem over prediction horizon h in each time step k. Accordingly, this reduces the right-hand side of equation (4.6) to the summation of objective terms from $k+1$ to $k+h$ at each specific time step k.

In order to maximize $\phi(\lambda)$ w.r.t. λ, the gradient is given by interaction error:

$$\nabla\phi(\lambda)|_{\lambda=\lambda^*} = \begin{bmatrix} \vdots \\ z_i - \sum_{j=1, j\neq i}^{M} h_{ij}(x_j) \\ \vdots \end{bmatrix} = \begin{bmatrix} \vdots \\ e_i \\ \vdots \end{bmatrix} = e \tag{4.7}$$

This interconnection error vector is used in the update procedure of λ_i.

In the case of linear interactions between subsystems, the equations (4.3) and (4.6) are rewritten as:

$$z_i(k) = \sum_{j=1, j\neq i}^{M} L_{ij} x_j(k) \tag{4.8}$$

and

$$L_i(x_i, u_i, z_i, \lambda_i) = J_i + \sum_{k=0}^{N-1} \left(\lambda_i^T z_i(k) - \sum_{j=1, j\neq i}^{M} \lambda_j^T L_{ji} x_i(k) \right) \tag{4.9}$$

where the vector of interaction inputs z_i is a linear combination of the states of the $M-1$ subsystems.

4.2.2 Distributed Control Algorithm

The coordination algorithm and the update procedure of λ_i can be summarized by the following steps:

1. Initialize subsystems and send the system data and initial coordination parameter values to all subsystems and the coordinator.

2. Solve the local optimization problem by using the MPC algorithm based on local and interaction variables.

3. Receive the local optimal solutions and updated state predictions from all subsystems.

4. Compute the interaction error e_i.

5. Update the value of λ_i for the next iteration.

6. Send the updated values of λ_i and z_i to all subsystems.

7. Repeat steps 2 to 6 for each time step k until $e_i \leq \epsilon$.

The coordinator's task is to update the Lagrange multiplier vector λ to decrease the interaction error e_i:

$$e_i = z_i - \sum_{j=1, j\neq i}^{M} h_{ij}(x_j) \leq \epsilon \tag{4.10}$$

where ϵ is defined as an error tolerance value, which, preferably, needs to be close to zero. Here, the coordination vector is $\begin{bmatrix} \lambda_i \\ z_i \end{bmatrix}$.

A simple description of this process for two subsystems is shown in Fig. 4.2.

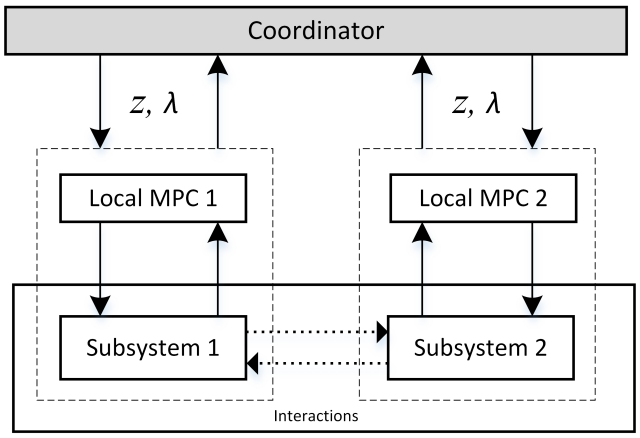

Figure 4.2: Example of distributed control for two subsystems

To update the interaction variables z_i, the coordinator has the last updated solutions obtained from the subsystems:

$$z_i^{l+1}(k) = \sum_{j=1}^{M} h_{ij}(x_j^l(k)) \tag{4.11}$$

where l is the iteration number. Different methods to update Lagrange multiplier vector λ_i exist, including the Alternating Direction Method of Multipliers (ADMM) [20], Multi-Step Gradient Method [56], Conjugate Gradient Method [39] and Accelerated Gradient Method [57]. In this research, we use the multi-step Gradient method for updating λ_i as follows:

$$\lambda_i^{l+1} = \lambda_i^l + \alpha.e_i^l + \beta(\lambda_i^l - \lambda_i^{l-1}) \tag{4.12}$$

where α and β are two fixed step-size parameters. This method is effective and simple for the model we deal with. In the coordinator level, an optimization problem is iteratively solved to update the Lagrange multiplier vector until the predicted interaction inputs from the local controllers are equal to the measured interaction inputs, therefore, achieving a global optimal solution. The Lagrange multiplier vector λ_i is used to tune the objective

function of the local MPC controllers; and is thereby also called Goal Coordination method. The complete algorithm flowchart is shown in Fig. 4.3, where the subsystems are separated from the coordinator by dashed lines.

4.3 Simulation Results

The simulation is done on a global nonlinear MVDC shipboard power system with 37 state variables [112] which includes two generators, one electrical driven propeller, four zonal service loads and an energy storage device. This model is partitioned into two subsystems as shown in Fig. 4.4. The model of subsystem one contains the main turbine generator, zonal load 1, zonal load 2 and one electrical propeller. The model of subsystem 2 includes the auxiliary turbine generator, zonal load 3, zonal load 4 and an energy storage device. The interaction variables between subsystems are currents. The decomposition coordination scheme acts as if the system is decomposed into two subsystems with two imaginary current sources placed at the cut points. These current sources are used to enable the subsystems to act independently on their control problem while the current sources are continuously adjusted to compensate for the lost interaction. The state variables of each subsystem converge to the desired values while its related current source is updated based on the obtained physical responses of devices of another subsystem.

In the following, the simulation results related to the centralized MPC and the distributed MPC controllers for the MVDC SPS with both continuous control inputs and discrete control inputs are demonstrated.

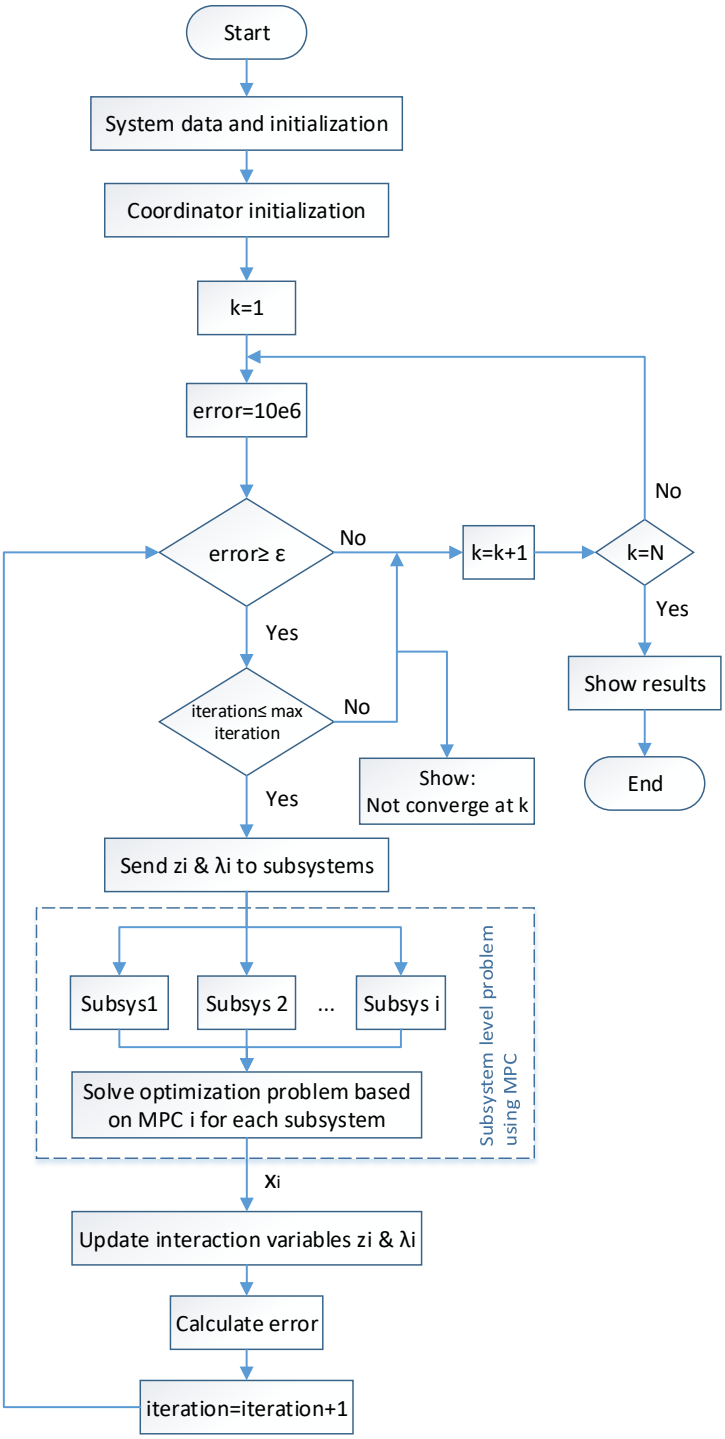

Figure 4.3: Algorithm Flowchart for the Distributed Control Structure

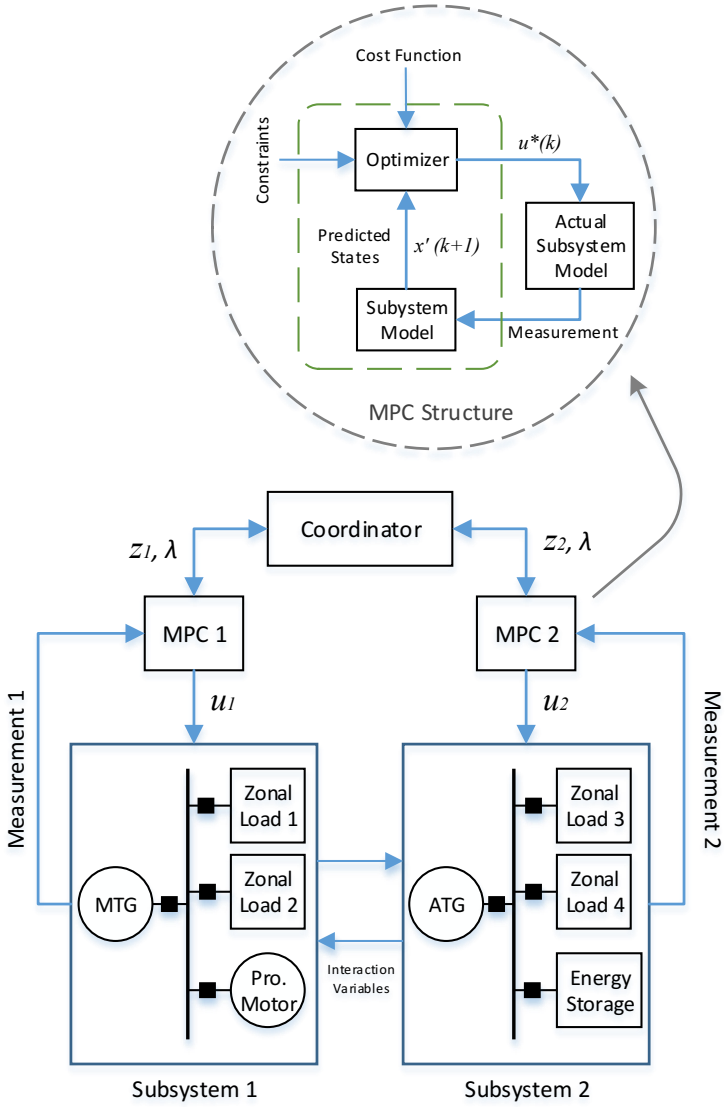

Figure 4.4: Distributed Control Structure for MVDC SPS

4.3.1 Performance Analysis of Continuous Centralized and Distributed MPC Control

To demonstrate the efficiency of distributed approach, a performance analysis is done by comparing the centralized and distributed MPC control of the global and partitioned MVDC models. The objective of the centralized MPC and each local MPC controller in the distributed case is to meet the voltage performance requirement of maintaining the bus voltage in 5 kV DC with minimal changes in the control inputs. Therefore, the centralized objective function for the global system is:

$$J = \sum_{k=0}^{N-1} (\|x(k) - x^*(k)\|_P + \|\Delta u(k)\|_R)$$

and the objective function for each local MPC in the distributed structure is described as follows:

$$L_i(x_i, u_i, z_i, \lambda_i) = \sum_{k=0}^{N-1} \Bigg(\|x_i(k) - x_i^*(k)\|_{P_i} + \|\Delta u_i(k)\|_{R_i} + \Big(\lambda_i^T z_i(k) - \sum_{j=1, j\neq i}^{M} \lambda_j^T h_{ji}(x_i(k))\Big)\Bigg)$$

where P, R, P_i and R_i are weighting matrices for $i = 1, 2$. The droop gain K_{droop} and the power reference P_{Gref} for each generator are defined as control inputs. Therefore, the centralized MPC controller has four control inputs ($K_{droop1}, P_{ref_{Gen1}}, K_{droop2}, P_{ref_{Gen2}}$), and the distributed controller has two control inputs for each subsystem. K_{droop1} and $P_{ref_{Gen1}}$ are control inputs of subsystem 1, and K_{droop2} and $P_{ref_{Gen2}}$ are control inputs of subsystem 2.

The constraints for continuous control inputs are defined as follows:

$$0.005 < K_{droop_1} < 0.09,$$

$$0.005 < K_{droop_2} < 0.09,$$

$$21.15 \times 10^6 < P_{ref_{Gen1}} < 25.85 \times 10^6,$$

$$2.97 \times 10^6 < P_{ref_{Gen2}} < 3.63 \times 10^6.$$

In the coordinator level, I choose $\epsilon = 0.02$, $\alpha = 0.001$ and $\beta = 0.01$ in the (4.10) and (4.12). The coupling constraints are (4.10) with $i = 1, 2$ and the local objective is to meet voltage performance requirement of maintaining $v_{dc_{sub1}}$ and $v_{dc_{sub2}}$ at 5 kV DC.

The simulation is done on a PC with Core i7-7700K CPU and 32.0 GB of RAM running on MATLAB R2016a. The horizon for the MPC controller with continuous inputs for both centralized and distributed cases is 2. The sampling time T_s is $0.01s$, the control interval T_c is $0.1s$ and v_{dc}^{ref} is $5\ kV$. In the objective function, the weighting factor related to the bus voltage tracking term is defined as 10000, and the weighting factor for the changes of K_{droop1} is 10. The MATLAB *fmincon* solver is used for the continuous MPC nonlinear optimization problems in both centralized and distributed control problems.

The centralized bus voltage and the voltage of subsystems 1 and 2 are shown in Fig. 4.5. The control inputs of both centralized and distributed controllers are given in Fig. 4.6. The computation time for the centralized MPC and distributed MPC is given in Table 4.1.

To make a better inference, Fig. 4.7 (a) shows the error between centralized bus voltage (v_{dc}) and the reference voltage (v_{dc}^{ref}). Fig. 4.7 (b) and (c) demonstrate the error between the distributed voltages of subsystem 1 ($v_{dc_{sub1}}$) and subsystem 2 ($v_{dc_{sub2}}$) with the reference voltage (v_{dc}^{ref}), respectively. Moreover, Fig. 4.7 (d) depicts the difference between the

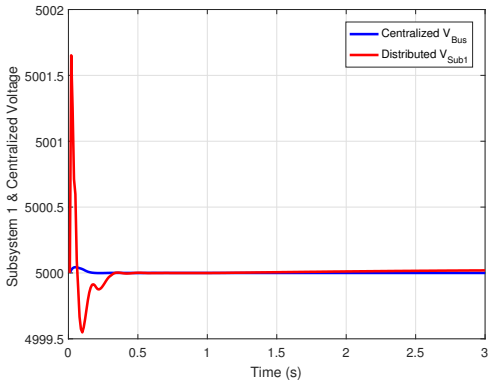

(a) Subsystem 1 and Centralized Voltages

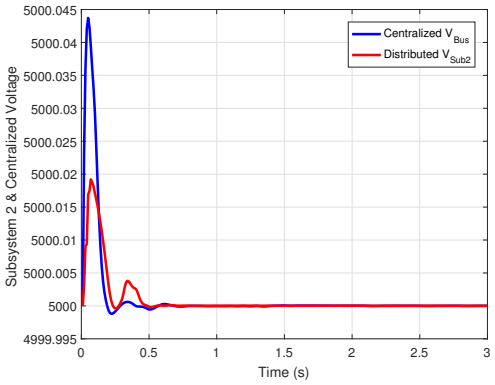

(b) Subsystem 2 and Centralized Voltages

Figure 4.5: Centralized and Distributed Voltages (Continuous Controller)

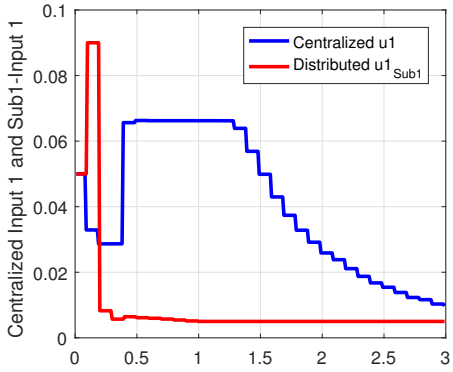

(a) Centralized Input 1 & Sub1-Input 1 (K_{droop1})

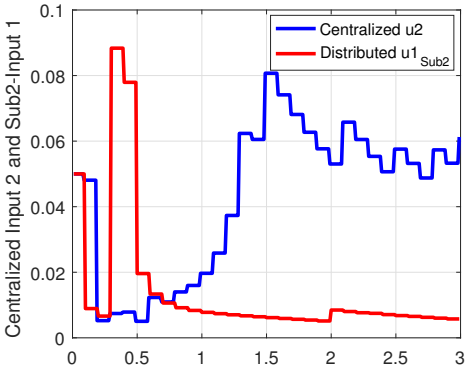

(b) Centralized Input 2 & Sub2-Input 1 (K_{droop2})

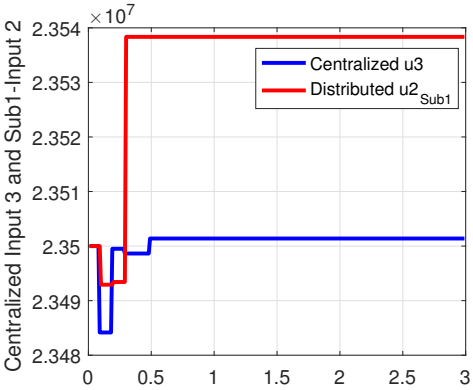

(c) Centralized Input 3 & Sub1-Input 2 (P_{G1-ref})

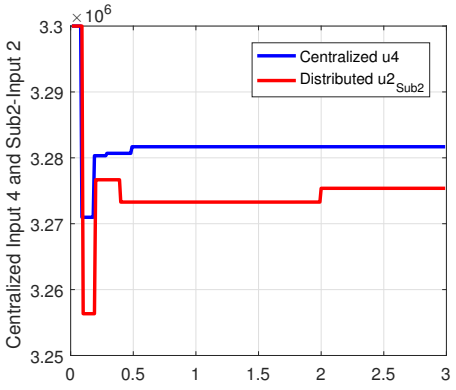

(d) Centralized Input 4 & Sub2-Input 2 (P_{G2-ref})

Figure 4.6: Centralized and Distributed Control Inputs (Continuous Controller)

centralized bus voltage and the distributed voltages ($v_{dc_{sub1}}$& $v_{dc_{sub2}}$). The average errors of these cases are given in Table 4.2.

4.3.2 Performance Analysis of Discrete Centralized and Distributed MPC Control

In this section, we first discretize the control inputs and then use a tree search algorithm to solve the optimization problem in the discrete MPC controller for both centralized and distributed cases. The size of control sets are given in Table 4.3.

The MPC objective functions and the parameters in the coordinator are chosen the same as the previous section. The horizon for MPC controller with discrete inputs for both centralized and distributed cases is 1. The sampling time T_s is $0.01s$, the control interval T_c is $0.1s$ and v_{dc}^{ref} is $5\ kV$. The centralized bus voltage and the voltage of subsystems 1 and 2 are shown in Fig. 4.8. The control inputs of both centralized and distributed controllers are given in Fig. 4.9. The computation time for the discrete centralized MPC and distributed MPC is given in Table 4.4. For the discrete control, the computational burden is significantly decreased by using the distributed MPC controller in comparison with the centralized one. To make a better inference, Fig. 4.10 (a) shows the error between centralized bus voltage v_{dc} and the reference voltage v_{dc}^{ref}. Fig. 4.10 (b) and (c) demonstrate the error between distributed voltages ($v_{dc_{sub1}}$ & $v_{dc_{sub2}}$) with the reference voltage v_{dc}^{ref}, respectively. Moreover, Fig. 4.10 (d) depicts the difference between the centralized bus voltage and the distributed voltages ($v_{dc_{sub1}}$& $v_{dc_{sub2}}$). The average errors of these cases are given in Table 4.5.

Table 4.1: Computation Time (Continuous Controller)

Centralized MPC	Distributed MPC
58.47 s	19.72 s
Speed up	**2.96**

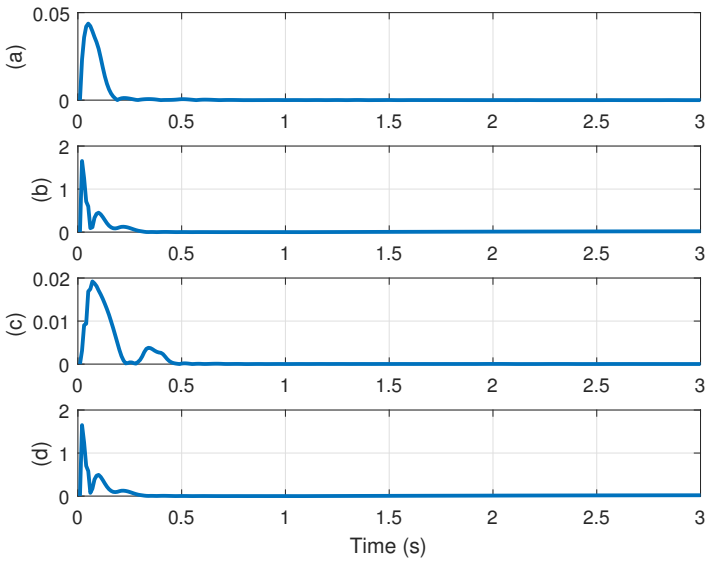

Figure 4.7: For the continuous controller (a) Error between centralized v_{dc} and v_{dc}^{ref}, (b) Error between distributed $v_{dc_{sub1}}$ and v_{dc}^{ref}, (c) Error between distributed $v_{dc_{sub2}}$ and v_{dc}^{ref}, (d) Error between the centralized and distributed voltages.

Table 4.2: Average Errors (Continuous Controller)

	Average Error (V)
$\frac{1}{N}\sum_{k=1}^{k=N}\|v_{dc}(k)-v_{dc}^{ref}\|$	0.0014
$\frac{1}{N}\sum_{k=1}^{k=N}\|v_{dc_{sub1}}(k)-v_{dc}^{ref}\|$	0.0353
$\frac{1}{N}\sum_{k=1}^{k=N}\|v_{dc_{sub2}}(k)-v_{dc}^{ref}\|$	9.41×10^{-4}
Average error between centralized voltage v_{dc} and distributed voltages ($v_{dc_{sub1}}$&$v_{dc_{sub2}}$): 0.0363 V	

Table 4.3: The Discretization of Control Inputs

Size of Control Sets	
	Centralized
Subsystem 1	$\|u_1\|=9$
Subsystem 1	$\|u_3\|=5$
Subsystem 2	$\|u_2\|=9$
Subsystem 2	$\|u_4\|=4$

Table 4.4: Computation Time (Discrete Controller)

Centralized MPC	Distributed MPC
131.49 s	3.06 s
Speed up	**42.97**

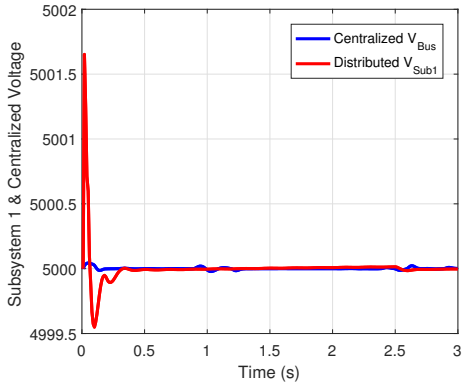

(a) Subsystem 1 and Centralized Voltages

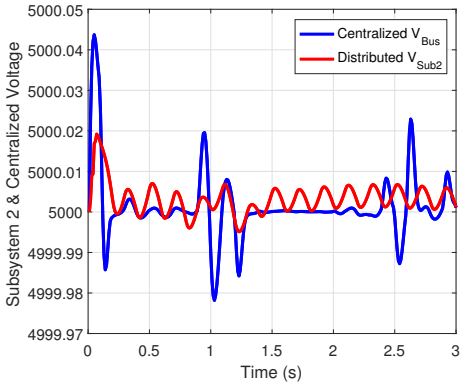

(b) Subsystem 2 and Centralized Voltages

Figure 4.8: Centralized and Distributed Voltages (Discrete Controller)

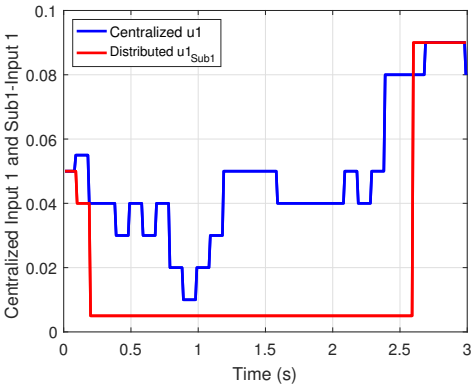

(a) Centralized Input 1 & Sub1-Input 1 (K_{droop1})

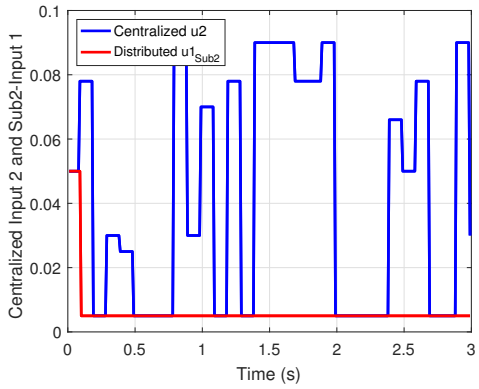

(b) Centralized Input 2 & Sub2-Input 1 (K_{droop2})

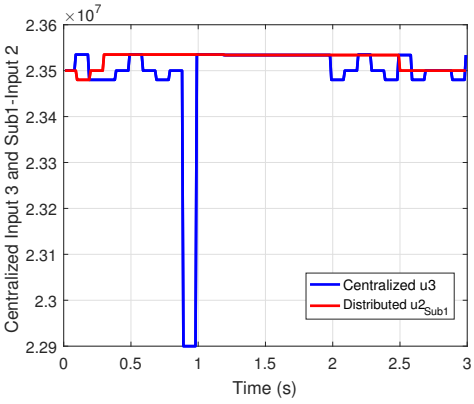

(c) Centralized Input 3 & Sub1-Input 2 (P_{G1-ref})

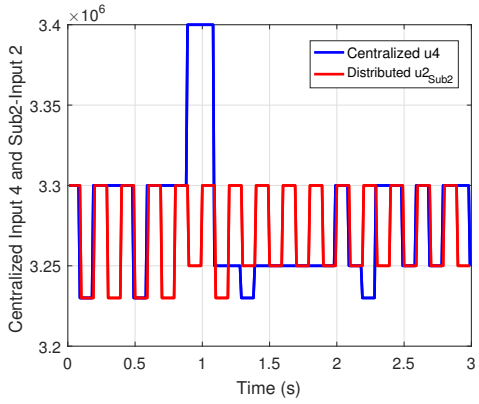

(d) Centralized Input 4 & Sub2-Input 2 (P_{G2-ref})

Figure 4.9: Centralized and Distributed Control Inputs (Discrete Controller)

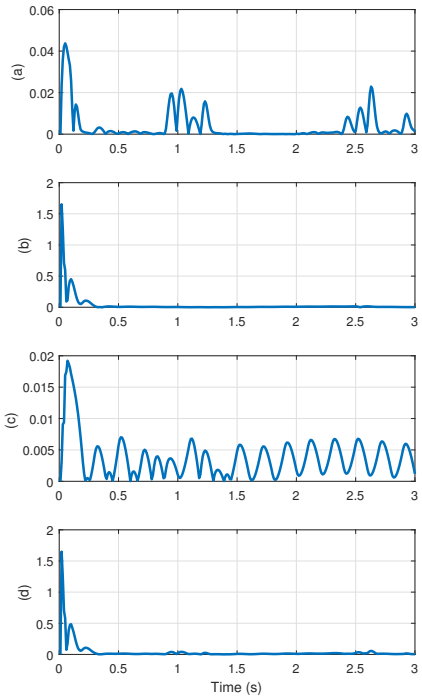

Figure 4.10: For the discrete controller (a) Error between centralized v_{dc} and v_{dc}^{ref}, (b) Error between distributed $v_{dc_{sub1}}$ and v_{dc}^{ref}, (c) Error between distributed $v_{dc_{sub2}}$ and v_{dc}^{ref}, (d) Error between centralized and distributed voltages.

Table 4.5: Average Errors (Discrete Controller)

	Average Error (V)
$\frac{1}{N}\sum_{k=1}^{k=N}\|v_{dc}(k) - v_{dc}^{ref}\|$	0.0040
$\frac{1}{N}\sum_{k=1}^{k=N}\|v_{dc_{sub1}}(k) - v_{dc}^{ref}\|$	0.0324
$\frac{1}{N}\sum_{k=1}^{k=N}\|v_{dc_{sub2}}(k) - v_{dc}^{ref}\|$	0.0037
Average error between centralized voltage v_{dc} and distributed voltages ($v_{dc_{sub1}}$&$v_{dc_{sub2}}$): 0.0388 V	

The simulation results of applying discrete and continuous controllers on the MVDC system demonstrate that the distributed control approach has a good overall performance with less computational overhead.

4.3.3 Scenario I: A Pulsed Load Control in Both the Centralized and the Distributed Cases

In this case scenario, the simulation results of both centralized and distributed MPC controllers are presented when the system encounters a pulsed load under the battle mode. Here, I the presented simulation results are just for continuous controllers. The control objectives and system constraints are the same as ones mentioned in the Subsection 4.3.1. The horizon for the MPC controllers for both centralized and distributed cases is 2. The pulsed load starts at $t = 1s$ with $1s$ duration. The centralized bus voltage and the voltage of subsystems one and two are shown in Fig. 4.11. The control inputs of both centralized and distributed controllers are given in Fig. 4.12. Fig. 4.13 (a) shows the error between centralized bus voltage v_{dc} and the reference voltage v_{dc}^{ref}. Fig. 4.13 (b) demonstrates the error between distributed voltages ($v_{dc_{sub1}}$ & $v_{dc_{sub2}}$) with the reference voltage v_{dc}^{ref}. The average errors of these cases are given in Table 4.6. The computation time for the centralized MPC and distributed MPC is given in Table 4.7.

The simulation results demonstrate that the proposed distributed MPC approach can effectively improve the DC bus voltage performance when we have a pulsed load in the system. In comparison with the centralized power system management, besides a good overall voltage performance, it also reduces the computational overhead significantly because of the system decomposition.

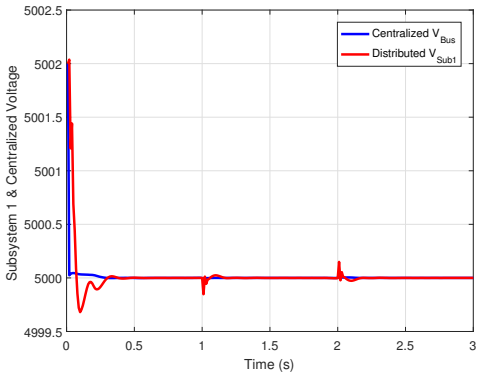

(a) Subsystem 1 and Centralized Voltages

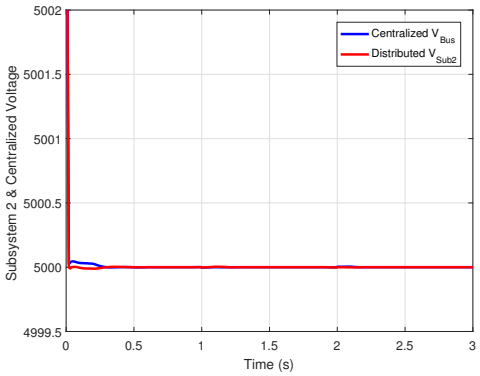

(b) Subsystem 2 and Centralized Voltages

Figure 4.11: Scenario I: Centralized and Distributed Voltages (Continuous Controller)

4.3.4 Scenario II: Changes in Load Demand in Both the Centralized and the Distributed Cases

In this case scenario, the simulation results of both continuous centralized and distributed MPC controllers are presented when the load demand is increasing gradually. Here, the control objectives and system constraints are the same as ones mentioned in the Subsection 4.3.1. The changes are considered in the load 1 in the global system in the centralized structure and in the load 1 in subsystem 1 in the distributed structure. In the distributed power management structure, the changes in the load demand occurring in the subsystem 1 and the coordinator aims to obtain the updated variables from each subsystem in each time step and share them with other subsystems to reach a global optimal solution. Therefore, the optimization problem for each local MPC is solved based on both local measurements and the latest interaction variables obtained from other subsystems through the coordinator.

The power changes in load 1 gradually start at $t = 5s$ and continue until $t = 10s$ from $1.25MW$ to $2.5MW$ as shown in Fig. 4.14 (a). The control inputs of both centralized

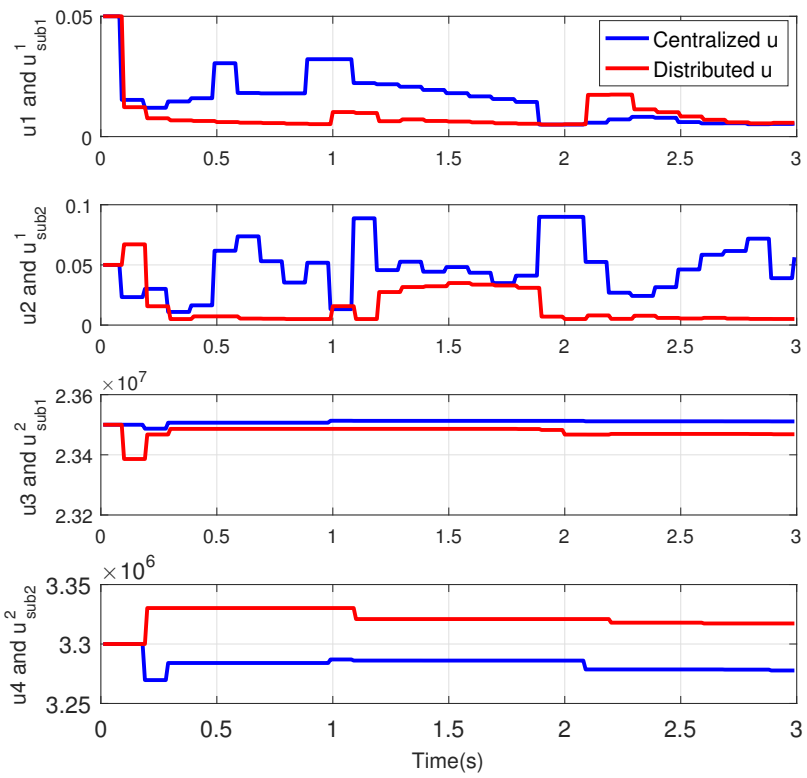

Figure 4.12: Scenario I: Centralized and Distributed Control Inputs

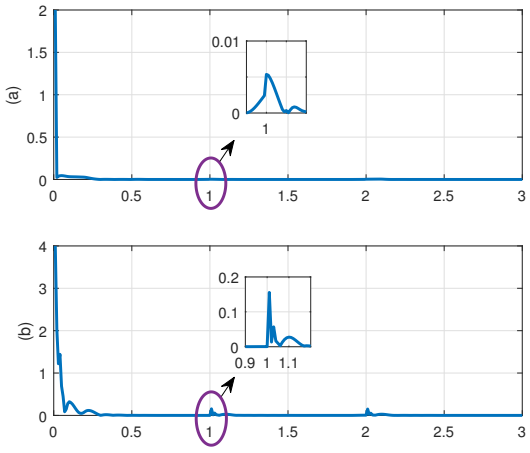

Figure 4.13: Scenario I: (a) Error between centralized v_{dc} and v_{dc}^{ref}, (b) Error between distributed voltages and v_{dc}^{ref}

Table 4.6: Scenario I: Average Errors

Scenario I	Average Error (V)
$\sum_{k=1}^{k=N} \frac{\|v_{dc}(k) - v_{dc}^{ref}\|}{N}$	0.0095
$\frac{1}{N} \sum_{k=1}^{k=N} \left(\|v_{dc_{sub1}}(k) - v_{dc}^{ref}\| + \|v_{dc_{sub2}}(k) - v_{dc}^{ref}\| \right)$	0.0464

Table 4.7: Scenario I: Computation Time (Continuous Controller with a Pulsed Load)

Centralized MPC	Distributed MPC
73.30 s	22.78 s
Speed up	**3.21**

and distributed controllers are given in Fig. 4.14 (b). The centralized bus voltage and the voltage of subsystems 1 and 2 are shown in Fig. 4.15. Fig. 4.16 shows the output power of generators for both centralized and distributed cases. Fig. 4.17 (a) shows the error between centralized bus voltage v_{dc} and the reference voltage v_{dc}^{ref}. Fig. 4.17 (b) demonstrates the error between distributed voltages ($v_{dc_{sub1}}$ & $v_{dc_{sub2}}$) with the reference voltage v_{dc}^{ref}. The average errors of these cases are given in Table 4.8. The computation time for the centralized MPC and distributed MPC is given in Table 4.9.

The simulation results demonstrate that the proposed distributed MPC approach can effectively handle the changes in load demand and improve the DC bus voltage performance. In comparison with the centralized power system management, it also reduces the computational overhead significantly because of the system decomposition.

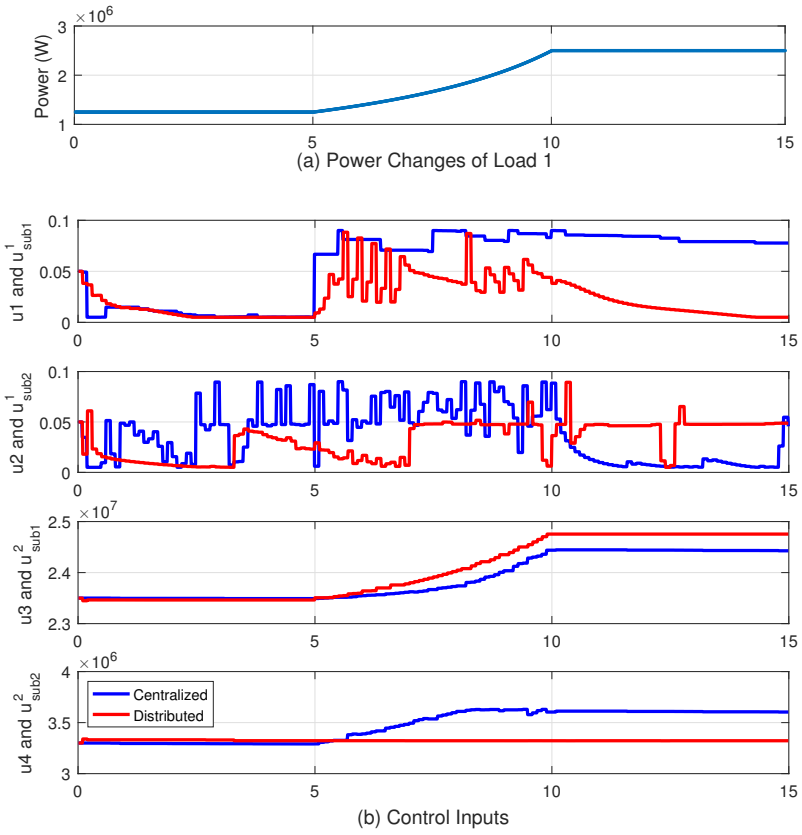

Figure 4.14: Scenario II: (a) Power changes in load 1 (b) Centralized and Distributed Control Inputs

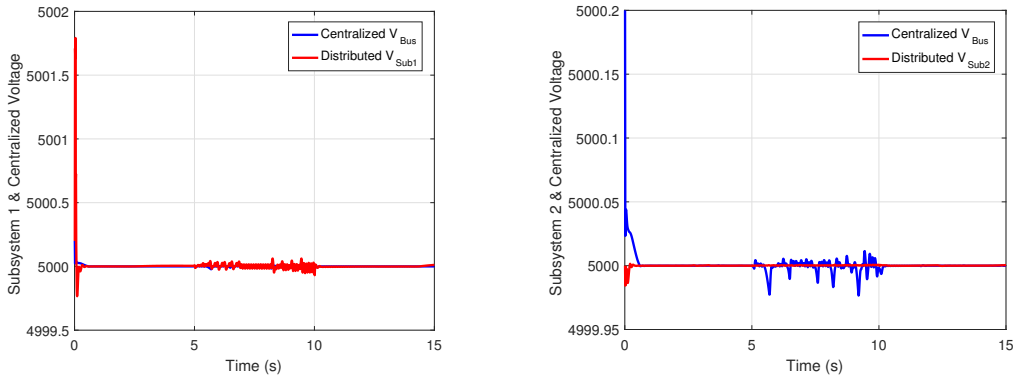

(a) Subsystem 1 and Centralized Voltages

(b) Subsystem 2 and Centralized Voltages

Figure 4.15: Scenario II: Centralized and Distributed Voltages (Continuous Controller)

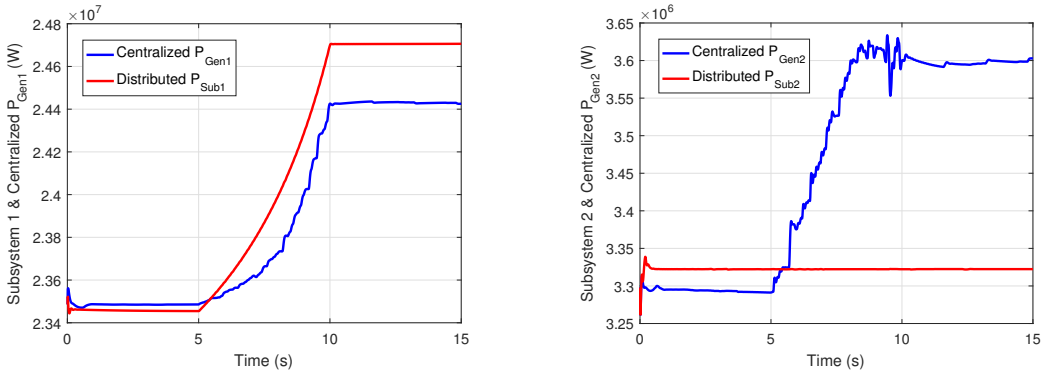

(a) Output power of generator 1

(b) Output power of generator 2

Figure 4.16: Scenario II: Output power of generators

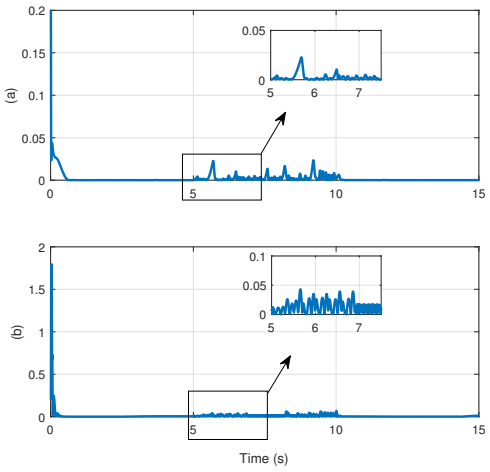

Figure 4.17: Scenario II: (a) Error between centralized v_{dc} and v_{dc}^{ref}, (b) Error between distributed voltages and v_{dc}^{ref}

Table 4.8: Scenario II: Average Errors

Scenario II ($N = \frac{15}{Ts}$)	Average Error (V)
$\sum_{k=1}^{k=N} \frac{\|v_{dc}(k) - v_{dc}^{ref}\|}{N}$	0.0021
$\frac{1}{N} \sum_{k=1}^{k=N} \left(\|v_{dc_{sub1}}(k) - v_{dc}^{ref}\| + \|v_{dc_{sub2}}(k) - v_{dc}^{ref}\| \right)$	0.0127

Table 4.9: Computation Time (Continuous Controller with Changes in Load Demand)

Centralized MPC	Distributed MPC
103.31 s	47.65 s
Speed up	**2.16**

Another situation when distributed controllers show their importance is when there are security concerns involved. In some situations, like a microgrid for example, a subsystem's owner might be reluctant to share their full system model with others, but they may be willing to share some limited data with a coordinator. In a different scenario, with some modifications in the control structure, subsystems can be added or removed online. However, this is not in the scope of current research.

4.4 Conclusion

This chapter proposes a distributed control architecture for a nonlinear MVDC shipboard power system. At first, the global model is partitioned into several interconnected subsystems. In the local control level, a model predictive control approach is chosen to manage each subsystem. The optimization problem for each local MPC is solved based on both local measurements and the latest interaction variables obtained from other subsystems with respect to subsystem's states and control inputs constraints. The goal coordination method is used for interacting variables between subsystems. The multi-step Gradient method is employed for updating Lagrange multipliers as a coordination algorithm in the distributed approach to achieve a global optimal solution. The simulation results are also given to

show the efficiency of the proposed distributed approach. At first the nonlinear MVDC model is divided into two subsystems and then a performance analysis is accomplished by comparing centralized and distributed control of the global and partitioned MVDC models for two cases of continuous and discrete control inputs. When we have discrete control inputs, the computational burden is significantly decreased by using the distributed MPC controller in comparison with the centralized one. According to case scenarios I and II, both the centralized and distributed control structures can efficiently manage the pulse load event and changes in the load demand. In general, the distributed power management structure improves overall performance, robustness and flexibility while minimizing computational overhead.

CHAPTER V

CONCLUSIONS AND FUTURE RESEARCH

This chapter concludes the contributions of this dissertation and states the possible future research directions.

5.1 Conclusions

The design of the latest MVDC shipboard power system needs careful consideration of the variety of system specifications, operating constraints and design requirements under different operating scenarios and mission profiles to maintain a stable, reliable and economically efficient operation. In this research, I first present a full description of the MVDC model under consideration. I also provide a complete list of significant transient and steady-state specifications and necessary operating constraints to address various aspects of the electric ship design. Then, I develop both centralized and distributed model predictive control architectures for a nonlinear MVDC shipboard power system to achieve different performance goals in the system.

During the last decade, model-based control has been widely considered and many results have been obtained for the system-wide automatic management. Among various model-based management methods, model predictive control is known as a promising control technique which attracts the interest of many researchers from academic and industry.

I use the MPC as the main control approach in our work for both centralized and distributed frameworks. For the centralized framework, the objective of the first MPC controller design is to meet voltage performance with minimal changes of the control inputs when dealing with a high power pulsed load in the system. The control inputs are chosen as the droop gain and power reference of each generator. The objective of the second proposed controller is to apply the appropriate reconfiguration algorithm based on the MPC controller to deliver maximum power to the loads in abnormal situations . In this case, the control inputs are defined as the status of switches related to each load and generator. Since the control inputs are discrete in this case, a tree search algorithm has been implemented to find the optimal switching configuration.

For the proposed distributed framework, each subsystem is controlled by a local model predictive controller using local state variables and parameters, and also interaction variables from other subsystems shared through a coordinator. The goal coordination approach is used for interacting information between subsystems. In this research, I use the multi-step Gradient method for updating Lagrange multiplier vector in the coordinator. For the MPC nonlinear optimization problems, the tree search algorithm and MATLAB *fmincon* solver are used when dealing with discretized control inputs and continuous control inputs, respectively. The simulation results demonstrate the effectiveness of the proposed distributed structure for the partitioned MVDC system by comparing centralized and distributed control methods for both continuous and discrete control inputs. Two scenarios are also provided to show how distributed control structure can manage a pulsed load or changes in the load demand

in the system. Accordingly, the proposed distributed control structure results in a good overall performance with less computational complexity.

5.2 Possible Future Directions

The contributions of this dissertation can lead to the following future research opportunities:

5.2.1 Different Subsystems Decompositions

In this work, I consider two subsystems' decomposition in the distributed case. In our case study, subsystem 1 contains the main turbine generator, zonal load 1, zonal load 2 and one electrical propeller, and subsystem 2 includes the auxiliary turbine generator, zonal load 3, zonal load 4 and an energy storage device. The interaction variables between subsystems are currents. However, the decomposition of the global MVDC system could have different subsystem configurations. It would yield different output results or even give a more applicable and efficient distributed control for the ship system if different subsystem decompositions are chosen. It is better that the elements of each subsystem closely interrelate with each other and have the same local objective. Also, the distributed control would be more efficient if subsystems are partitioned with minimal interaction between them. Therefore, it is important to investigate the system closely in order to find the proper decomposition.

5.2.2 Framework Extension of Distributed Control for the General MVDC System

In this research, the centralized and distributed controllers are mainly developed for a nonlinear MVDC model which consists of two generators (MTG & ATG) and one propulsion load. However, the general baseline MVDC model which is given in [6] includes four generators (2 MTGs & 2 ATGs) and two propulsion modules. New configuration of the MVDC model also includes more that four zonal loads in the system. Since the general system includes more elements in the system resulting in a complicated model, centralized model-based control would not be an efficient choice for the power management. The distributed control structure simplifies any possible expansions and maintenance of the control system. Moreover, it would be easier to implement a distributed control scheme due to its lower computational requirements. It has less computational overhead because a difficult problem is replaced by several smaller-scale problems. Fig. 5.1 shows a possible extended distributed model predictive control structure for the general baseline MVDC system.

5.2.3 Communication Delays in the Coordinator

The proposed distributed control approach can be extended when delays exist in the system states or in the coordinator communication. These delays, either constant or time varying, can reduce the performance of the designed controllers that do not consider delays. Therefore, much research work is needed to develop systematic control methods to design advanced distributed controllers to consider communication delays.

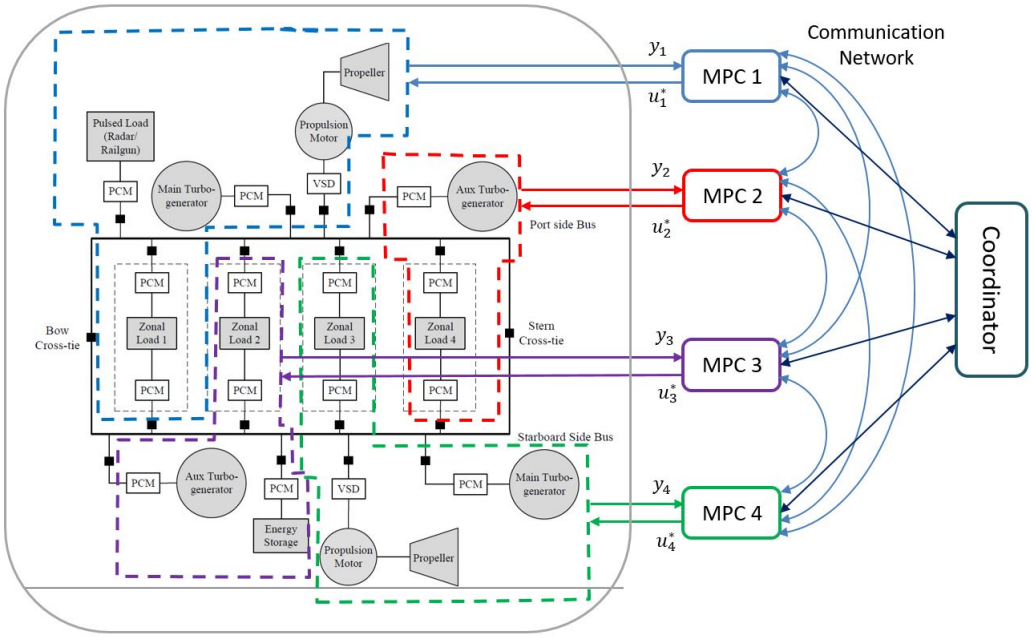

Figure 5.1: Extension of Distributed Control Framework

5.2.4 Control Hardware In Loop Implementation

The main purpose of using hardware in loop simulation is to test the proposed control approaches before implementing it in the real plant (MVDC SPS). It is also very useful for the training purpose and also testing methods without damaging the real equipment. Controller hardware-in-the-loop (CHIL) is a popular approach which provides flexible and effective tools to study and examine the design challenges in many applications, including the MVDC electric ship research.

5.2.5 SPS Stochastic Hybrid Modeling and Power Management

It is worth mentioning that a shipboard power system, like any other physical system, has uncertainty and randomness in its behavior. For instance, load power consumption is not completely deterministic. Several parameters like measurement difficulty, temperature

dependency, and random fluctuation of environment cause uncertainty in the SPS. Due to increasing demand for electric power in the SPS such as electrical weaponry and electric propulsion, optimal power distribution is an important issue, especially during a mission or critical situation. Besides, unpredictable sea states can lead to stochastic time-varying propulsion loads. As a future work, stochastic modeling of power systems and hydrodynamics of an SPS would be an interesting research. In this regard, stochastic hybrid systems would be a useful modeling approach to reach this goal, including the interaction of continuous dynamics, discrete dynamics and probabilistic uncertainty.

REFERENCES

[1] *Electric Power, Alternating Current*, Tech. Rep. MIL-STD- 1399 Section 300B, Department of Defense, Apr. 2008.

[2] *High Voltage Electric Power, Alternating Current*, Tech. Rep. MIL-STD-1399 Section 680, Department of Defense, Apr. 2008.

[3] "IEEE Guide for the Design and Application of Power Electronics in Electrical Power Systems on Ships," *IEEE Std 1662-2008*, Mar. 2009, pp. 1–72.

[4] "IEEE Recommended Practice for 1 kV to 35 kV Medium-Voltage DC Power Systems on Ships," *IEEE Std 1709-2010*, Nov. 2010, pp. 1–54.

[5] *Documentation for Notional Baseline System Models*, Version 0.7, ESRDC, 2012.

[6] *Notional System Models: Technical Report*, Tech. Rep., ESRDC, The Office of Naval Research, 2013.

[7] *Mission Analysis - Methods, Metrics, and Mission Definition for Electric Ships*, Esrdc, Mississippi State University, 2014.

[8] R. Amgai and S. Abdelwahed, "Power Management of Shipboard Power Systems Using Interaction Balance Principle," *North American Power Symposium (NAPS), 2014*. 2014, pp. 1–6, IEEE.

[9] S. Anand, B. G. Fernandes, and J. Guerrero, "Distributed Control to Ensure Proportional Load Sharing and Improve Voltage Regulation in Low-Voltage DC Microgrids," *IEEE Transactions on Power Electronics*, vol. 28, no. 4, 2013, pp. 1900–1913.

[10] G. Antonelli, "Interconnected Dynamic Systems: An Overview on Distributed Control," *IEEE Control Systems*, vol. 33, no. 1, 2013, pp. 76–88.

[11] V. Arcidiacono, A. Monti, and G. Sulligoi, "Generation Control System for Improving Design and Stability of Medium-Voltage DC Power Systems on Ships," *IET Electrical Systems in Transportation*, vol. 2, no. 3, 2012, pp. 158–167.

[12] P. B. Backlund, C. C. Seepersad, and T. M. Kiehne, "All-Electric Ship Energy System Design Using Classifier-Guided Sampling," *IEEE Transactions on Transportation Electrification*, vol. 1, no. 1, 2015, pp. 77–85.

[13] S. Barsali, C. Miulli, and A. Possenti, "A Control Strategy to Minimize Fuel Consumption of Series Hybrid Electric Vehicles," *IEEE Transactions on energy conversion*, vol. 19, no. 1, 2004, pp. 187–195.

[14] M. Bash, R. Chan, J. Crider, C. Harianto, J. Lian, J. Neely, S. Pekarek, S. Sudhoff, and N. Vaks, "A medium voltage DC testbed for ship power system research," *Electric Ship Technologies Symposium, 2009. ESTS 2009. IEEE*. IEEE, 2009, pp. 560–567.

[15] S. Batiyah, N. Zohrabi, S. Abdelwahed, and R. Sharma, "An MPC-Based Power Management of a PV/Battery System in an Islanded DC Microgrid," *2018 IEEE Transportation Electrification Conference and Expo (ITEC)*. IEEE, 2018, pp. 231–236.

[16] A. Bidram, A. Davoudi, and F. L. Lewis, "Distributed Control for AC Shipboard Power Systems," *Electric Ship Technologies Symposium (ESTS), 2013 IEEE*. 2013, pp. 282–286, IEEE.

[17] T. I. Bø and T. A. Johansen, "Battery Power Smoothing Control in a Marine Electric Power Plant Using Nonlinear Model Predictive Control," *IEEE Transactions on Control Systems Technology*, vol. 25, no. 4, 2017, pp. 1449–1456.

[18] S. Bose, S. Pal, B. Natarajan, C. M. Scoglio, S. Das, and N. N. Schulz, "Analysis of Optimal Reconfiguration of Shipboard Power Systems," *IEEE Transactions on Power Systems*, vol. 27, no. 1, 2012, pp. 189–197.

[19] G. E. Box, G. M. Jenkins, G. C. Reinsel, and G. M. Ljung, *Time series analysis: forecasting and control*, John Wiley & Sons, 2015.

[20] S. Boyd, N. Parikh, E. Chu, B. Peleato, and J. Eckstein, "Distributed Optimization and Statistical Learning via the Alternating Direction Method of Multipliers," *Foundations and Trends® in Machine Learning*, vol. 3, no. 1, 2011, pp. 1–122.

[21] G. Buja, A. da Rin, R. Menis, and G. Sulligoi, "Dependable design assessment of integrated power systems for all electric ships," *Electrical Systems for Aircraft, Railway and Ship Propulsion (ESARS), 2010*. IEEE, 2010, pp. 1–8.

[22] K. L. Butler-Purry and N. D. R. Sarma, "Self-Healing Reconfiguration for Restoration of Naval Shipboard Power Systems," *IEEE Transactions on Power Systems*, vol. 19, no. 2, 2004, pp. 754–762.

[23] E. F. Camacho and C. B. Alba, *Model Predictive Control*, Springer Science & Business Media, 2013.

[24] S. Castellan, R. Menis, A. Tessarolo, and G. Sulligoi, "Power Electronics for All-Electric Ships with MVDC Power Distribution System: An Overview," *Ecological Vehicles and Renewable Energies (EVER), 2014 Ninth International Conference On*. 2014, pp. 1–7, IEEE.

[25] J. P. Certuche-Alzate and M. Velez-Reyes, "A Reconfiguration Algorithm for a DC Zonal Electric Distribution System Based on Graph Theory Methods," *Electric Ship Technologies Symposium, 2009. ESTS 2009. IEEE*. 2009, pp. 235–241, IEEE.

[26] J. Chalfant, "Early-Stage Design for Electric Ship," *Proceedings of the IEEE*, vol. 103, no. 12, 2015, pp. 2252–2266.

[27] J. Chalfant, M. Ferrante, and C. Chryssostomidis, "Design of a Notional Ship for Use in the Development of Early-Stage Design Tools," *Electric Ship Technologies Symposium (ESTS), 2015 IEEE*. 2015, pp. 239–244, IEEE.

[28] J. S. Chalfant, *Vulnerability Metric Implementation: Technical Report*, Tech. Rep., MIT Sea Grant College Program, Massachusetts Institute of Technology, May 2010.

[29] J. S. Chalfant and C. Chryssostomidis, "Analysis of various all-electric-ship electrical distribution system topologies," *Electric Ship Technologies Symposium (ESTS), 2011 IEEE*. IEEE, 2011, pp. 72–77.

[30] H. Chen and F. Allgöwer, "A Quasi-Infinite Horizon Nonlinear Model Predictive Control Scheme with Guaranteed Stability," *Automatica*, vol. 34, no. 10, 1998, pp. 1205–1217.

[31] Chief of Naval Operations, *Survivability Policy and Standards for Surface Ships and Craft of the U.S. Navy*, Tech. Rep. OPNAVINST 9070.1A, DEPARTMENT OF THE NAVY, Sept. 2012.

[32] P. D. Christofides, R. Scattolini, D. M. de la Pena, and J. Liu, "Distributed Model Predictive Control: A Tutorial Review and Future Research Directions," *Computers & Chemical Engineering*, vol. 51, 2013, pp. 21–41.

[33] J. G. Ciezki and R. W. Ashton, "Selection and Stability Issues Associated with a Navy Shipboard DC Zonal Electric Distribution System," *IEEE Transactions on power delivery*, vol. 15, no. 2, 2000, pp. 665–669.

[34] A. M. Cramer, *Metric Based Design of Integrated Engineering Plants for Robust Performance during Hostile Disruptions*, doctoral dissertation, Purdue University, 2007.

[35] A. M. Cramer, S. D. Sudhoff, and E. L. Zivi, "Performance Metrics for Electric Warship Integrated Engineering Plant Battle Damage Response," *IEEE Transactions on Aerospace and Electronic Systems*, vol. 47, no. 1, 2011, pp. 634–646.

[36] J. M. Crider and S. D. Sudhoff, "Reducing impact of pulsed power loads on microgrid power systems," *IEEE Transactions on Smart Grid*, vol. 1, no. 3, 2010, pp. 270–277.

[37] M. Cupelli, F. Ponci, G. Sulligoi, A. Vicenzutti, C. S. Edrington, T. El-Mezyani, and A. Monti, "Power Flow Control and Network Stability in an All-Electric Ship," *Proceedings of the IEEE*, vol. 103, no. 12, 2015, pp. 2355–2380.

[38] R. M. Cuzner and D. A. Esmaili, "Fault tolerant shipboard MVDC architectures," *Electrical Systems for Aircraft, Railway, Ship Propulsion and Road Vehicles (ESARS), 2015 International Conference on*. IEEE, 2015, pp. 1–6.

[39] Y.-H. Dai and Y. Yuan, "A Nonlinear Conjugate Gradient Method with a Strong Global Convergence Property," *SIAM Journal on optimization*, vol. 10, no. 1, 1999, pp. 177–182.

[40] K. Davey, "Ship Component in Hull Optimization," *Marine Technology Society Journal*, vol. 39, no. 2, 2005, pp. 39–46.

[41] N. Doerry, "Designing Electrical Power Systems for Survivability and Quality of Service," *Naval Engineers Journal*, vol. 119, no. 2, 2007, pp. 25–34.

[42] N. Doerry, "Next Generation Integrated Power Systems (NGIPS) for the Future Fleet," *IEEE Electric Ship Technologies Symposium*, 2009.

[43] N. Doerry, "Naval Power Systems: Integrated Power Systems for the Continuity of the Electrical Power Supply.," *IEEE Electrification Magazine*, vol. 3, no. 2, 2015, pp. 12–21.

[44] N. Doerry and J. Amy, "DC Voltage Interface Standards for Naval Applications," *Electric Ship Technologies Symposium (ESTS), 2015 IEEE*. 2015, pp. 318–325, IEEE.

[45] N. Doerry and J. Amy, "MVDC Shipboard Power System Considerations for Electromagnetic Railguns," *Proc. 6th DoD Electromagn. Railgun Workshop*, 2015.

[46] N. Doerry and J. Amy Jr, "MVDC Distribution Systems," *Advanced Machinery Technology Symposium (AMTS)*. ASNE, 2018.

[47] N. Doerry and K. McCoy, *Next Generation Integrated Power System: NGIPS Technology Development Roadmap*, Tech. Rep., DTIC Document, 2007.

[48] N. Doerry and K. McCoy, *Next generation integrated power system: NGIPS technology development roadmap*, Tech. Rep., Naval Sea Systems Command Washington DC, 2007.

[49] N. H. Doerry, "Sizing Power Generation and Fuel Capacity of the All-Electric Warship," *Electric Ship Technologies Symposium, 2007. ESTS'07. IEEE*. 2007, pp. 1–6, IEEE.

[50] N. H. Doerry and J. V. Amy, "Implementing Quality of Service in Shipboard Power System Design," *Electric Ship Technologies Symposium (ESTS), 2011 IEEE*. 2011, pp. 1–8, IEEE.

[51] N. H. Doerry and D. H. Clayton, "Shipboard Electrical Power Quality of Service," *Electric Ship Technologies Symposium, 2005 IEEE*. 2005, pp. 274–279, IEEE.

[52] A. T. Elsayed and O. A. Mohammed, "A comparative study on the optimal combination of hybrid energy storage system for ship power systems," *Electric Ship Technologies Symposium (ESTS), 2015 IEEE*. IEEE, 2015, pp. 140–144.

[53] U. Eren, A. Prach, B. B. Koçer, S. V. Raković, E. Kayacan, and B. Açıkmeşe, "Model Predictive Control in Aerospace Systems: Current State and Opportunities," *Journal of Guidance, Control, and Dynamics*, 2017.

[54] M. Farhadi and O. Mohammed, "Adaptive energy management in redundant hybrid DC microgrid for pulse load mitigation," *IEEE Transactions on Smart Grid*, vol. 6, no. 1, 2015, pp. 54–62.

[55] A. Feliachi, K. Schoder, S. Ganesh, and H.-J. Lai, "Distributed Control Agents Approach to Energy Management in Electric Shipboard Power System," *Power Engineering Society General Meeting, 2006. IEEE*. 2006, pp. 6–pp, IEEE.

[56] E. Ghadimi, I. Shames, and M. Johansson, "Multi-Step Gradient Methods for Networked Optimization," *IEEE Transactions on Signal Processing*, vol. 61, no. 21, 2013, pp. 5417–5429.

[57] S. Ghadimi and G. Lan, "Accelerated Gradient Methods for Nonconvex Nonlinear and Stochastic Programming," *Mathematical Programming*, vol. 156, no. 1-2, 2016, pp. 59–99.

[58] S. Hannapel, N. Vlahopoulos, and D. Singer, "Including Principles of Set-Based Design in Multidisciplinary Design Optimization," *12th AIAA Aviation Technology, Integration, and Operations (ATIO) Conference and 14th AIAA/ISSMO Multidisciplinary Analysis and Optimization Conference*, 2012, p. 5444.

[59] B. Hassanzadeh, H. Pakravesh, J. Liu, and J. F. Forbes, "Coordinated-distributed MPC of nonlinear systems based on price-driven coordination," *American Control Conference (ACC), 2013*. IEEE, 2013, pp. 3153–3158.

[60] H. He, J. Guo, and C. Sun, "Road Grade Prediction for Predictive Energy Management in Hybrid Electric Vehicles," *Energy Procedia*, vol. 105, 2017, pp. 2438–2444.

[61] H. He, H. Li, S. Chen, and H. Xiong, "Warship Power System Survivability Evaluation Based on Complex Network Theory," *2015 International Industrial Informatics and Computer Engineering Conference*. 2015, Atlantis Press.

[62] D. Jia, *Distributed coordination in multiagent control systems through model predictive control*, doctoral dissertation, PhD Thesis, Department of Electrical and Computer Engineering, Carnegie Mellon University, 2003.

[63] W. Jiang, R. Fang, J. Khan, and R. Dougal, "Performance Prediction and Dynamic Simulation of Electric Ship Hybrid Power System," *Electric Ship Technologies Symposium, 2007. ESTS'07. IEEE*. 2007, pp. 490–497, IEEE.

[64] Z. Jin, G. Sulligoi, R. Cuzner, L. Meng, J. C. Vasquez, and J. M. Guerrero, "Next-generation shipboard dc power system: Introduction smart grid and dc microgrid technologies into maritime electrical netowrks," *IEEE Electrification Magazine*, vol. 4, no. 2, 2016, pp. 45–57.

[65] F. D. Kanellos, J. M. Prousalidis, and G. J. Tsekouras, "Control System for Fuel Consumption Minimization–gas Emission Limitation of Full Electric Propulsion Ship Power Systems," *Proceedings of the Institution of Mechanical Engineers, Part M: Journal of Engineering for the Maritime Environment*, vol. 228, no. 1, 2014, pp. 17–28.

[66] S.-Y. Kim, S. Choe, S. Ko, and S.-K. Sul, "A Naval Integrated Power System with a Battery Energy Storage System: Fuel efficiency, reliability, and quality of power.," *IEEE electrification magazine*, vol. 3, no. 2, 2015, pp. 22–33.

[67] S. Kulkarni and S. Santoso, "Impact of pulse loads on electric ship power system: With and without flywheel energy storage systems," *Electric Ship Technologies Symposium, 2009. ESTS 2009. IEEE*. IEEE, 2009, pp. 568–573.

[68] J. Kuseian, "Naval power systems technology development roadmap," *Electric Ships Office, PMS*, vol. 320, 2013.

[69] S. Lahiri, K. Miu, H. Kwatny, G. Bajpai, A. Beytin, and J. Patel, "Fuel Optimization under Quality of Service Constraints for Shipboard Hybrid Electric Drive," *Resilient Control Systems (ISRCS), 2011 4th International Symposium On*. 2011, pp. 137–141, IEEE.

[70] M. Larsson, D. J. Hill, and G. Olsson, "Emergency Voltage Control Using Search and Predictive Control," *International journal of electrical power & energy systems*, vol. 24, no. 2, 2002, pp. 121–130.

[71] J. H. Lee, "Model Predictive Control: Review of the Three Decades of Development," *International Journal of Control, Automation and Systems*, vol. 9, no. 3, 2011, pp. 415–424.

[72] B. P. Loop, S. D. Sudhoff, S. H. Zak, and E. L. Zivi, "Estimating Regions of Asymptotic Stability of Power Electronics Systems Using Genetic Algorithms," *IEEE Transactions on Control Systems Technology*, vol. 18, no. 5, 2010, pp. 1011–1022.

[73] J. M. Maestre and R. R. Negenborn, *Distributed Model Predictive Control Made Easy*, vol. 69, Springer Science & Business Media, 2013.

[74] S. Mashayekh and K. L. Butler-Purry, "Assessing the Dynamic Secure Region for an All-Electric Ship Model," *North American Power Symposium (NAPS), 2012*. 2012, pp. 1–6, IEEE.

[75] J. Mayer and O. Wasynczuk, "An efficient method of simulating stiffly connected power systems with stator and network transients included," *IEEE Transactions on Power Systems*, vol. 6, no. 3, 1991, pp. 922–929.

[76] D. Q. Mayne, "Model Predictive Control: Recent Developments and Future Promise," *Automatica*, vol. 50, no. 12, 2014, pp. 2967–2986.

[77] P. Mitra and G. K. Venayagamoorthy, "An adaptive control strategy for DSTATCOM applications in an electric ship power system," *IEEE Transactions on power electronics*, vol. 25, no. 1, 2010, pp. 95–104.

[78] P. Mitra and G. K. Venayagamoorthy, "Implementation of an Intelligent Reconfiguration Algorithm for an Electric Ship's Power System," *IEEE Transactions on Industry Applications*, vol. 47, no. 5, 2011, pp. 2292–2300.

[79] A. Mohamed, V. Salehi, and O. Mohammed, "Real-time energy management algorithm for mitigation of pulse loads in hybrid microgrids," *IEEE Transactions on Smart Grid*, vol. 3, no. 4, 2012, pp. 1911–1922.

[80] A. Monti, S. D'Arco, L. Gao, and R. Dougal, "Energy storage management as key issue in control of power systems in future all electric ships," *Power Electronics, Electrical Drives, Automation and Motion, 2008. SPEEDAM 2008. International Symposium on*. IEEE, 2008, pp. 580–585.

[81] K. Morison, L. Wang, and P. Kundur, "Power System Security Assessment," *IEEE Power and Energy Magazine*, vol. 2, no. 5, 2004, pp. 30–39.

[82] H. Park, J. Sun, S. Pekarek, P. Stone, D. Opila, R. Meyer, I. Kolmanovsky, and R. DeCarlo, "Real-Time Model Predictive Control for Shipboard Power Management Using the IPA-SQP Approach," *IEEE Transactions on Control Systems Technology*, vol. 23, no. 6, 2015, pp. 2129–2143.

[83] A. Riccobono and E. Santi, "Comprehensive Review of Stability Criteria for DC Power Distribution Systems," *IEEE Transactions on Industry Applications*, vol. 50, no. 5, 2014, pp. 3525–3535.

[84] J. Rodriguez, M. P. Kazmierkowski, J. R. Espinoza, P. Zanchetta, H. Abu-Rub, H. A. Young, and C. A. Rojas, "State of the Art of Finite Control Set Model Predictive Control in Power Electronics," *IEEE Transactions on Industrial Informatics*, vol. 9, no. 2, 2013, pp. 1003–1016.

[85] V. Salehi, B. Mirafzal, and O. Mohammed, "Pulse-load effects on ship power system stability," *IECON 2010-36th Annual Conference on IEEE Industrial Electronics Society*. IEEE, 2010, pp. 3353–3358.

[86] J. D. Schuddebeurs, C. D. Booth, G. M. Burt, and J. R. McDonald, "Impact of Marine Power System Architectures on IFEP Vessel Availability and Survivability," *Electric Ship Technologies Symposium, 2007. ESTS'07. IEEE*. 2007, pp. 14–21, IEEE.

[87] G. Seenumani, J. Sun, and H. Peng, "Real-Time Power Management of Integrated Power Systems in All Electric Ships Leveraging Multi Time Scale Property," *IEEE Transactions on Control Systems Technology*, vol. 20, no. 1, 2012, pp. 232–240.

[88] F. Shariatzadeh, C. B. Vellaithurai, S. S. Biswas, R. Zamora, and A. K. Srivastava, "Real-Time Implementation of Intelligent Reconfiguration Algorithm for Microgrid," *IEEE Transactions on Sustainable Energy*, vol. 5, no. 2, 2014, pp. 598–607.

[89] J. Shi, S. Abdelwahed, W. Zhu, and R. Amgai, "Development of a Control-Based Performance Management System for Shipboard Power Systems," *Electric Ship Technologies Symposium (ESTS), 2015 IEEE*. 2015, pp. 129–134, IEEE.

[90] J. Shi, R. Amgai, and S. Abdelwahed, "Modelling of Shipboard Medium-Voltage Direct Current System for System Level Dynamic Analysis," *IET Electrical Systems in Transportation*, vol. 5, no. 4, 2015, pp. 156–165.

[91] J. Siegers, S. Arrua, and E. Santi, "Stabilizing Controller Design for Multibus MVdc Distribution Systems Using a Passivity-Based Stability Criterion and Positive Feedforward Control," *IEEE Journal of Emerging and Selected Topics in Power Electronics*, vol. 5, no. 1, 2017, pp. 14–27.

[92] J. Siegers and E. Santi, "Stability Analysis and Control Design for an All-Electric Ship MVDC Power Distribution System Using a Passivity Based Stability Criterion and Power Hardware-in-the-Loop Simulation," *Electric Ship Technologies Symposium (ESTS), 2015 IEEE*. 2015, pp. 86–92, IEEE.

[93] D. J. Singer, N. Doerry, and M. E. Buckley, "What Is Set-Based Design?," *Naval Engineers Journal*, vol. 121, no. 4, 2009, pp. 31–43.

[94] R. Soman, M. M. Steurer, T. A. Toshon, M. O. Faruque, and R. M. Cuzner, "Size and weight computation of MVDC power equipment in architectures developed using the smart ship systems design environment," *IEEE Journal of Emerging and Selected Topics in Power Electronics*, vol. 5, no. 1, 2017, pp. 40–50.

[95] S. Srivastava and K. L. Butler-Burry, "Expert-System Method for Automatic Reconfiguration for Restoration of Shipboard Power Systems," *IEE Proceedings-Generation, Transmission and Distribution*, vol. 153, no. 3, 2006, pp. 253–260.

[96] M. Steurer, M. Andrus, J. Langston, L. Qi, S. Suryanarayanan, S. Woodruff, and P. Ribeiro, "Investigating the impact of pulsed power charging demands on shipboard power quality," *Electric Ship Technologies Symposium, 2007. ESTS'07. IEEE*. IEEE, 2007, pp. 315–321.

[97] S. D. Sudhoff, *Stability Technical Report*, Esrdc, Office of Naval Research, Aug. 2012.

[98] S. D. Sudhoff, S. F. Glover, P. T. Lamm, D. H. Schmucker, and D. E. Delisle, "Admittance Space Stability Analysis of Power Electronic Systems," *IEEE Transactions on Aerospace and Electronic Systems*, vol. 36, no. 3, 2000, pp. 965–973.

[99] S. D. Sudhoff, S. D. Pekarek, S. F. Glover, S. H. Zak, E. Zivi, J. D. Sauer, and D. E. Delisle, *Stability Analysis of a Dc Power Electronics Based Distribution System*, Tech. Rep., SAE Technical Paper, 2002.

[100] A. Tessarolo, S. Castellan, R. Menis, and G. Sulligoi, "Electric Generation Technologies for All-Electric Ships with Medium-Voltage DC Power Distribution Systems," *Electric Ship Technologies Symposium (ESTS), 2013 IEEE*. 2013, pp. 275–281, IEEE.

[101] D. Trentesaux, "Distributed Control of Production Systems," *Engineering Applications of Artificial Intelligence*, vol. 22, no. 7, 2009, pp. 971–978.

[102] G. J. Tsekouras, F. D. Kanellos, and J. Prousalidis, "Simplified Method for the Assessment of Ship Electric Power Systems Operation Cost Reduction from Energy Storage and Renewable Energy Sources Integration," *IET electrical systems in transportation*, vol. 5, no. 2, 2014, pp. 61–69.

[103] U.S. Department of Defense, "DoD Guide for Achieving Reliability, Availability, and Maintainability," Aug. 2005.

[104] P. M. J. van den Hof, C. Scherer, P. S. C. Heuberger, and O. Bosgra, eds., *Model-Based Control: Bridging Rigorous Theory and Advanced Technology*, Springer, New York, NY, 2009, OCLC: 836954282.

[105] S. Vazquez, J. I. Leon, L. G. Franquelo, J. Rodriguez, H. A. Young, A. Marquez, and P. Zanchetta, "Model Predictive Control: A Review of Its Applications in Power Electronics," *IEEE Industrial Electronics Magazine*, vol. 8, no. 1, 2014, pp. 16–31.

[106] L. Wang, *Model Predictive Control System Design and Implementation Using MATLAB®*, Springer Science & Business Media, 2009.

[107] W. Wu, D. Wang, A. Arapostathis, and K. Davey, "Optimal Power Generation Scheduling of a Shipboard Power System," *Electric Ship Technologies Symposium, 2007. ESTS'07. IEEE*. 2007, pp. 519–522, IEEE.

[108] H. Zakeri and P. J. Antsaklis, "Local passivity analysis of nonlinear systems: A sum-of-squares optimization approach," *American Control Conference (ACC), 2016*. IEEE, 2016, pp. 246–251.

[109] H. Zakeri and S. Ozgoli, "A sum of squares approach to robust PI controller synthesis for a class of polynomial multi-input multi-output nonlinear systems," *Nonlinear Dynamics*, vol. 76, no. 2, 2014, pp. 1485–1495.

[110] H. Zakeri and M. S. Sadeghi, "A 2-DoF multi-objective H_∞/L_1 robust controller design for a high purification distillation column using LMIs," *2010 International Conference on Computer Applications and Industrial Electronics*, Dec 2010, pp. 683–687.

[111] T. Zhang, "A Method for Evaluating Power Generation Concepts Considering the Optimal Concept of Operations," 2013.

[112] W. Zhu, J. Shi, and S. Abdelwahed, "End-to-end system level modeling and simulation for medium-voltage DC electric ship power systems," *International Journal of Naval Architecture and Ocean Engineering*, vol. 10, no. 1, 2018, pp. 37–47.

[113] N. Zohrabi and S. Abdelwahed, "On the application of distributed control structure for medium-voltage DC shipboard power system," *Control Technology and Applications (CCTA), 2017 IEEE Conference on*. IEEE, 2017, pp. 1201–1206.

[114] N. Zohrabi and S. Abdelwahed, "Efficient Load Management in Electric Ships: A Model Predictive Control Approach," *Applied Power Electronics Conference and Exposition (APEC), 2019 IEEE*. IEEE, 2019.

[115] N. Zohrabi, S. Abdelwahed, and J. Shi, "Reconfiguration of MVDC shipboard power systems: A model predictive control approach," *Electric Ship Technologies Symposium (ESTS), 2017 IEEE*. IEEE, 2017, pp. 253–258.

[116] N. Zohrabi, J. Shi, and S. Abdelwahed, "Ship-wide transient specifications and criteria for Medium-Voltage DC Shipboard Power System," *Transportation Electrification Conference and Expo (ITEC), 2016 IEEE*. IEEE, 2016, pp. 1–6.

[117] N. Zohrabi, J. Shi, and S. Abdelwahed, "An overview of design specifications and requirements for the MVDC shipboard power system," *International Journal of Electrical Power & Energy Systems*, vol. 104, 2019, pp. 680–693.

[118] N. Zohrabi, J. Shi, M. Babaei, and S. Abdelwahed, "Steady-State Specifications and Design Requirements for Medium-Voltage DC Shipboard Power System," *ASNE Advanced Machinery Technology Symposium*, 2016.

APPENDIX A

MATHEMATICAL MODEL FORMULATION OF THE MVDC SPS

A.1 General Structure of the MVDC Ship Power Model

The continuous power system dynamics included in the MVDC SPS can be mathematically described by the following nonlinear differential-algebraic equation (DAE):

$$\begin{aligned} \dot{x}(t) &= f(x(t), u(t), y(t)), \quad x(0) = x_0 \\ 0 &= g(x(t), y(t)) \end{aligned} \tag{A.1}$$

where $x(t) \in \mathbb{R}^n$ is a vector of state variables included in dynamic components of the system such as gas turbines, synchronous machines, and exciters. $u(t)$ denotes the control inputs and x_0 is a vector of initial values for the state variables. $y(t) \in \mathbb{R}^m$ represents a vector of the algebraic state variables such as distribution network variables and other nonlinear algebraic state variables associated with on-board components where no derivatives are present. The system contains one Main Turbine Generator (MTG), one Auxiliary Turbine Generator (ATG), four zonal service loads, one propulsion motor which connected to DC bus via Variable Speed Drive (VSD), one energy storage device and a high power pulsed load like free electron lasers or electromagnetic guns. Fig. A.1 shows the general architecture of the MVDC SPS used in this research. A complete explanation about this MVDC model along with its detailed formulations are given in [112].

In the following sections, the system model shown in Fig. A.1 is broken to different modules. Accordingly, each section provides the necessary explanations and the related mathematical formulations of each functional module.

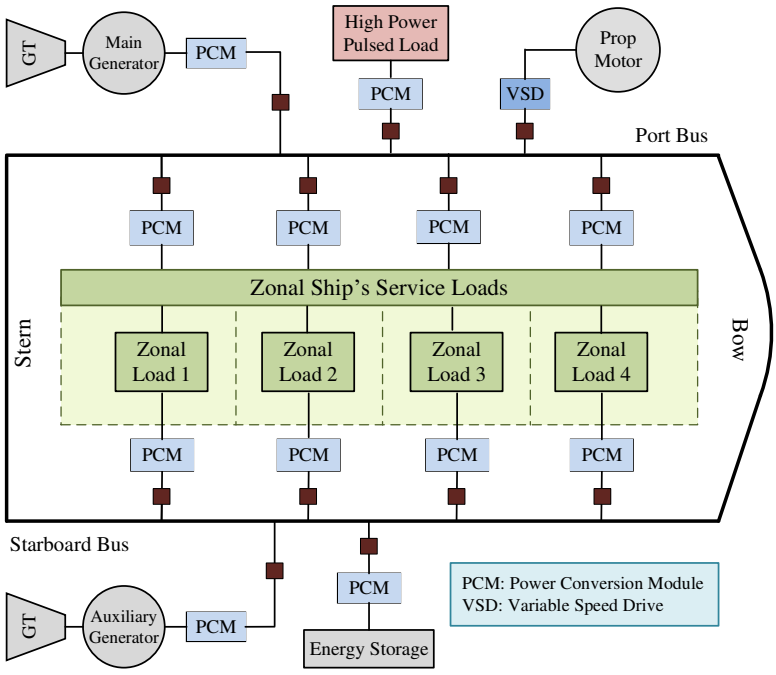

Figure A.1: MVDC SPS Architecture

A.2 Power Generators: MTG and ATG

The system includes two power generators (MTG, ATG) to supply power to the propulsion module and loads on the ship. In the generator, a gas turbine is used as the prime mover for the Wound Rotor Synchronous Machine (WRSM). Different models for a gas turbine are available in the literature. Here, the considered model for the gas turbine can be formulated as follows [112, 75]:

$$\begin{aligned}
\frac{dSG}{dt} &= K_a\left(1-\frac{\omega_r}{\omega_b}\right) - \frac{K_b}{\omega_b}\frac{d\omega_r}{dt}, \\
\frac{dVP}{dt} &= -\frac{1}{T_1}V_P + \frac{1}{T_1}\left(\frac{SG}{W_1} + W_2\right), \\
\frac{dFS}{dt} &= -\frac{1}{T_2}FS + \frac{1}{T_2}VP.
\end{aligned} \tag{A.2}$$

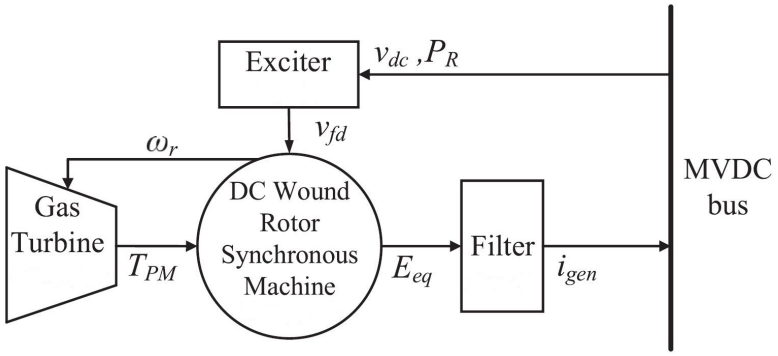

Figure A.2: Power Generation Module [112]

The mechanical torque is the output of gas turbine which is defined as [112]:

$$T_{pm} = T_{base}\left[W_1(FS - W_2) + T_1\left(1 - \frac{\omega_r}{\omega_b}\right)\right] \tag{A.3}$$

The DC current flowing through the filter is formulated as follows :

$$\frac{di_{gen}}{dt} = \frac{\frac{3\sqrt{3}}{\pi}\sqrt{2}E_{eq} - \left(r_{dc} + \frac{3}{\pi}L_c\omega_b + 2r_s\right)i_{gen} - v_{dc}}{L_{dc} + 2L_t} \tag{A.4}$$

A simplified PI controller based exciter is employed in this work. The related formulations for the exciter are as follows [112]:

$$\begin{aligned}\frac{dv_{fd}}{dt} &= -\frac{v_{fd}}{T_{ex}} + \frac{x_G}{T_{ex}} - \frac{K_{ps}}{T_{ex}}\left(v_{dc}^{ref} + K_{droop}(P_r - P_{tg}) - v_{dc}\right)\\ \frac{dx_G}{dt} &= K_{is}\left(v_{dc}^{ref} + K_{droop}(P_r - P_{tg}) - v_{dc}\right)\end{aligned} \tag{A.5}$$

Fig. A.2 illustrates the complete architecture of power generation module. All the state variables and parameters used in this module are also provided in the section A.7.

A.3 Propulsion Module

The propulsion module consists of a three-phase Induction Motor (IM), the associated Pulse-Width Modulation (PWM) Variable Speed Drive (VSD) with filter, a notional fixed pitch propeller and a notional ship hydrodynamics model.

The related equations for different elements of the propulsion module are given below [112].

- Propeller filter: This filter is employed between the distribution bus and PWM to eliminate the harmonics. The related equations are as follows:

$$\begin{aligned} \frac{di_{prop}}{dt} &= \frac{1}{L_f}(v_{dc} - v_f - r_f i_{prop}) \\ \frac{dv_f}{dt} &= \frac{1}{C_f}(i_{prop} - i_{LC}) \end{aligned} \tag{A.6}$$

- PWM-VSI: The PWM-VSI consists of three-phase two-level IGBT bridge that is built by an average model. The current drawn from the DC distribution bus based on d-q coordinates is formulated as follows:

$$i_{LC} = \frac{3}{2}\left(m_d i_{sdm} + m_q i_{sqm}\right) \tag{A.7}$$

- Direct torque controller (DTC) of induction motor consists of two PI controllers that is formulated as follows:

$$\begin{aligned} \frac{d_{x_L}}{dt} &= K_{LI}\left(\lambda_{sref} - \lambda_s\right) \\ \frac{dx_T}{dt} &= K_{TI}\left(T_{ref} - T_{em}\right) \end{aligned} \tag{A.8}$$

- Induction motor: A non-saturable induction machine model in stationary reference frame is used in this work.

The induction motor dynamics are represented by the following equations:

$$\begin{aligned}
\frac{d\lambda_s}{dt} &= v_{sdm} - r_{sm} i_{sdm} \\
\frac{d\lambda_{rd}}{dt} &= -r_{rm} i_{rdm} - \lambda_{rq} \left(P\omega_m - \omega_b ss\right) \\
\frac{d\lambda_{rq}}{dt} &= -r_{rm} i_{rqm} - \lambda_{rd} \left(\omega_b ss - P\omega_m\right) \\
\frac{d\omega_m}{dt} &= \frac{1}{J_m} \left(T_{em} - T_{prop}\right)
\end{aligned} \tag{A.9}$$

- Propeller and ship hydrodynamic: The propeller torque and mechanical thrust are formulated as follows:

$$\begin{aligned}
T_{prop} &= K_Q \left(\frac{\omega_m}{2\pi}\right)^2 \rho D^5 \\
F_{prop} &= K_T \left(\frac{\omega_m}{2\pi}\right)^2 \rho D^4
\end{aligned} \tag{A.10}$$

  Here, the model just considers the ship forward motion. Therefore, the ship dynamics can be formulated as follows:

$$\frac{dv_s}{dt} = \frac{2F_{prop}(1 - t_d) - F_r}{m \cdot m_a} \tag{A.11}$$

Fig. A.3 illustrates the complete architecture of the propulsion module. All the state variables and parameters used in this module are also provided in the section A.7.

A.4 Energy Storage

In this system, a super-capacitor is used as an energy storage device. Fig. A.4 shows the structure of the energy storage module. The related formulations for this module are as follows:

$$\begin{aligned}
i_{cap} &= \frac{v_{dc} - v_{sc}}{R_s} \\
\frac{dv_{sc}}{dt} &= \frac{v_{dc} - v_{sc}}{C_s R_s} - \frac{v_{sc}}{C_s R_p}
\end{aligned} \tag{A.12}$$

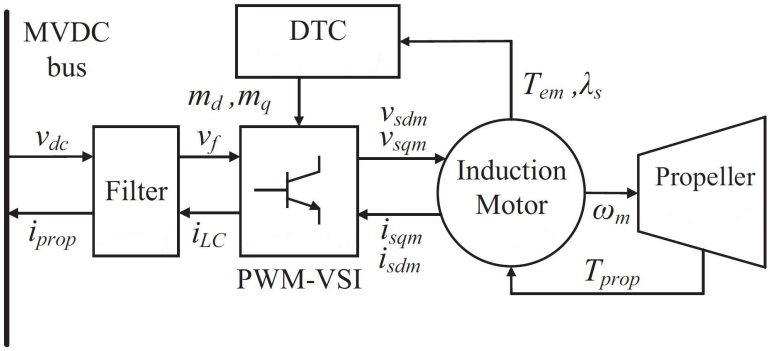

Figure A.3: Propulsion Module [112]

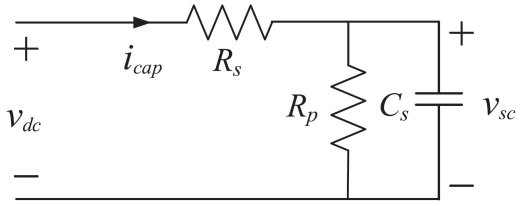

Figure A.4: Energy Storage Module [112]

A.5 Loads

In this work, two types of loads are considered in the system. The first type is zonal loads which represents the service loads on the ship. The second one is pulsed loads which represents weaponry loads including electromagnetic launch systems, electromagnetic guns and free electron lasers. Fig. A.5 shows the structure of the power loads used here. Zonal loads are represented in their Norton equivalents form consisting of a resistor in parallel with a Controlled Current Source (CCS). The current of a zonal load (i_{zonal}) can be formulated as follows:

$$i_{zonal} = \frac{v_{dc}}{R_L} + \frac{P_{zonal}}{v_{dc}} \tag{A.13}$$

A high power pulsed load draws a very high short-time current from the system. As shown in A.5, the time varying power requirement of a pulsed load can be approximated by a square wave. The current of a pulsed load (i_{pulsed}) can be represented as follows:

$$i_{pulsed} = \frac{P_{pulsed}}{v_{dc}} \tag{A.14}$$

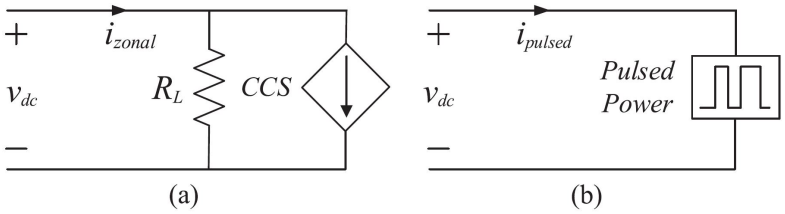

Figure A.5: Power Loads [112]

A.6 Power Distribution Module

All the components of the system are connected to the MVDC distribution bus via Power Conversion Modules (PCMs) and DC disconnect switches. By using the nodal method, a current entering the network from a source has a positive sign, while a current leaving the network to a load has a negative sign. Accordingly, the voltage of the DC distribution bus can be formulated as follows:

$$\frac{dv_{dc}}{dt} = \frac{i_{gen1} + i_{gen2} - i_{pulsed} - i_{cap} - i_{prop} - \sum_{k=1}^{4} i_{zonal}^{k}}{C_{dc}} \tag{A.15}$$

A.7 State Variables and Parameters

In the following, Table A.1 and Table A.2 provide the state variables and the parameters used for different components of the MVDC SPS model, respectively. Readers can also refer to [112] for the comprehensive information about the system model, its mathematical formulations and the exact values of the parameters used in the MVDC model.

Table A.1: A List of Representative State Variables of the MVDC SPS Model

Symbol	Description	Symbol	Description
v_{dc}	DC Bus Voltage	v_{fd}	Field winding excitation voltage
i_{gen}	Generator Current	ω_m	Rotor speed of propeller
v_s	Ship Speed	SG	Internal system state variable of the speed governor
x_G	Internal state variable of PI controller	VP	Internal system state variable of the valve positioner
i_{LC}	Induction Motor Current	FS	Internal system state variable of the fuel system
ω_r	Rotor Speed	v_{sc}	Super-Capacitor Voltage
x_L, x_T	State variables of DTC	i_{prop}	Current flown through the filter into the propulsion module
v_f	State variable of propeller filter	$\lambda_{rd}, \lambda_{rq}$	d-q axis flux linkage of rotor in induction motor
λ_s	Stator flux linkage	v'_{ref}, X_I, v_{of}	State variables of power conversion module

Table A.2: A List of Representative Parameters of the MVDC SPS Model

Power Generators Parameters:			
ω_b	Base rotating speed of the gas turbine rotor	T_{base}	Base value of the mechanical torque
r_{dc}	Resistance of the LC filter	L_{dc}	Inductance of the LC filter
r_s	Synchronous machine stator resistance	L_c	Equivalent line commutating inductance
L_t	Transient commutating inductances	v_{dc}^{ref}	Reference bus voltage
K_{PS}, K_{is}	Proportional and integral gains of exciter	T_{ex}	Integration time constant
P_r	Requested power from the generator	K_{droop}	Power droop factor
Propulsion Module Parameters:			
L_f	Inductance of the propeller filter	r_f	Resistance of the propeller filter
C_f	Capacitance of the propeller filter	i_{LC}	Filtered current
m_d, m_q	Modulation ratio in d-q coordinates	i_{sdm}, i_{sqm}	d-q axis currents into the propulsion motor
λ_{sref}	Flux linkage reference	T_{em}	IM output electrical torque
T_{ref}	Torque reference	v_{sdm}, v_{sqm}	d-q axis voltages
i_{rdm}, i_{rqm}	d-q axis currents of rotor	r_{sm}, r_{rm}	Resistances of stator and rotor
J_m&P	Inertia & pole pairs	T_{prop}	Load torque of the propeller
K_T	Thrust coefficient of the propeller	K_Q	Torque coefficient of the propeller
F_{prop}	Mechanical thrust	t_d	Thrust deduction fraction
m, m_a	Ship mass and added mass	F_r	Ship resistance
ρ	Seawater density	D	Propeller diameter